University of Kentucky
UKnowledge

Theses and Dissertations--Plant Pathology | Plant Pathology

2018

ROLE OF GLYCEROL-3-PHOSPHATE PERMEASES IN PLANT DEFENSE

Juliana Moreira Soares
University of Kentucky, soaresjm6@gmail.com
Digital Object Identifier: https://doi.org/10.13023/ETD.2018.134

Right click to open a feedback form in a new tab to let us know how this document benefits you.

Recommended Citation

Moreira Soares, Juliana, "ROLE OF GLYCEROL-3-PHOSPHATE PERMEASES IN PLANT DEFENSE" (2018). *Theses and Dissertations--Plant Pathology*. 23.
https://uknowledge.uky.edu/plantpath_etds/23

This Doctoral Dissertation is brought to you for free and open access by the Plant Pathology at UKnowledge. It has been accepted for inclusion in Theses and Dissertations--Plant Pathology by an authorized administrator of UKnowledge. For more information, please contact UKnowledge@lsv.uky.edu.

STUDENT AGREEMENT:

I represent that my thesis or dissertation and abstract are my original work. Proper attribution has been given to all outside sources. I understand that I am solely responsible for obtaining any needed copyright permissions. I have obtained needed written permission statement(s) from the owner(s) of each third-party copyrighted matter to be included in my work, allowing electronic distribution (if such use is not permitted by the fair use doctrine) which will be submitted to UKnowledge as Additional File.

I hereby grant to The University of Kentucky and its agents the irrevocable, non-exclusive, and royalty-free license to archive and make accessible my work in whole or in part in all forms of media, now or hereafter known. I agree that the document mentioned above may be made available immediately for worldwide access unless an embargo applies.

I retain all other ownership rights to the copyright of my work. I also retain the right to use in future works (such as articles or books) all or part of my work. I understand that I am free to register the copyright to my work.

REVIEW, APPROVAL AND ACCEPTANCE

The document mentioned above has been reviewed and accepted by the student's advisor, on behalf of the advisory committee, and by the Director of Graduate Studies (DGS), on behalf of the program; we verify that this is the final, approved version of the student's thesis including all changes required by the advisory committee. The undersigned agree to abide by the statements above.

Juliana Moreira Soares, Student

Dr. Pradeep Kachroo, Major Professor

Dr. Lisa J. Vaillancourt, Director of Graduate Studies

ROLE OF GLYCEROL-3-PHOSPHATE PERMEASES IN PLANT DEFENSE

DISSERTATION

A dissertation submitted in partial fulfillment
of the requirements for the degree of Doctor of Philosophy in the College of
Agriculture, Food and Environment at the University of Kentucky

By
Juliana Moreira Soares
Lexington, Kentucky
Director: Dr. Pradeep Kachroo, Professor of Plant Pathology
Lexington, Kentucky
2018
Copyright © Juliana Moreira Soares 2018

ABSTRACT OF DISSERTATION

ROLE OF GLYCEROL-3-PHOSPHATE PERMEASES IN PLANT DEFENSE

Systemic acquired resistance (SAR) is a type of plant defense mechanism that is induced after a localized infection and confers broad-spectrum immunity against related or unrelated pathogens. During SAR, a number of chemical signals and proteins generated at the site of primary infection travel to the uninfected tissues and are thought to alert the distal sites against secondary infections. Glycerol-3-phosphate (G3P) is one of the chemical signals that play an important role in SAR. G3P is synthesized in the cytosol and chloroplasts via the enzymatic activities of G3P Dehydrogenase (G3Pdh) or Glycerol Kinase (GK). Interestingly, a mutation in three of the five G3Pdh isoforms or GK impairs SAR by lowering the pathogen induced G3P pool. This suggests that total cellular pool of G3P is critical for SAR. To determine factors contributing to G3P flux between various subcellular compartments I analyzed the role of putative G3P transporters in G3P flux and SAR. The Arabidopsis genome encodes five isoforms of G3P Permeases (G3Pp) and these transmembrane proteins are predicted to localize to plasma membrane, chloroplast or mitochondria. At least two G3Pp isoforms (G3Pp1 and G3Pp3) were able to complement the *Escherichia coli* mutant impaired in the uptake of G3P into the cytoplasm. Characterization of Arabidopsis G3Pp mutants showed that a mutation in G3Pp2, G3Pp3 and G3Pp4 compromised SAR but not local resistance. Furthermore, this SAR defect could only be complemented by exogenous application of G3P. The G3Pp mutants accumulated wild-type-like levels of G3P suggesting that the subcellular compartmentalization of G3P might contribute to the induction of SAR.

KEY WORDS: Glycerol-3-phosphate (G3P), Systemic acquired resistance, G3P Permease, Plant defense

Juliana Moreira Soares

May 3rd, 2018

ROLE OF GLYCEROL-3-PHOSPHATE PERMEASES IN PLANT DEFENSE

By
Juliana Moreira Soares

Pradeep Kachroo
_____
Director of Dissertation

Lisa J. Vaillancourt
_____
Director of Graduate Studies

May 3rd, 2018
_____
Date

DEDICATION

In memory of my father, Nereu Jose Soares, who always emphasized the value of education and the importance of helping others.

ACKNOWLEDGMENTS

I would like to acknowledge first and foremost my advisor, Dr. Pradeep Kachroo, for his guidance and assistance. I am thankful for the opportunity to be trained as a scientist in his lab and be able to learn from him the value of time. I would like to thank Dr. Aardra Kachroo for providing critical insight that was essential to my training and education.

I sincerely thank all my committee members, Dr. Bruce Downie, Dr. Christopher Schardl, Dr. David Hildebrand and the outside examiner Dr. Jan Smalle, for their useful comments and suggestions during my committee meetings as well as for their valuable insights that substantially improved the quality of this dissertation.

Furthermore, there is no way I would survive these last six years of graduate school without the kindness and unselfish support of Dr. Ludmila Lapchyk, who became more than a lab manager for me. I would like to extend my gratitude to Wendy Havens for the technical support and for always share her knowledge and experiences. I would like to thank John Johnson for helping me with GC-MS quantifications and Amy Crume for maintaining our plant growth facility and the greenhouse. I would also like to acknowledge the plant pathology department staff, which have always been very friendly, helpful and make me feel very welcome.

I would also like to sincerely thank my lab mates for providing both insight into research and an enjoyable work environment. I would like to thank all my friends for their companionship throughout my PhD program specially my dearest Katia for

standing by my side during the most stressful years of my life. I could not have finished without her love and support.

Finally, I would like to thank my family. My mother Néia for sending me positive thoughts and especially thanks to my sister Natália, for her emotional support and encouragement. I appreciate our numerous and long conversations whenever I was feeling homesick. I would like to especially thank my nephew Kaique, your love have helped to push me to this point.

Table of Contents

Acknowledgments iii
Table of Contents v
List of Tables xii
List of Figures xiii
CHAPTER 1- INTRODUCTION 1
Non-host resistance 1
Host resistance 2
PAMP-triggered immunity (PTI) 2
Effector-triggered immunity (ETI) 2
Systemic immunity 3
Salicylic acid (SA) dependent branch of SAR pathway 4
SA independent branch of SAR pathway 5
SAR associated transport of chemical signals 5
Dissertation Goals 6
CHAPTER 2- MATERIALS AND METHODOS 9
Plant growth conditions 9
Pathogen infection 9
Pseudomonas syringae pv. tomato 9
Colletotrichum higginsianum 10
Genetics analysis 10
Bacterial transformation 11
Sequencing 12
Arabidopsis transformation 12
Plant treatments 13
Trypan-blue staining 13
DNA extraction 14
RNA extraction and northern analysis 14
Synthesis of probe and hybridization 15
Synthesis of cDNA 16
Fatty acid profiling 16
Extraction and quantification of azelaic acid (AzA) 16
Extraction and quantification of glycerol-3-phosphate (G3P) 17

Petiole exudate collection 18
G3P quantification of petiole exudates (HPLC) 19
Quantification of AzA, SA and G3P in exudates by GC-MS 19
Hidrogen Peroxide (H_2O_2) Quantification (DAB staining) 20
Escherichia coli complementation assay 20
Confocal microscopy 21
Protein extraction and western blotting 21
CHAPTER 3- ROLE OF G3P PERMEASE IN PLANT DEFENSE 25
Introduction 25
Results and Discussion 28
Characterization of G3P Permeases (G3Pp) 28
Analysis of G3Pp isoforms 28
G3Pp1 and G3Pp3 proteins function as membrane transporters 30
Role of G3Pp in plant defense 31
Exogenous G3P restores defective SAR in *g3pp* mutants 34
AZI and DIR are stable *g3pp* background 36
CHAPTER 4- CHARACTERIZATION OF *gly1-1* SUPPRESSORS 66
Introduction 66
Results and Discussion 67
Defense phenotypes are restored in the suppressor of *gly1-1* 67
AzA and SA confer SAR on *gly1 Sup3* 68
CHAPTER 5- CONCLUSION AND FUTURE PROSPECTS 76
APPENDIX 1- LIST OF ABREVIATIONS 77
REFERENCES 81
VITA 90

List of Tables

Table 2. 1. Seed materials used in this study. 23
Table 2. 2. List of primers used in this study 24
Table 3. 1. G3Pp protein isoforms and mutant alleles 40
Table 3. 2. Isoforms predicted subcellular localization 41
Table 3. 3. Knockouts ordered from the Arabidopsis database. 41

List of Figures

Figure 1. 1. Plant immune system scheme 7
Figure 1. 2. SAR model containing chemicals, proteins and their transport routes 8
Figure 3. 1. G3P Transporter (GlpT) adapted from (Moradi et al, 2015) 38
Figure 3. 2. Inferred phylogenetic relationship of G3Pp isoforms 39
Figure 3. 3. Transcript levels in the *35S-G3Pp-GFP* transgenic lines 42
Figure 3. 4. Protein levels in the *35S-G3Pp-GFP* transgenic lines 43
Figure 3. 5. Fosfomycin mode of action adapted from (Blazquez & Alexandro, 2013) 44
Figure 3. 6. G3Pp complementation assay in ΔG3Pp *E. coli* strain 45
Figure 3. 7. Insertion position and semi-quantitative RT-PCR of *g3pp* knockouts 46
Figure 3. 8. *g3pp3 ssi2* double and single mutant morphological phenotypes 47
Figure 3. 9. Fatty acid (FA) profile in *g3pp* 48
Figure 3. 10. Basal defense in *g3pp* knockouts 49
Figure 3. 11. Cell death phenotype in *g3pp* mutants 50
Figure 3. 12. SAR phenotype in *g3pp* KOs 51
Figure 3. 13. Analysis of transgenic lines overexpressing *35S-G3Pp2-GFP* in *g3pp2* mutant background 52
Figure 3. 14. FA profile in *g3pp gly1-1* double and single mutants 54
Figure 3. 15. Basal defense phenotype in the double mutants *g3pp gly1-1* 55
Figure 3. 16. *g3pp ssi2* double mutant phenotypes 57
Figure 3. 17. Effect of G3Pp mutation on the SA pathway 58
Figure 3. 18. Effect of G3Pp mutation on H_2O_2-mediated SAR and H_2O_2 levels 60
Figure 3. 19. Effect of G3Pp mutation on AzA-mediated SAR and AzA levels 62
Figure 3. 20. Effect of G3Pp mutation on G3P-mediated SAR and G3P levels 63
Figure 3. 21. SAR signaling generation and perception in *g3pp* mutants 64
Figure 3. 22. AZI stability in *g3pp* mutant backgrounds 64
Figure 3. 23. DIR stability in *g3pp* mutant backgrounds 65
Figure 4. 1. *gly1-1 Sup* genotyping and FA profile 70
Figure 4. 2. Basal defense responses in the *Sup* plants 71
Figure 4. 3. SAR phenotype in *gly1-1 Sup* plants 72
Figure 4. 4. SAR response in F3 population derived from *gly1-1 Sup3* x *gly1-1* backcross 73
Figure 4. 5. SAR response in F3 plants derived from the *gly1-1 S3* x Col-0 cross 74
Figure 4. 6. AzA and SA chemically induced SAR on *gly1 Sup3* 75

CHAPTER 1

INTRODUCTION

During the course of evolution plants have developed a sophisticated set of defense mechanisms that they use to recognize and counter growth of pathogens and pests (Agrios, 2005). The plant innate immunity can be classified into following two broad categories that are based on recognition of pathogen by the host and the extent of pathogen colonization on the host (Jones & Dangl, 2006).

Non-host resistance

Non-host resistance (NHR) is one of the most common form of defense that allows plants to resist microbes that are pathogenic on select plant species (Gill et al, 2015). NHR is durable, broad ranged and ensures immunity against any genetic variants of a non-adapted pathogen species. Therefore, NHR can potentially be used as a genetic source of resistance for crop improvement. NHR is subdivided in Type I and Type II based on presence or absence of visual symptoms (Mysore & Ryu, 2004). Type I NHR is most common and is characterized by the complete absence of symptoms on plant tissues. The first barrier that pathogens encounter on Type I NHR include structural components such as cell walls and antimicrobial compounds that prevent pathogen entry into the cell (Freialdenhoven et al, 1996). The inducible plant defense functions as a second barrier, resulting in the generation of phytoalexins, a low molecular weight antimicrobial compound (Glazebrook et al, 1997). In spite of the absence of symptoms, several molecular changes are known to take place during Type I NHR. Type II NHR is manifested by the appearance of a hypersensitive response (HR) like visual symptoms at the site of pathogen infection and induction of defense responses typically associated with host resistance. Thus, signal transduction pathways induced against host and non-host pathogens share many common features (Peart et al, 2002).

Host resistance

PAMP-triggered immunity (PTI)

Host resistance is associated with recognition of pathogens, which in turn activates defense response against the pathogens. The first line of defense is induced when the pathogen associated molecular pattern (PAMP) is recognized by the plant membrane-anchored protein receptors (Pattern Recognition Receptors-PRRs) resulting in induction of PAMP-triggered immunity (PTI) **(Figure 1.1A)** (Jones & Dangl, 2006). One of the common examples of PTI includes recognition of *Pseudomonas syringae* pv. *tomato* (*Pst*) flagellin (fl22) by the host receptor kinase FLS2 (Flagellin Sensing 2) (Zipfel et al, 2004). Orthologs of FLS2 have been characterized in tomato (Robatzek et al, 2007) and other crops (Boller & Felix, 2009). The recognition of flg22 by FLS2 involves physically interaction between the receptor and the PAMP (Chinchilla et al, 2006). The PTI against fungal pathogen involves host specific recognition of PAMPS including chitin (N-Acetyl Chitooligosaccharides), which are recognized by CERK1 (Chitin Elicitor Receptor Kinase 1) in *Arabidopsis thaliana*. The perception of fungi chitin oligomers (Miya et al, 2007) results in dimerization of the CERK1 receptor and triggers chitin-induced immune signaling (Liu et al, 2012). Thus both FLS2 and CERK1 serve as positive regulators of basal defense against specific virulent pathogens (Gómez-Gómez & Boller, 2000; Miya et al, 2007).

Effector-triggered immunity (ETI)

The pathogen-encoded effectors act as virulence factors targeting one or more cellular functions. Plants in turn have evolved resistance (R) proteins, which function by recognizing specific pathogen effectors called avirulence factors (avr proteins) and this in turn results in induction of a robust and strong defense response. This form of defense is called effector-triggered immunity (ETI) and is mediated via direct or indirect interaction between R and avr proteins **(Figure 1.1B)** (Jones & Dangl, 2006). A number of structurally diverse R proteins have been identified from different plant

species and of these a majority of the R proteins belong to Nucleotide Binding Site (NBS) and Leucine Rich Repeat (LRR) families of proteins. The NBS-LRR R proteins are further sub categorized as Toll and interleukin-1 receptor (TIR)-domain-containing (TNL) or coiled-coils (CC)-domain-containing (CNL) proteins based on the domain present on their N-terminus **(Figure 1.1C)** (McHale et al, 2006).

Notably, a majority of R and avr interaction occurs in an indirect manner and involves one or more host proteins known as guard proteins. The R protein is activated in response to pathogen effector mediated change in the guard protein and this guard model has been verified for several R-avr factor interactions. For instance, R protein RPM1 (Resistance to *Pseudomonas syringae* pv. *maculicola 1*) is activated in response to avrRpm1-mediated phosphorylation of the host protein RIN4 (RPM1-Interacting Protein) (Mackey et al, 2002). Interestingly, RIN4 is also a target of avrRpt2 and the avrRpt2-mediated proteolysis of RIN4 activates RPS2 (Resistant to *Pseudomonas syringae* 2) (Mackey et al, 2003). The R and guard proteins are thought to be under constant selection pressure with the evolution favoring pathogens fitness (van der Hoorn & Kamoun, 2008).

Systemic immunity

Induction of local resistance is also associated with the activation of systemic defense responses known as systemic acquired resistance (SAR) and induced systemic resistance (ISR). ISR involves root-shoot signaling and is induced in response to root colonizing beneficial bacteria (Choudhary et al, 2007). In contrast, SAR is triggered in response to pathogen infection and involves generation and transport of mobile signal(s) via phloem to uninfected parts (Kuć, 1982; Spoel & Dong, 2012; Tuzun & Kuć, 1985). Both SAR and ISR confer broad-spectrum disease resistance against pathogen infections (Kachroo & Robin, 2013; Spoel & Dong, 2012). The time-frame for the production of the SAR mobile signal(s) at the site of infection occurs within four to six hours of primary infection (Chanda et al, 2011; Chaturvedi et al, 2012). Many mobile signals been discovered and include salicylic acid (SA) (Gaffney et al, 1993) and its methylated derivative (MeSA) (Park et al, 2007), the dicarboxylic acid

azelaic acid (AzA) (Jung et al, 2009), auxin (Truman et al, 2010), the non-protein amino acid pipecolic acid (Pip) (Návarová et al, 2012), the diterpenoid dehydroabietinal (DA) (Chaturvedi et al, 2012), free radicals nitric oxide (NO) and reactive oxygen species (ROS) (Wang et al, 2014) and glycerol-3-phosphate (G3P) (Chanda et al, 2011). Normal induction of SAR also requires lipid-transfer-like proteins (LTPs), Defective in Induced Resistance (DIR1) (Maldonado et al, 2002) and AzA insensitive (AZI1) (Jung et al, 2009), galactolipids (Gao et al, 2014b) and an intact cuticle (Xia et al, 2009; Xia et al, 2012; Xia et al, 2010). Systemic immunity can be inherited across several generations and is associated with modification in the chromatin structure (Luna et al, 2012; Slaughter et al, 2012). Recent findings suggest that SAR is induced via two parallel branches which are regulated by SA and NO-ROS-AzA-G3P **(Figure 1.2)** (Wang et al, 2014; Wendehenne et al, 2014).

Salicylic acid (SA) dependent branch of SAR pathway

Pathogen infection is well known to trigger accumulation of SA in infected tissues. A low level of SA also accumulates in the distal uninfected tissues (Gao et al, 2014a). Mutations compromising SA biosynthesis or signaling compromise SAR, highlighting an important role of SA in SAR (Cao et al, 1994; Shine et al, 2016; Wildermuth et al, 2001). SA-mediated signaling involves NPR1 (Non-expressor of Pathogenesis-Related Protein 1) protein, a key transcriptional regulator of SA-mediated defense responses. NPR1 localizes to the cytosol and is present in a multimeric form in an un-induced state. A pathogen triggered increase in SA levels is thought to create reducing conditions that result in dissociation of cytoplasmic NPR1 to monomeric form followed by localization of these monomers to the nucleus (Mou et al, 2003; Spoel et al, 2009; Tada et al, 2008). Nuclear NPR1 interacts with TGA transcription factors which then bind to promoters and activate gene expression. The CUL3-mediated degradation, phosphorylation and S-nitrosylation of NPR1 are all required for SAR establishment. NO-mediated S-nitrosylation of NPR1 has yielded conflicting results and was shown to promote both nuclear accumulation (Lindermayr et al, 2010) and

oligomerization (Tada et al, 2008). It is possible that mono- or oligomerization of NPR1 may be dependent on the cellular concentrations of NO (Singh et al, 2017).

NO-ROS-AzA-G3P branch of SAR pathway

NO and ROS act synergistically as signaling species coordinating one of the earliest visible manifestations of host induced HR. In addition to the HR these free radicals are also involved in activation of many defense-related genes (Delledonne et al, 2001; Kulik et al, 2015). In the SAR pathway, NO/ROS mediate AzA biosynthesis by facilitating cleavage of the double bond present on carbon 9 of C18 fatty acids present on digalactosyldiacylglycerol (DGDG) and monogalatosyldiacylglycerol (MGDG) lipids. These two species of galactolipids function non-redundantly in the SAR. In addition to serving as the precursor for AzA, the DGDG lipid is also required for pathogen induced biosynthesis and/or accumulation of NO (Gao et al, 2014b). AzA formed from C18 fatty acids modulates SAR by upregulating *GLY* and *GLI1* genes that catalyze biosynthesis of G3P, a three carbon phosphorylated sugar derivative. Plants impaired in G3P biosynthesis show compromised SAR and this defect can be compensated by the exogenous application of G3P (Chanda et al, 2011). G3P functions in a feedback loop with DIR1 and AZI1 and is required for their stability (Yu et al, 2013).

SAR associated transport of chemical signals

An efficient systemic transport of SAR-associated signals is critical for manifestation of SAR. Phloem is likely the conduit for translocation of these chemicals (Tuzun & Kuć, 1985). The molecules movement inside of the plant cells can occur either via apoplastic or symplastic routes. The plasmodesmata (PD) forms symplastic communication between cells and facilitate movement of ions, metabolites, and hormones between cells. The apoplast is a continuous space involving the outer side of the plasma membrane and like PD serves as a transport route for phloem loading of solutes (Lee, 2015; Stahl & Faulkner, 2016). Recent work has shown that AzA and

G3P are transported via PD while SA transport from local- to distal-leaves occurs via the apoplast **(Figure 1.2)**. The transport of these molecules appears to be tightly regulated since only a small percentage of these chemicals (5-15%) are transported to the distal tissues (Chanda et al, 2011; Lim et al, 2016; Yu et al, 2013). A majority of G3P, AzA and SA present in the distal leaves are synthesized *de novo* (Singh et al, 2017). The plasmodesmata localizing proteins (PDLP) 1 and PDLP5 are responsible for PD gating and consequently regulate the symplastic transport of AzA and G3P. These proteins also regulate the stability and localization of Azelaic Acid Induced protein 1 (AZI1), an important component of the G3P and AzA mediated SAR (Lim et al, 2016).

OBJECTIVES

Translocation of signals is crucial for the establishment of SAR and this can occur both at inter- and intra-cellular levels. G3P is synthesized in multiple subcellular locations in the cell and a mutation in G3P biosynthesis enzymes present in either chloroplast or cytosol impairs SAR. This suggests that the total cellular pool of G3P might be in a continuous flux between various subcellular compartments. In this study, I have investigated the role of G3P Permeases in G3P flux and SAR.

The goals of my dissertation research were:

I) Evaluate defense associated functions of G3P Permeases

II) Determine the contribution of G3P Permeases to the total G3P pool and G3P-mediated SAR signaling

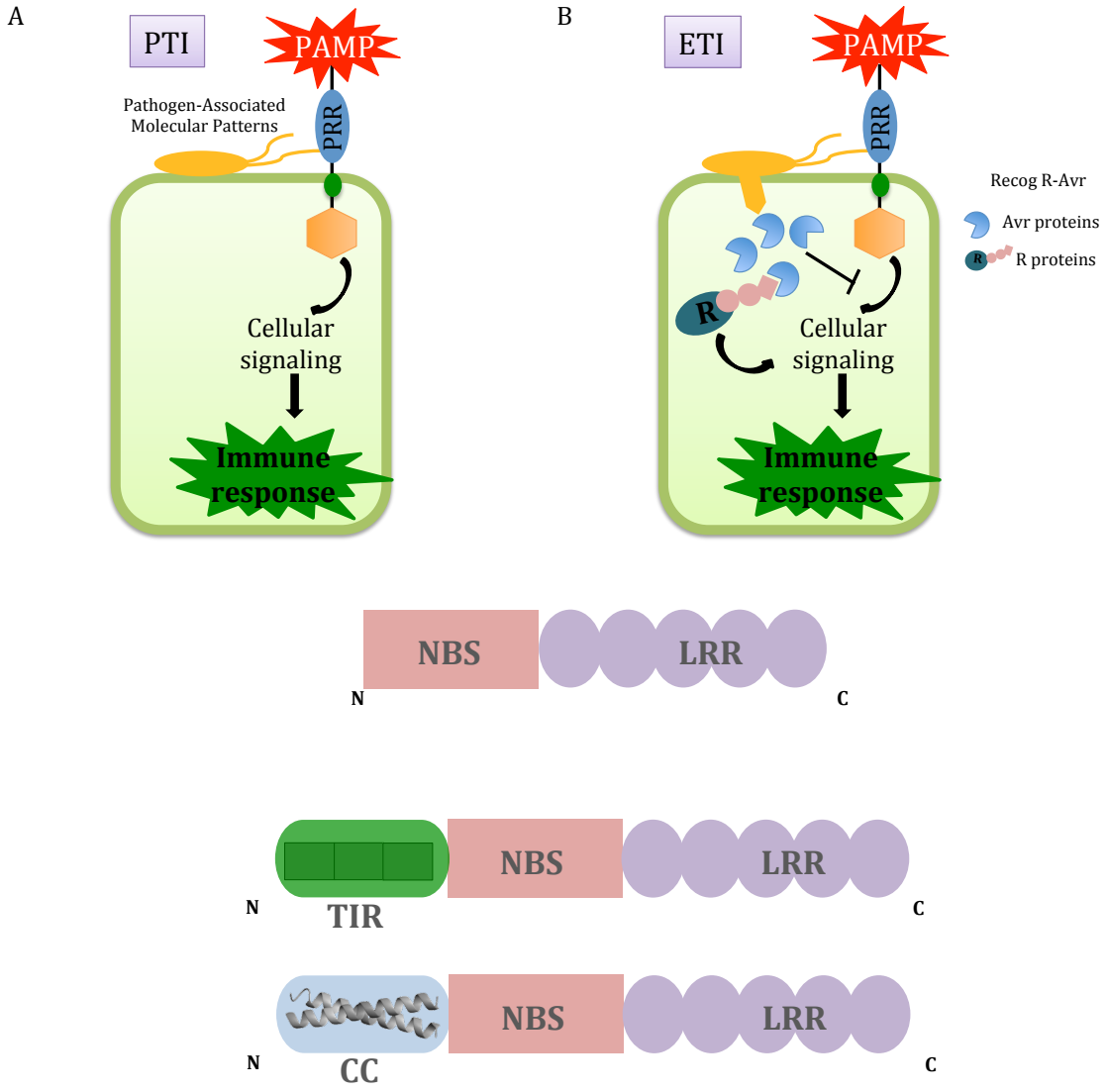

Figure 1.1. Plant immune system scheme adapted from (Pieterse et al, 2009)

(A) Pathogen-associated molecular patterns (PAMPs) recognized by host extracellular pattern-recognition receptors (PRRs), leading to a downstream signaling cascade culminating in PAMP-triggered immunity (PTI). **(B)** Plant pathogen evolved to produce avr proteins (blue pacman) that are directly injected into plant cells suppressing of PTI and resulting in effector-triggered susceptibility (ETS). In turn, plants evolved to produce resistance proteins (R-proteins), which have the ability to recognize the pathogen avr proteins, leading to effector-triggered immunity (ETI). **(C)** R-protein scheme showing two different types of protein domain (TIR and CC).

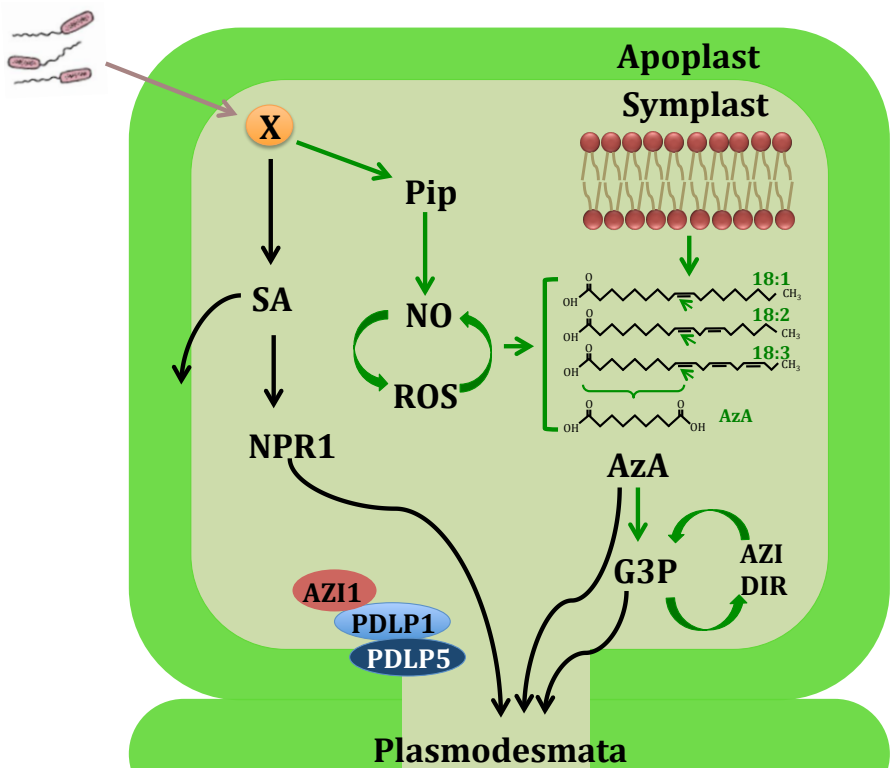

Figure 1.2. SAR model containing chemicals, proteins and their transport routes adapted from (Singh et al, 2017)

Plant pathogenic bacteria infecting a plant cell and triggering accumulation of an unknown signal (indicated by X) that together with digalactosyldiacylglycerol (DGDG) leads to the induction of salicylic acid (SA) and NO/ROS in two parallel branches. SA together with NPR1 protein mediates the induced SAR throughout the SA dependent branch of the pathway. The SA independent branch is coordinated by accumulation of free radicals nitric oxide (NO) and reactive oxygen species (ROS). The ROS operate in a feedback loop with NO and catalyze oxidative cleavage at carbon 9 of C18 D9 unsaturated fatty acids to form azelaic acid (AzA). AzA confers SAR by inducing biosynthesis of glycerol-3-phosphate (G3P). AzA and G3P are transported via plasmodesmata (PD) and SA moves throughout the apoplastic space. The PD localizing protein (PDLP) 5 regulates PD permeability; The PDLP1, PDLP5 and AZI1 proteins interact with each other forming a complex.

CHAPTER 2

MATERIALS AND METHODS

Plant growth conditions

Arabidopsis wild type and mutant seeds were sown on steam-sterilized PRO-MIX BX containing 1% (w/w) marathon. The seeds were kept overnight at 4°C to enhance the synchrony for completion germination. The plant were grown in walk-in MTPS 144 chambers (Conviron, Winnigen, MN, Canada) maintained at 22°C, 65% relative humidity and 14 h photoperiod. These chambers were equipped with cool white fluorescent bulbs (Sylvania, F096/841/XP/ECO). The photon flux density (PFD) of the day period was 106.9 µmoles m^{-2} s^{-1} (measured using a digital light meter, Phytotronic Inc, MO). A list of the genotypes used in this study is provided **(Table 2.1)**.

Pathogen infection

Pseudomonas syringae pv. *tomato*

The strains used in this work included *Pseudomonas syringae* pv. *tomato* DC3000 and *P. syringae* expressing avrRpt2. For plant inoculations, the bacterial stock was first streaked on King's B (King et al, 1954) agar plates containing antibiotics rifampicin (25 µg/mL) and kanamycin (50 µg/mL) (Sigma, St. Louis, MO-USA) and incubated at 29°C for two days. A single bacterial colony from the plate was cultured overnight in 10 mL King's B medium containing rifampicin (25 µg/mL) and kanamycin (50 µg/mL) (King's B 1 L broth contains: 20 g of peptone, 10 mL of glycerol, 1.5 g of K_2HPO_4, 1.5 g of $MgSO_4$ and pH was adjusted to 7.5; for plates, 15 g agar was added). The cultured cells were centrifuged at 936 x g for 10 min, washed twice with 10 mM $MgCl_2$ and then suspended in 10 mM $MgCl_2$. The cell density was quantified using a spectrophotometer (A_{600}) and the cells were suspended at a concentration of 10^5-10^7

CFU/mL. For plant inoculations, the bacterial suspension was infiltrated into the abaxial surface of the leaf using a needle-less syringe. Plants were sampled at 0 and 3 days post inoculation (dpi), three leaf discs from the inoculated leaves were harvested, ground and homogenized in 10 mM $MgCl_2$. For 0 dpi, 100 µL of the leaf extract was plated on King's B plates. For 3 dpi the leaf extract was diluted 10^3- or 10^4-fold and 100 µL was then plated on King's B plates. The plates were kept at 29°C for two days and the colonies were manually counted.

Colletotrichum higginsianum

Colletotrichum higginsianum Sacc. (IMI 349063) was obtained from CABI Bioscience (CABI Inc., Oslo, Norway). Oatmeal agar (Difco, NJ, USA) was used for growth and sporulation of the fungus. The concentration of spore suspensions used in all of the experiments was $2x10^6$ spores/mL. For spot inoculations 7 µL of spore suspension was placed in the middle of the ad-axial side of true rosette leaves and lesion size was measured using digital Vernier calipers (Fischer scientific, PA, USA). For each experiment, lesions were measured from at least 30 leaves. Statistical significance was determined using a Student's *t-test*. Spray inoculated plants were photographed 2-4 days after infection. To maintain high humidity plants were kept in trays covered with a plastic dome, these trays were placed into a bigger plastic container containing water and wrapped with plastic wrap. These containers were placed in a PGV36 Conviron walk-in chamber and the disease symptoms were recorded between 3-11 dpi.

Genetics analysis

For crosses, pollen from the donor flower was used to pollinate the stigma of recipient flowers. Prior to pollination, the sepals, petals and stamen were removed from the recipient flowers.

To isolate homozygous double mutants, wild type and mutant alleles were identified using cleaved amplified polymorphic sequence (CAPS) (Konieczny & Ausubel, 1993)

or derived (d)-CAPS (Neff et al, 1998). For the tDNA knockout lines, PCR using tDNA border primer in combination with gene specific primers were used. PCR primer sequences are provided **(Table 2.2)**.

Bacterial transformation

Escherichia coli transformations were performed using heat shock and/or electroporation. To prepare the heat-shock competent cells, a single colony of DH5α strain (Invitrogen) was inoculated into 5 mL LB (Luria-Bertani medium) broth and the culture was incubated overnight at 37°C with constant shaking. Next morning, 50 µL inoculum from the overnight culture was transferred into 100 mL LB broth and incubated until it reached an OD 0.5 (A_{600}). The culture was then chilled on ice for 15 min, and the cells were centrifuged at 936 x g for 10 min at 4°C. The pellet was re-suspended in 50 mL ice-cold transformation buffer 1 containing 30 mM potassium acetate [CH_3CO_2K] pH 5.8, 100 mM $RbCl_2$, 10 mM $CaCl_2$ and 15% (v/v) glycerol and kept on ice for 30 min. The cells were again centrifuged at 936 x g for 10 min and the pellet was re-suspended in 5 mL of ice-cold transformation buffer 2 (10 mM MOPS pH 6.5, 75 mM $CaCl_2$ 10 mM $RbCl_2$, 15% v/v glycerol). The competent cells were aliquoted and stored at -80°C until further use.

For transformation, ~50-100 ng of DNA was mixed with 100 µL of competent cells, incubated on ice for 30 min, the tubes were transferred to 42°C water bath for 90 seconds and immediately chilled on ice for 5 min. The cells were then mixed with 1 mL of LB broth and incubated at 37°C in a shaker at 240 rpm for 60 min. The transformed cells were plated on LB agar containing appropriate antibiotics.

For electroporation competent cells, a single colony of *E. coli* DH5α or *Agrobacterium tumefaciens* MP90 or LBA4404 strains were cultured overnight in 5 mL LB at 37°C or 29°C, respectively. A 50µL inoculum of bacteria culture was transferred into 100 mL LB broth, grown to an OD of 0.5 (A_{600}) and chilled on ice for 15 min. The cells were

centrifuged at 936 x g for 10 min at 4°C, and the pellet was suspended in ice-cold solution of 8.0% (v/v) glycerol. Following 15 min incubation on ice, 20 µL of these cells were aliquoted into 1.5 mL microfuge tubes and stored at -80°C until further use.

For electro-transformation ~50-100 ng of plasmid DNA was added to 20 µL competent cells and this mixture were placed in a pre-chilled cuvette and electroporated using 25 µF capacitance, 200 Ω resistance and 2 volt pulse. After the electro-shock, the cells were mixed with 800 µL of LB broth and incubated at 37°C (*E. coli* strain, 1 h) or 29°C (*A. tumefaciens* strains, 2 h) with constant shaking (240 rpm). After incubation the transformed cells were plated on LB-agar plates containing appropriate antibiotic and incubated at 37°C (*E. coli*, overnight) or 29°C (*A. tumefaciens*, 2 days).

Sequencing

For sequencing, 50-100 ng of PCR- or purified plasmid DNA (Qiagen, CA-USA) were used. The reactions were performed using 1 µL of 5 µM primer, 2 µL of reaction buffer and 0.5 µL of BigDye Terminator V3.1 (Applied Biosystems, CA-USA), the volume was made up to 10 µL. The reactions product were precipitated, washed with 70% (v/v) ethanol and air-dried and sequenced at the Advanced Genetic Technologies Center (AGTC) facility at University of Kentucky.

Arabidopsis transformation

Arabidopsis was transformed with *A. tumefaciens* containing the binary plasmid of interest. The Agrobacterium culture was streaked on a LB plate containing appropriate antibiotic and incubated at 29°C for two days. From this plate, a single colony was cultured overnight in 5 mL LB at 29°C with constant shaking (240 rpm). This overnight culture was inoculated into 500 mL LB and cultured overnight at 29°C with constant shaking (240 rpm). The culture was centrifuged for 10 min at 3,743 x g

to pellet the cells. The pellet was re-suspended in transformation buffer (1 L contained 2.15 g of 1/2X Murashige and Skoog [MS] basal salt mixture, 30 g of sucrose (3% w/v), 0.5 mL of Silwet L77, and the solution pH was adjusted to 5.7 with 1 M KOH). The transformation buffer was distributed into square containers and plants were dipped (pot upside-down) into the transformation buffer for 20-30 seconds. Plants were kept under a dome overnight, rinsed gently under tap water and allowed to set seeds. The seeds from transformed plants were collected after ~4-6 weeks, surface-sterilized with 70% (v/v) ethanol for 1 min, washed with 5% (v/v) bleach for ~20-30 min in a rotary shaker (240 rpm) and washed 4-5 times with sterile water. The transgenic seeds were plated on solid 1/2X Murashige and Skoog media (MS) medium, 1% (w/v) agarose, containing appropriate antibiotic.

Plant treatments

For SAR assays, plants were treated with varying volumes of G3P (100 μM; Sigma-Aldrich, MO, USA), SA (500 μM; Hydroxybenzoic acid, Sigma-Aldrich, MO, USA), or H_2O_2 (500 μM; Sigma-Aldrich, MO, USA). The stocks of all these chemicals were prepared in water and aliquots frozen to be thawed just before use. Azelaic acid (1 mM; Sigma-Aldrich, MO, USA) stock was prepared in 0.01% (v/v) methanol and diluted in water prior to leaf infiltrations.

Trypan-blue staining

The leaves were placed in a six-well plate and overlaid with trypan-blue stain until they were fully immersed in the stain. Trypan-blue stain was prepared by mixing 10 mL of acidic phenol, 10 mL of glycerol, 20 mL of sterile water and 10 mg of trypan blue. The leaves were placed under vacuum until the samples were completely infiltrated with the dye. The plate was incubated for 2 min in a boiling water bath and then left at room temperature for 2-12 h. The leaves were de-stained with chloral hydrate (25 g/10 mL sterile water; Sigma, St. Louis, MO-USA) and mounted in

glycerol. Microscopic images were captured using AxioCam camera (Zeiss, Germany) and analyzed using Openlab 3.5.2 (Improvision) software.

DNA extraction

For small scale DNA extraction, leaves were frozen in liquid nitrogen, ground with a disposable pestle (Fisher Scientific, PA, USA) and suspended in 150 µL of DNA extraction buffer containing 200 mM Tris-HCl pH 8.0, 25 mM EDTA, 1% (w/v) SDS and 250 mM NaCl. The homogenate was extracted with 75 µL of phenol: chloroform: isoamyl alcohol (25:24:1) and centrifuged at 12,850 x g for 10 min to separate phases. The upper phase was transferred to a fresh microfuge tube, precipitated with 100 µL of isopropanol, mixed by inversion and centrifuged to collect DNA pellet (12,850 x g for 10 min). The pellet was air dried and re-suspended in 50-80 µL Tris:EDTA (10:1, pH 8.0) or sterile water.

RNA extraction and northern analysis

For RNA extraction ~100 mg of Arabidopsis leaves were frozen in liquid nitrogen, ground using a disposable pestle and homogenized in 1 mL trizol reagent (Invitrogen, CA, USA). For phase separation, 200 µL of chloroform was added to the trizol followed by vigorous mixing and centrifugation at 13,523 x g for 12 min. The RNA present in the supernatant was precipitated with 500 µL of isopropanol, washed with 1 mL of 75% (v/v) ethanol, air-dried and suspended in 20-30 µL of DEPC-treated water. The RNA samples were fractionated on a 1.5% (w/v) agarose gel containing 3% (v/v) formaldehyde and 1X MOPS (4.18 g MOPS, 680 mg NaOAc, 37 mg EDTA in 1 L sterile water, pH 7.0). The RNA was quantified using spectrophotometer (A_{260}). Approximately seven µg total RNA mixed with 12-14 µL of loading buffer (39 µg/mL ethidium bromide, 0.39 X MOPS, 13.7% (v/v) formaldehyde and 39% (v/v) formamide) and 2 µL of loading dye (50% (v/v) glycerol, 1mM EDTA, 0.4% (w/v) bromophenol blue and 0.4% (w/v) xylene cyanol) were loaded into the RNA gel. For Northern hydridization the RNA gel was washed with 2xSSC (1 X SSC is: Meniatus et

al. 2003) and blotted onto Hybond TMNX (Amersham Biosciences, NJ, USA) nylon membrane. After overnight wet-transfer in 20X SSC (3 M NaCl and 0.3 M Na citrate), RNA was cross-linked to the nylon membrane under ultraviolet (UV) light for 0.9 min in a CL-1000 ultraviolet Cross-linker (Khandjian, 1986). The membrane was dried at 65°C oven for 20 min. Prior to hybridization, the membrane was washed with 2xSSC for 15 min and dried at 65°C. Hybridization was carried out in sodium phosphate buffer (200 mM, pH 7.0) containing sheared salmon sperm DNA (100 μg/mL), 7% (w/v) SDS and 1.25 mM EDTA.

DNA labeling and hybridization

The DNA fragment used for labeling was either a PCR amplicon or derived from a plasmid after restriction digestion (Qiagen, MD-USA). The DNA fragment was boiled for 10 min in water bath for denatured. The labeling reaction, assembled on ice, contained 1 μL of DNA polymerase I Klenow enzyme (NEB, 2,000U/mL), hexanucleotide primers, dATP, dGTP, dTTP, BSA and 25 μCi α-^{32}P-dCTP (Perkin Elmer, USA). The reaction was incubated at 37°C for 2 h, chromatographed on a G-50 Sephadex spin column which was centrifuged at 587 x g for 3 min to elute the incorporated fraction. The probe was denatured with 2N NaOH (1/10 vol), neutralized with 1M Tris pH 7.5 (1/10 vol). Before adding the probe to the hybridization bottle, the membranes were pre-hybridized for 30 min in hybridization oven at 65°C. To the same bottle, the probe was added and incubated overnight. The membrane was washed twice with 2xSSC, 0.5% (w/v) SDS for 30 min each (at 65°C) and once with 1xSSC, 0.1% (w/v) SDS for 20 min (at 65°C). The membrane was wrapped and exposed on a Storage Phosphor Screen (Amersham Biosciences, CA USA) and scanned on a Typhoon 9400 Variable Mode Imager (GE Healthcare, NJ-USA). The signal intensity was quantified using ImageQuant TL V2005 software.

Synthesis of cDNA

RNA used for cDNA synthesis was analyzed by gel electrophoresis to verify its quality. Approximately 7 µg to total RNA was mixed with oligo dT primer (0.5 µg) in a 10 µL volume, denatured at 65°C for 10 min, chilled on ice for 2 min, mixed with 1 µL Superscript reverse transcriptase (200 U/µL), 1 µL RNase inhibitor (40 U/µL), 2 µL 10 mM dNTP mixture, 4 µL 2X Superscript buffer and 2 µL of 10 mM DTT. The reaction was incubated at 42°C for 1 h and denatured at 65°C for 15 min prior to PCR.

Fatty acid analysis

Quantification of fatty acid (FA) levels were carried out using 100 mg of plant tissues. Into disposable glass tubes, 2 mL of 3% (v/v) H_2SO_4 in methanol containing 0.001% (w/v) butylated hydroxytoluene (BHT) were dispensed followed by the addition of samples tissues as well as 10 µg of 17:0 FA used as internal standard. The tubes were incubated in water bath at 80°C until ¾ of the volume was left and 1 mL of hexane with 0.001% (w/v) BHT was added. The tubes were vortexed and the samples and the supernatant containing FA was transferred to gas chromatography (GC) vials. For detection, one microliter of the samples were injected into the GC on a Varian FAME 0.25 mm x 50 m column and quantified with flame ionization detection. The relative FA levels were calculated based on flame ionization detector peak areas. The FA identification was determined by comparing the retention time of the peaks with known FA standards. The peak area given in the GC was divided by the FA molecular weights, for the Mole value calculation.

Extraction and quantification of azelaic acid (AzA)

For azelaic acid estimations, 150 mg of leaf tissues previously infected with *Pst* avrRpt2 (at 10^6 after 24h) or 10mM $MgCl_2$ (as mock control) were collected into microcentrifuge tubes and frozen in liquid nitrogen. The frozen tissues were transferred to test tubes (13 mm x 100 mm), ground and homogenized with 1 mL of

chloroform:methanol (2:1). As internal standard, 5 µg of sebacic acid (Sigma-Aldrich, MO, USA) was used (with stock of 100 ng/µL use 50 µL). To this mixture 200 µL of glacial acetic acid and 1 mL of 0.9% (w/v) KCl was added, vigorously vortexed and centrifuged (2.5 x g) using a tabletop swing arm centrifuge (Beckman) for 1 min. The lower phase was transferred to another test tube; 1 mL of chloroform was added to the original test tube, vigorous vortexed and centrifuged (as above). The lower phase of the original tube was combined with the lower phase of the other test tube and completely dried under nitrogen gas stream. For sample methylation, 500 µL of sodium methoxide (4.8% w/v suspended in methanol) was added and samples were maintained shaking at 150 rpm for 45 min at room temperature. Following the incubation time, 200 µL of glacial acetic acid, 1 mL of 0.9 (w/v) KCl and 1 mL of chloroform were added, the mixture was vortexed and centrifuge (as above). The lower phase was transferred to another tube and the extraction process repeated one more time by adding 1 mL of chloroform, vortexing and centrifugation (as above). The combined extract was evaporated under a stream of nitrogen gas and methylated using 10 drops of diazomethane, which was evaporated using stream of nitrogen gas and stopped immediately after complete evaporation. The samples were re-suspended in 150 µL of isooctane, vortexed and transferred to GC glass vials containing glass inserts. For the gas chromatograph analysis a Varian FAME 0.25 mm × 50 m column equipped with mass spectrometry were used and 1 µL samples were injected into the GC-MS. The azelaic acid peaks were identified using mass spectrometry.

Extraction and quantification of glycerol-3-phosphate (G3P)

To assay G3P levels, 100 mg of plant tissue inoculated with *Pst* avrRpt2 (at 10^6 after 24h) or 10 mM $MgCl_2$ (as control) were collected and frozen into liquid nitrogen. The samples were ground using pestle and homogenized with ethanol containing 20% (v/v) phosphatase inhibitor (100x stock solution prepared in water: 1mM sodium phosphate, 6.25 mM sodium orthophosphate, 1mM beta glycophosphate, pryrophosphate). Immediately after crushing, 10 µg of suberic acid (TCI America,

Portland, OR) was added as an internal standard. The tubes were capped with plastic clamps, boiled in a water bath for 5 min and cooled in ice. The mixture was vortexed and centrifuged at 15871 x g for 10 min. The upper phase was transferred to GC glass vials, dried completely under a nitrogen gas steam. For the reaction, 50 µL of acetonitrile (dehydrated using 3A zeolite ceramic pellets as a molecular sieve) and 50 µL of N-Methyl-N-(trimethylsilyl)trifluoroacetamide (MSTFA) were added to the GC vial, vortexed and incubated at 65°C for 1 h. For the detection, one microliter of the samples was injected into a Varian FAME 0.25 mm x 50 m GC column and quantified with flame ionization detection. The relative G3P levels were calculated based on flame ionization detector peak areas. The G3P identification was determined by comparing the retention time of the peaks with known G3P standard. The peak area given in the GC was divided by the G3P molecular weights, for the Mole values calculation.

Collection of petiole exudate

Leaves for petiole exudate collection were harvested 12h after inoculation with *P. syringae* pv. *tomato* containing avrRpt2 at a concentration of 10^6 or mock-treated with 10 mM of $MgCl_2$. The leaves were rinsed in 50% (v/v) ethanol, 1mM EDTA solution (pH 8, in water) and a second time in 1mM EDTA. To collect exudates a solution containing 1mM EDTA pH 8 and 100 µg/mL of ampicillin were prepared (in water) and aliquot into microcentrifuge tubes. Approximately 15 leaves were placed petioles down and in contact with the collection solution in opened lid microcentrifuge tubes. The tubes were kept under glass dome and placed inside of the plant growth chamber. The plant exudates were collected during 2 days, freeze-dried, re-suspended in 500 µL of water and filtered using a 0.45 µm microcentrifuge filter (Spin-X centrifuge tube filter, Costar, 0.45 µm nylon, 2 mL tube, CN: 8170). The protein concentration was estimated using the Bradford assay (Bradford, 1976).

Quantification of G3P in petiole exudate

Approximately 200 µL of exudate was transferred to High-performance liquid chromatography (HPLC) vials containing glass inserts and 25 µL was injected onto a High performance anion exchange chromatograph (ICS 3000; Dionex Inc., Palo Alto, CA, USA) for analysis (Downie, 1994). A PA1 column was used with pulsed electrochemical detection (ED40 Pulsed Electrochemical detector, Dionex Inc., Palo Alto, CA, USA). Eluents included; A: water; B: 200 mM NaOH; C: 200 mM NaOH and 500 mM NaOAc; the flow rate was 1 mL/min. The conditions for operation was: isocratic initial conditions for 0-12 min: %B=80; %C=20, a 10 minute gradient from 12.1 min from initial conditions to %B=0; %C=100 at 22 min; back to initial conditions at 22.1 min: %B=80; %C=20 and column re-equilibration from 22.1-32 min prior to injection of the next sample.

Quantification of AzA, SA and G3P in petiole exudate

The reaction was performed in GC vials where 10 µg of exudates as well as 100 ng of internal standards (SA: anisic acid; AzA: fatty acid 17:0; G3P: suberic acid) were added. After completely drying the mixture under nitrogen gas steam, 500 µL of acetone was added, vortexed and dried. For AzA and SA derivatization, 90 µL of acetonitrile (dried with molecular sieve) and 90 µL of *N*-*tert*-Butyldimethylsilyl-*N*-methyltrifluoroacetamide (MTBSTFA), was added to the vials, vortexed and incubated in 110°C oven for 2h. For G3P derivatization, 50 µL of acetonitrile (dried with molecular sieve) and 50 µL of MSTFA was used, vortexed and incubated in 65°C oven for 1 h.

For the detection, one microliter of the sample was injected into GC on a Varian FAME 0.25 mm x 50 m column and quantified with flame ionization detection. The relative metabolite levels were calculated based on flame ionization detector peak areas. The metabolite identification was determined by comparing the retention time of the peaks with known metabolite standard.

Hydrogen peroxide (H_2O_2) Quantification (DAB staining)

Plant leaves were used for H_2O_2 quantifications. The plants were previously inoculated with avrRpt2 at a concentration of $5x10^5$ CFU or mock-treated with 10 mM of $MgCl_2$. The time point for sample collection was 24 h after inoculation and collected leaves were placed in 6-well plates. To the leaves were added 2 mL DAB (3,3'-diaminobenzidine) staining solution (200 mM of Na_2HPO_4, 25 µL of Tween 20, 1 mg/mL of DAB dissolved into water and the pH adjusted to 3.0 using 0.2 M HCl). The plates were covered with aluminum foil and a gentle vacuum was applied for 5 min to the samples. The plates were incubated at room temperature for 8 h shaking at 150 rpm in an orbital shaker (Varion Inc., model T, New Jersy, USA). De-stained containing ethanol:acetic acid:glycerol (3:1:1) was added to the leaves and the plates were boiled in a water bath for 15 min. The leaf samples were scanned using a white background. Samples were mounted on microscope slides using glycerol.

***Escherichia coli* complementation assay**

Each G3Pp protein isoforms were amplified from plant cDNA using high fidelity enzyme (Platinum Taq DNA Polymerase –Invitrogen, Thermo Fisher scientific USA). The amplicon was cloned into pET vectors. G3Pp isoforms 1 and 3 were cloned into pET21d and isoforms 2 and 5 cloned into pET21a. The constructs were transformed in ΔG3Pp (strain JW22-34) (Baba et al, 2006) as well as Rosetta (Invitrogen, Thermo Fisher scientific USA) competent cells.

For protein induction, a single colony was inoculated into 10 mL SOC media (Super Optimal Broth with Catabolite repression: 2% w/v tryptone, 0.5% w/v Yeast extract, 8.56 mM NaCl or 10 mM NaCl, 2.5 mM KCl, 20 mM glucose, 10 mM $MgCl_2$ and 10 mM $MgSO_4$) (or LB) and grown overnight (o/n). Fresh SOC media was inoculated with the o/n culture (dilution of 100 fold), which grew until reach OD of 0.6-0.8. The culture was cooled on ice for 15 min and 1 mM of IPTG was added for the induction. The conditions used were: 37°C for 4h and/or 16°C (o/n).

For the complementation assay, the pET21 constructs containing G3Pp isoforms previously transformed into ΔG3Pp were used and *E. coli* mutant strain containing empty vector (pET21a and pET21d) was included as control. The antibiotic fosfomycin, known to be uptake by *E. coli* GlpT transporter (G3P Transporter) was used for the assay. To SOC plates supplied with kanamycin (50 μg/mL), ampicillin (100 μg/mL) and fosfomycin (128 μg/mL) the constructs as well as empty vector cells were streaked. As a control, the cells were streaked in SOC plates containing kanamycin (50 μg/mL) and ampicillin (100 μg/mL) but without fosfomycin. The plates were incubated at 37°C and the bacterial growth assayed next day.

Confocal microscopy

For confocal imaging, samples were scanned on an Olympus FV1000 microscope (Olympus America, Melvile, NY). GFP was excited using 488 nm laser line. Constructs were made using pGWB (Nakagawa et al, 2007) binary vectors using Gateway technology and introduced in *Agrobacterium tumefaciens* strain LBA4404 or MP90 for agroinfiltration into *Nicotiana benthamiana* or *A. thaliana*, respectively. For transient expression, Agrobacterium strains carrying various constructs were infiltrated into wild type (WT) or transgenic *N. benthamiana* plants expressing CFP-tagged nuclear protein H2B or RFP-tagged ER. Forty-eight hours later, water-mounted sections of leaf tissue were examined by confocal microscopy. The leaf tissue of Arabidopsis transgenic lines were also water-mounted and examined by confocal microscopy.

Protein extraction and western blotting

Proteins were extracted in buffer containing 50 mM Tris-HCl, pH 7.5, 10% glycerol, 150 mM NaCl, 10 mM $MgCl_2$, 5 mM EDTA, 5 mM DTT, and 1 X protease inhibitor cocktail (Sigma-Aldrich, St. Louis, MO). Protein concentration was measured by the Bio-RAD protein assay (Bio-Rad, CA).

For Ponceau-S staining, PVDF membranes were incubated in Ponceau-S solution (40% methanol (v/v), 15% acetic acid (v/v), 0.25% Ponceau-S). The membranes were destained using deionized water.

Proteins (50-150 μg) were fractionated on a 7%–10% SDS-PAGE gel and subjected to immunoblot analysis using α-GFP antibody (Sigma-Aldrich, St. Louis, MO). Immunoblots were developed using ECL detection kit or alkaline-phosphatase-based color detection.

Table 2.1. Seed materials used in the study.

SI No.	Mutants and transgenic seeds	References
1	Columbia-0 (Col-0)	(Kachroo et al, 2003)
2	Nössen (Nö)	(Kachroo et al, 2001)
3	*gly1-1* (Col-0)	(Miquel & Cassagne, 1998)
4	*ssi2* (Nö)	(Kachroo et al, 2001)
5	*E. coli gpsA*	(Shen et al, 2010)
6	*35S-DIR-GFP*	(Lim et al, 2016)
7	*35S-AZI-Myc*	(Pitzschke et al, 2014)
8	*g3pp4-1*; SALK071338; *At4G17550* (Col-0)	(Ramaiah et al, 2011)
9	*g3pp4-2*; GK230D07-014316; *At4G17550* (Col-0)	(Ramaiah et al, 2011)
10	*g3pp2*; GK742G10-023520; *At4G25220* (Col-0)	This dissertation
11	*g3pp3*; SAIL452-B07; *At1G30560* (Col-0)	This dissertation
12	*35S-G3Pp1-GFP* (Col-0)	This dissertation
13	*35S-G3Pp2-GFP* (Col-0)	This dissertation
14	*35S-G3Pp5-GFP* (Col-0)	This dissertation
15	*35S-G3Pp2-GFP* (*g3pp2*)	This dissertation
16	*35S-G3Pp2-GFP* (*g3pp3*)	This dissertation
17	*35S-G3Pp2-GFP* (*g3pp4-1*)	This dissertation

Table 2.2. List of primers used in this study.

Genotype	Primer name	Primer sequence
GK742 (*g3pp2*)	AT4G25220-NcoI-Fwd	CAACCATGGCGTCATGGACTTCATCC
	AT4G25220-BglII-Rev	CAAAGATCTTCAAACGAGGACATC
	LB (GABI T-DNA)	ATATTGACCATCATACTCATTGC
S071338 GK230 (*g3pp4)*	SALK-071338 RP	TGGTTCTTTAATTGCTGCTGG
	SALK-071338 LP	TCAGATCATTGTTTCTGCAATTG
	LBb1-3	ATTTTGCCGATTTCGGAAC
SAIL452 (*g3pp3*)	AT1G30560-NcoI-Fwd	CAACCATGGCGTCGTGGACTTCATCT
	AT1G30560-BamHI-Rev	CAAGGATCCTCATATGAGGACATC
	LB2-SAIL C/390-423	GCTTCCTATTATATCTTCCCAAATTAC CAATACA
gly1-1 (*BstNI*)	*tw2-1* dCAPS Fwd	AACCGATGTTCTTGAGCGTACTCGCC
	tw2-1 dCAPS Rev	CAACAACCTAAAAACCCCCAGATT C
ssi2 (*NsiI*)	*ssi2* dCAPS NsiI-Fwd	TTGGTGGGGGACATGATCACAGAAGAT GCA
	ssi2 dCAPS NsiI-Rev	AAGTAGGACTAGCACCTGTTTCATCCC TAA
GFP lines	GFP-Fwd (~350 bp)	ATGGTGAGCAAGGGCGAGGAG
	GFP-Rev (~350 bp)	ATGCGGTTCACCAGGGTGTCG
AZI-Myc	AZI1-qRT (Fwd)	TCCGGAAACAGCTGTCCTAT
	MYC-tag Rev	CAAGTCTTCCTCGGAGATTAGCTT
β-*Tubulin*	β-Tubulin Fwd	CGTGGATCACAGCAATACAGAGCC
	β-Tubulin Rev	CCTCCTGCACTTCCACTTCGTCTTC
gpsA E. coli	35S promoter Fwd	AAGTGGATTGATGTGATATC
	GPSA5 no site Rev	CCAACAATGAACCAACGTAA

CHAPTER 3

Role of G3P Permease in plant defense

Introduction

Glycerol-3-phosphate is required for basal defense against *Colletotrichum* as well as systemic acquired resistance (SAR) induced in response to avirulent *Pseudomonas syringae pv tomato* (*Pst*). The identification of G3P and its association with other SAR signals has established signaling events that orchestrate induction of SAR in plants (Chanda et al, 2011; Gao et al, 2014a; Kachroo & Robin, 2013; Kachroo & Kachroo, 2018; Lim et al, 2016; Wang et al, 2014; Wang et al, 2018; Wendehenne et al, 2014; Yu et al, 2013). These analyses have also determined movement of SAR associated chemicals from local to distal tissues. The cell-to-cell and long-distance movements of mobile signals play an important role in SAR. The long distance transport occurs via phloem (Jenns & Kuc, 1979; Tuzun & Kuć, 1985) and the cell to cell transport involves both apoplastic and symplastic routes (Lim et al, 2016). The apoplastic space includes space outside of the plasma membrane. The transport of biomolecules between the cytosol to the apoplastic space requires either exo- or endo-cytosis mediated by secretory vesicles (Toyooka & Matsuoka, 2009) or an active transport involving membrane associated transporters (Robert & Friml, 2009).

The symplastic pathway utilizes the space inside of the plasma membrane and is mediated by cytoplasmic connections between adjacent cells called plasmodesmata-PD for metabolites translocation. The symplastic route allows the passage of molecules ranging in sizes from 800-1,000 Da (Oparka, 1993). Some signals such as G3P and AzA preferably use the symplastic pathway for their movement, while SA is transported via the apoplastic route (Lim et al, 2016). Although G3P uses the symplastic pathway, a large amount of G3P can also be detected in the apoplastic space (Lim et al, 2016). Since G3P cannot readily diffuse across cell membranes, it is likely that G3P transport into the apoplast is mediated via transporters. Likewise, transport of G3P across various subcellular compartments might also involve transporters.

The Arabidopsis genome encodes five isoforms of a transmembrane protein G3P Permease (G3Pp) that shows homology to the *Escherichia coli* G3P Transporter (GlpT) (Ramaiah et al, 2011). The GlpT transporter is driven by a Pi electrochemical gradient and mediates an antiport type of exchange between G3P and inorganic phosphate (Pi) across the cytoplasmic membrane (Huang et al, 2003). GlpT belongs to the major facilitator superfamily (MFS), which is composed of 400 to 600 amino acid long proteins. These proteins contain 12 transmembrane α helices surrounding a central pore, with two cytosolic loops, one at the N-terminus and one situated between the 6th and 7th transmembrane domains (TMDs), with both the N- and C-termini located in the cytosol (Hirai et al, 2003; Hirai et al, 2002; Maiden et al, 1987; Pao et al, 1998) **(Figure 3.1A)**. Metabolite exchange occurs by alternations in protein conformation to be inward facing (Ci) or outward facing (Co) relative to the cytosolic space. During this process a single binding site in a central cavity is available only on one side of the membrane. Once inside the pore, interconversion between the two conformations (antiporter) releases the metabolite to the other side of the membrane **(Figure 3.1B)** (Kaback & Wu, 1997; West, 1997).

G3P Permeases also meditate intracellular transport of glycerol-2-phosphate, arsenate and the antibiotics fosfomycin and fosmidomycin (Elvin et al, 1985; Ramaiah et al, 2011). Fosfomycin and fosmidomycin are antibiotics produced by several species of *Streptomyces* genus. Fosfomycin inhibits bacteria cell wall synthesis and is used to treat urinary tract infections (Blazquez & Alexandro, 2013; Venkateswaran & Wu, 1972). Fosmidomycin is an antimalarial drug affecting a key enzyme in the non-mevalonate pathway of isoprenoid biosynthesis in the malaria parasite, *Plasmodium falciparum* (Jomaa et al, 1999). Arsenate is taken up by phosphate transport systems because of its molecule resemblance to phosphate. This chemical is commonly present in the environment and is used in anticancer and antiprotozoan therapies (Yang et al, 2012).

A complex cross-talk across different nutrient signaling pathways has been suggested to regulate Arabidopsis *G3Pp* genes. Seedlings grown on rich media lacking nitrogen-N, potassium-K, and iron-Fe, showed differences in the relative expression levels of *G3Pp* isoforms (Ramaiah et al, 2011). The *G3Pp1-G3Pp4* genes are up regulated in response to phosphate starvation, suggesting that the proteins they encode may play a role in phosphate homeostasis (Ramaiah et al, 2011). The G3Pp was also suggested to play a role in seedling development (Ramaiah et al, 2011). The G3Pp4 isoform is localized in the chloroplast and has been shown to transport G3P in an *E. coli* heterologous system (Kawai et al, 2014). The G3Pp4 protein has also been suggested to participate in the accumulation of storage lipids during late embryo development (Kawai et al, 2014). However, the *in planta* function of G3Pp proteins in relation to G3P transport and their defense related functions (if any) remain unknown. The main goal of the present work was to characterize G3Pp protein isoforms in relation to SAR and G3P transport. We hypothesize that G3Pps are required for metabolite translocation during SAR induction.

Results and discussion

Characterization of G3P Permeases

Analysis of G3Pp isoforms

The nomenclature of the Arabidopsis *G3Pp* genes used in this study, mutant allele characterized in this study, the predicted protein length and molecular weights are listed in **Table 3.1A**. Except for *G3Pp3*, all other *G3Pp* genes contained a ~100 bp intron which did not show any homology to each other. The human *G3Pp*, which shows 43% and 30% homology to Arabidopsis permease gene (Takahashi et al, 2000) and *E. coli GlpT* (Eiglmeier et al, 1987), respectively, contains 19 coding exons and 7 untranslated exons that are generated via alternate splicing (Bartoloni et al, 2000). Similarly, Arabidopsis *G3Pp1* and *G3Pp5* genes were shown to have two and three splice variants, respectively. The function of these alternate splice forms remains unknown.

ClustalW alignment of full-length protein sequences was used to determine the phylogenetic relationship among G3Pp isoforms. Because the GlpT from *E. coli* is homologous to G3Pp, though less closely related than the Arabidopsis isoforms themselves, its protein sequence (http://www.uniprot.org/uniprot/P08194) was used in the phylogenetic analysis as an outgroup. An outgroup in the phylogenetic analysis enables the root of the tree to be located in the correct evolutionary pathway (Williams, 2014). The G3Pp2 and G3Pp3 proteins showed high identity (83%) and were grouped together in the same clade. The remaining G3Pp proteins showed 53-63% relatedness and were positioned in different branches of the phylogenetic tree **(Figure 3.2)**. The subcellular localization of G3Pp were determined based on computational predictions using ChloroP, MitoProII, SecretomP, TargetP and SignalP programs (Meinken & Min, 2012). All the programs suggested plasma membrane localization for the isoforms G3Pp1, G3Pp2 and G3Pp3 **(Table 3.2)**. ChloroP predicted the isoforms G3Pp4 and G3Pp5 to localize to the chloroplast. However,

MitoProtII and TargetP predicted mitochondrial localization for G3Pp4 **(Table 3.2).** The ChloroP prediction for G3Pp4 is consistent with transient and stable expression of G3Pp4-yellow fluorescence protein (YFP) which localizes to chloroplast (Kawai et al, 2014). To examine the subcellular localization of G3Pp isoforms, *35S-G3Pp1-GFP*, *35S-G3Pp2-GFP* and *35S-G3Pp5-GFP* constructs were generated in the pGWB5 vector where these genes were expressed under the control of the 35S promoter. In spite of repeated efforts, *G3Pp3* and *G3Pp4* could not be cloned into the pGWB5 vector. It was possible that the leaky expression of *35S-G3Pp4* and *35S-G3Pp5* genes in *E. coli* was causing lethality. To address this issue, generation of native promoter (NP) based constructs for *NP-G3Pp3-GFP* and *NP-G3Pp4-GFP* isoforms in the pGWB4 vector were attempted. The promoter length used for these constructs was based on their ability to drive expression of the GUS reporter gene (Ramaiah et al, 2011). In spite of repeated attempts I was unable to generate G3Pp4::*NP-G3Pp4-GFP* construct. However, I was able to construct the G3Pp3::*NP-G3Pp3-GFP* clone. All the constructs were transformed into *Agrobacterium tumefaciens* strain LBA4404 and transiently expressed in *Nicotiana benthamiana*. For the transient expression experiments, *35S-AGD2- Like Defense Response Protein1* (*ALD1-GFP*) construct was included as positive control. ALD1 encodes an aminotransferase that converts lysine to Pip (Wang et al, 2018). Except ALD1-GFP, none of the constructs showed any detectable fluorescence in the transient assays (data not shown). Notably, earlier studies have also indicted difficulties associated with cloning and/or expression of *G3Pp* genes (Elashvili et al, 1998; Frohlich et al, 2010; Gubellini et al, 2011; Kawai et al, 2014). To test if these constructs would express better in the native plant system, Arabidopsis transgenic lines overexpressing *35S-G3Pp1-GFP*, *35S-G3Pp2-GFP* and *35S-G3Pp5-GFP* transgenes were generated. Transgenic plants were assayed for transcript levels and plants showing high, moderate or low expression of the transgene were **(Figure 3.3A-F)** analyzed by protein gel blots and under a confocal microscope. Western analysis detected very low levels of protein in transgenic lines expressing *35S-G3Pp1-GFP* and *35S-G3Pp2-GFP* **(Figure 3.4A-B)**.

G3Pp1 and G3Pp3 proteins function as membrane transporters

The G3P transporter (GlpT) in *E. coli* functions in rocker-switch model (Huang et al, 2003). Since the Arabidopsis G3Pp shows homology to GlpT, it was possible that G3Pp function similarly to GlpT. To test this we assayed complementation of *E. coli glpt* mutant with Arabidopsis G3Pp protein isoforms. The *E. coli* strain *glpt* obtained from the *E. coli* database shows resistance to the antibiotic fosfomycin; therefore, this antibiotic was used in the complementation assays. Uptake of fosfomycin in *E. coli* is mediated via GlpT and UhpT (Hexose phosphate Transporter) and inactivation in either of these transporters confers resistance to fosfomycin (Blazquez & Alexandro, 2013; Castaneda-García et al, 2009). Fosfomycin acts by binding to MurA enzyme and blocking the initial steps of the cell wall biosynthesis in *E. coli* **(Figure 3.5A-B)**. For complementation assays, *G3Pp* amplified from plant cDNAs were cloned into pET21 vectors and transformed into *glpt E. coli* mutant strain. In spite of repeated attempts *G3Pp4* gene could not be cloned. Also, for reasons unclear at present, the cDNA sequences amplified for *G3Pp2* and *G3Pp5* genes always contained their respective introns. The presence of this intron is predicted to result in a premature stop codon and a truncated protein (~36-38 kDa). Thus, only G3Pp1 and G3Pp3 provided conclusive results with regards to their ability to complement *glpt* mutation. Consistent with their predicted biological function, both G3Pp1 and G3Pp3 were able to complement the *glpt E. coli* mutant strain defect. Unlike the *glpt* mutant transformed with pET21d empty vector, the G3Pp1 and G3Pp3 expressed in *glpt* mutant background showed sensitivity to fosfomycin (**Figure 3.6)**. These results suggest that both G3Pp1 and G3Pp3 proteins function as membrane transporters.

Role of G3Pp in plant defense

Next, the expression profiles from *G3Pp* genes in Arabidopsis plants subjected to various abiotic and biotic stresses were obtained by mining through available microarray datasets (http://www.expressionbrowser.com) (Zhang et al, 2010). This analysis showed that different *P. syringae* strains induced the expression of *G3Pp1* gene; *G3Pp1* gene was induced ~42-fold after *P. syringae* pv. *maculicola* infection and ~4-fold in plants inoculated with avirulent bacteria expressing *avrRpt2*, *avrRpm1* or *avrB*. The *G3Pp1* gene was also induced in response to Xanthomonas, *Botrytis cinerea* and *Blumeria graminis* f. sp. *hordei* **(Table 3.1B)**. Likewise, *G3Pp4* and *G3Pp5* genes were also induced in response to pathogen infection but *G3Pp2* and *G3Pp3* showed basal level expression in pathogen inoculated plants. The *G3Pp* genes were induced by at least one of the abiotic stress treatments including nutrient starvation, cold, heat, abscisic acid, drought or osmotic stresses **(Table 3.1B)**. Together, the expression data suggests that *G3Pp* genes might play a role in biotic and/or abiotic stress responses.

To assay a role for G3Pp in plant defense, putative T-DNA knockout (KO) lines were obtained from the Arabidopsis database. The mutants were screened to isolate homozygous T-DNA insertion lines in both the copies of the gene **(Table 3.3)**. The homozygous KO lines were assayed for *G3Pp* transcript level by semi-quantitative reverse transcription polymerase chain reaction (RT-PCR). This analysis was able to identify KO mutants in *G3Pp2* (GK742G10-023520), *G3Pp3* (SAIL452-B07) and *G3Pp4* (SALK071338 and GK230D07-014316) but not in *G3Pp1* or *G3Pp5* **(Figure 3.7A-B)**. The KO lines were derived from Col-0 (*g3pp2* and *g3pp4*) or Col-3 (*g3pp3*) backgrounds and were compared to their respective wild-type parents. The KO plants showed wild-type-like growth phenotypes and leaf morphology **(Figure 3.8A)**. The *g3pp* plants showed a wild-type-like fatty acid profile (**Figure 3.9A-B)**, suggesting that these plants are not affected in the G3P pool that is utilized for lipid biosynthesis.

To determine if the absence of G3Pp2, G3Pp 3, and G3Pp 4 proteins rendered plants defective in defense, the local responses to virulent bacterial pathogen and to a hemibiotrophic pathogen *Colletotrichum higginsianum* were assayed. The KO plants showed wild type-like (*g3pp3* and *g3pp4*) or better resistance (*g3pp2*) to bacterial pathogens **(Figure 3.10C-D)**. Notably, the *g3pp2* and *g3pp4* KO plants showed reduced pathogen induced cell death, which was monitored by assaying ion leakage, or visualized by staining with trypan blue. In contrast, the *g3pp3* KO plants showed increased cell death **(Figure 3.11A-B)**. Clearly, a nominal change in the cell death phenotype had no effect on the local resistance to bacterial pathogens. Likewise, the KO plants showed wild type-like resistance to *C. higginsianum* **(Figure 3.10A-B)**.

Next, I evaluated SAR in *g3pp* mutants. Wild type (WT) plants as well as *g3pp* mutants were first inoculated with buffer (mock) or *Pst* avrRpt2 and two days later the distal leaves were challenged with *Pst* DC3000 virulent strain. Three days after virulent inoculation, the distal leaves were sampled, homogenized and appropriate dilutions of homogenates plated on King's B medium to quantify the bacterial growth. As expected, both Col-0 and Col-3 plants showed normal SAR; plants inoculated locally with *Pst* avrRpt2 showed ~7-10-fold less growth of the virulent bacteria compared to mock-inoculated plants **(Figure 3.12A-C)**. Interestingly, unlike WT, the *g3pp2*, *g3pp3* and *g3pp4* plants all showed compromised SAR **(Figure 3.12A-C)**, suggesting that these genes were specifically required for systemic immunity. Two independent KO lines were analyzed for *g3pp4* and both showed compromised SAR. However, only one KO line was available for *g3pp2* and *g3pp3*. To confirm that compromised SAR in *g3pp2* and *g3pp3* was not due to a second site mutation, the WT copy of *g3pp2* gene was overexpressed in its mutant background and SAR assayed in the T2 generation of plants. The *GFP* transcript levels in the transgenic lines used for these analyses are shown in the **Figure 3.13A**. Two independent lines were used and both showed normal SAR **(Figure 3.13B)**. Together, these results suggest that compromised SAR seen in *g3pp2* and *g3pp4* KO plants is due to loss-of-function mutation in these genes. With regards to the isoform 3, *g3pp3*, the complementation assay for SAR defective phenotype was not performed yet. For this analysis, native promoter based line was

generated in mutant background and T2 seeds were collected for further evaluation. Overexpression of *35S-G3Pp1-GFP* and *35S-G3Pp2-GFP* genes did not affect basal defense against *Pst* DC3000 **(Figure 3.14C)**.

A possible explanation for the compromised SAR response in *g3pp* plants is that a mutation in *G3Pp* alters G3P levels and/or its compartmentalization. The G3Pps are transmembrane proteins, which might mediate the movement of G3P across different sub-cellular compartments. The plastidal localization of G3Pp4 (Kawai et al, 2014) prompted me to investigate the levels of G3P in different compartments of *g3pp* before and after pathogen infection. In spite of many attempts, G3P levels could not be detected in the chloroplast fraction by either HPLC or gas chromatography-mass spectrometry (GC-MS). This was surprising considering an important role of chloroplastic G3P in lipid biosynthesis. In contrast to G3P, most common neutral sugars were detected in the chloroplast fraction. It is possible that cellular fractionation could result in escape of G3P from the plastids. As an alternate, I used mutants altered in G3P levels to determine if G3Pp regulates SAR by modulating G3P flux. In these assays, defense and morphological phenotypes of *g3pp* were analyzed in *gly1* and *ssi2* mutant backgrounds. The *gly1* plants have a point mutation in one of the chloroplastic isoform of G3P Dehydrogenase (G3Pdh) enzyme, which impairs the prokaryotic pathway of lipid biosynthesis resulting in reduced accumulation of hexadecatrienoic acid (16:3) acid. The *gly1* plants contain reduced levels of G3P, which in turn is associated with compromised local resistance, and a defective SAR (Chanda et al, 2008; Kachroo et al, 2004; Miquel & Cassagne, 1998). *ssi2* plants contain a loss-of-function mutation in Stearoyl Acyl Carrier Protein Desaturase (S-ACP-DES), which converts 18:0-ACP to 18:1-ACP. Consequently, the *ssi2* plants accumulate reduced levels of oleic acid. The *ssi2* plants are dwarf, develop constitutive cell death, exhibit enhanced disease resistance to pathogens and constitutively express defense genes including *Pathogenesis-Related Protein 1 (PR-1)* (Kachroo et al, 2003; Kachroo et al, 2001; Shah et al, 2001; Shah et al, 1997). Interestingly, the *gly1* mutation restores *ssi2*-triggered phenotypes, suggesting that a

balance between G3P and 18:1 is critical for the regulation of defense pathways (Kachroo et al, 2004).

The *gly1* and *ssi2* mutants were crossed with *g3pp* KO lines and the double mutants obtained from these crosses were analyzed for defense and morphological phenotypes. The *g3pp gly1* homozygous double mutant plants showed *gly1*-like slightly narrow leaves and flowered early like *gly1* plants. Furthermore, like *gly1*, the *g3pp gly1* plants showed reduced 16:3 levels **(Figure 3.14A-C)**. Interestingly, the *g3pp3 gly1* and *g3pp4 gly1* plants showed better basal resistance to *Pst* DC3000 **(Figure 3.15A)** and *g3pp2 gly1* showed wild-type-like response to *C. higginsianum* **(Figure 3.15B-C)**.

In contrast to the defense related phenotypes observed in *g3pp gly1* plants, the *g3pp ssi2* double mutant plants showed *ssi2*-like morphological phenotypes **(Figure 3.8B)**. Consistent with their morphology the *g3pp ssi2* showed *ssi2*-like levels of 18:0 (higher than wild-type) 18:1 (lower than wild-type), *PR-1* gene expression and constitutive cell death phenotype **(Figure 3.16A-D)**.

Exogenous G3P restores defective SAR in *g3pp* mutants

SAR is induced in response to either G3P or SA treatments and these chemical signals induce distinct branches of the SAR pathway (Gao et al, 2014b; Wang et al, 2014). To determine if the SAR defective phenotype in *g3pp* mutants was associated with SA- and/or the G3P-branch of the pathway, SAR in *g3pp* mutants was assayed after treatments with SA and G3P. Since, H_2O_2 and AzA function upstream of G3P, these chemicals were also used to assay SAR in the *g3pp* mutants. For chemically induced SAR, the local leaves of WT and mutant plants were treated with the water or chemical and 24 h post inoculation distal leaves were inoculated with *Pst* DC3000. Exogenous SA induced robust SAR on wild-type plants but not on *g3pp* mutants **(Figure 3.17A-B)**. Inability of *g3pp* plants to respond to SA was not due to their insensitivity to SA since pathogen inoculation induced wild-type-like levels of the SA marker gene *PR-1* in all *g3pp* genotypes **(Figure 3.17C)**. To test if defective SAR was

associated with impaired transport of SA, petiole exudates (PEX) were collected from the WT and *g3pp* mutants 12 h after pathogen infection. SA levels in PEX collected from pathogen-inoculated leaves were significantly higher than the levels seen in mock treated plants and more importantly *g3pp* accumulated wild-type-like levels of SA in their PEX **(Figure 3.17D-E)**. Together these results suggested that the impaired SAR observed in *g3pp* was not associated with the SA branch of the SAR pathway.

Next, SAR responses to chemicals that operate in parallel to SA were evaluated. These include NO, ROS, AzA and G3P (Wang et al, 2014). NO/ROS mediates cleavage of C18 unsaturated fatty acid resulting in biosynthesis of AzA (Wang et al, 2014; Yu et al, 2013). To determine if compromised SAR in *g3pp* plants was associated with ROS or AzA, WT and KO plants were treated with either H_2O_2 (500 μM) or AzA (1mM), followed by inoculation with *Pst* DC3000 at 24 h post chemical treatment. As expected, H_2O_2 **(Figure 3.18A)** and AzA **(Figure 3.19A)** induced normal SAR on WT plants but not on *g3pp* mutants. These results suggested that the defective SAR in *g3pp* mutants was not associated with ROS or AzA steps in the SAR pathway. To ascertain this I quantified H_2O_2 and AzA levels in *g3pp* and WT plants after pathogen infection. Indeed, all *g3pp* KO plants induced wild-type-like H_2O_2 **(Figure 3.18B)** and AzA levels **(Figure 3.19B)**. The *g3pp* mutants also showed normal transport of AzA; the *g3pp* plants accumulated wild-type-like levels of AzA in PEX collected from mock- and pathogen-inoculated leaves **(Figure 3.19C)**.

Next, I assayed SAR in response to exogenous G3P. For this experiment, G3P was co-infiltrated together with *Pst* avrRpt2. As shown in the **Figure 3.20A-B**, *Pst* avrRpt2 alone was unable to confer SAR in any of the *g3pp* KO mutants. However, *Pst* avrRpt2 co-infiltrated with 50 or 100 μM G3P was able to restore SAR in *g3pp* plants **(Figure 3.20A-B)**. To determine if *g3pp* mutants were altered in G3P transport, pathogen induced G3P levels in PEX collected from mutant and WT plants were assayed. All *g3pp* mutants showed an increase in G3P after pathogen infection but *g3pp2* and *g3pp4* mutants showed a nominal reduction compared to WT **(Figure 3.20B)**.

Normal or near normal induction of G3P in mutants suggests that compromised SAR phenotype in *g3pp* mutants might not be associated with the total pool of G3P. This was further consistent with the result that avrRpt2-PEX collected from WT plants or *g3pp2*- and *g3pp3* mutants was able to induce systemic resistance on WT but not on mutant plants **(Figure 3.21A-B)**. However, avrRpt2-PEX from *g3pp4* did not induce normal SAR on either WT or *g3pp4* plants. This suggests that unlike *g3pp2* and *g3pp3*, the *g3pp4* plants were defective in generation of mobile signal.

Since G3Pp proteins are thought to mediate G3P transport, it is possible that SAR phenotype of *g3pp* plants is associated with compartmentalization of G3P. However, the fact that exogenous application of either 50 or 100μM of G3P restored the defective SAR in all of the *g3pp* mutants was puzzling since the *g3pp* mutants accumulated normal levels of G3P in the infected leaves and PEX. It is possible that G3P levels and/or compartmentalization of transported G3P in the distal leaves play an important role in SAR. Normal levels of ROS and AzA in the *g3pp* mutants suggest that these are not affected in steps that function upstream of G3P.

AZI and DIR are stable *g3pp* background

Defective In Induced Resistance 1 (DIR1) and AZI1 are lipid transfer proteins that together with G3P orchestrate SAR (Yu et al, 2013). The DIR1 and AZI1 proteins are unstable in low G3P background mutants such as *gly1* and *gli1* (Yu et al, 2013). The fact that G3Pp function as transporters and that low levels of G3P reduce DIR1 and AZI1 transcripts/protein, prompted me to examine whether G3Pp isoforms play a role in DIR/AZI stability. The DIR1-GFP and AZI1-Myc overexpression lines were crossed with the *g3pp* mutants and analyzed for transcript and protein levels. The DIR1-GFP and AZI1-Myc protein levels correlated with transcript levels of the respective transgene, suggesting that DIR1 and AZI1 proteins are not unstable in *g3pp* plants **(Figure 3.22A-B; Figure 3.23A-B)**.

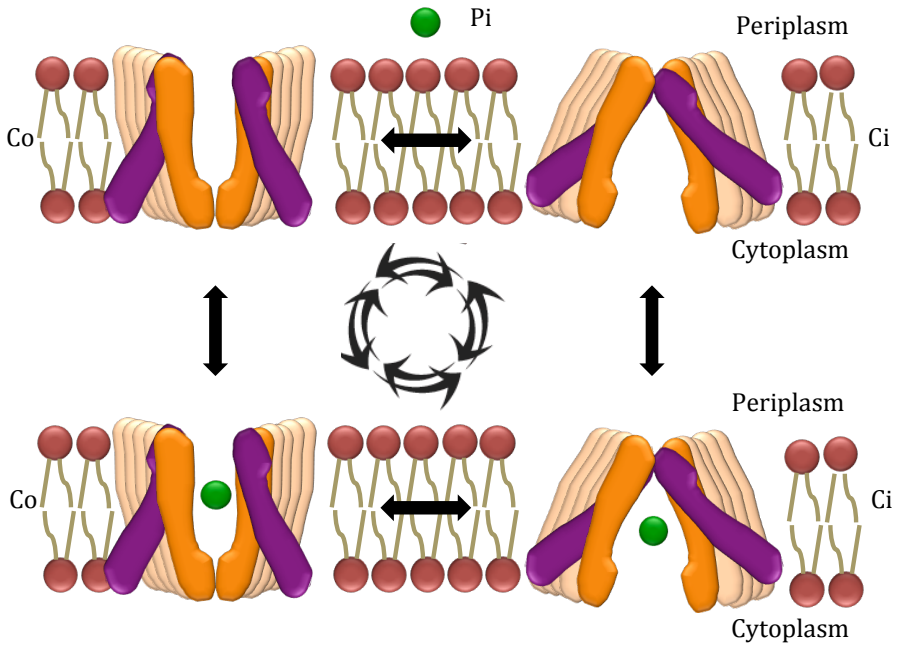

Figure 3.1. G3P Transporter (GlpT) adapted from (Moradi et al, 2015).

Escherichia coli G3P Transporter (GlpT) mediating anti-porter type of molecules exchange from periplasm to cytoplasm and vice-versa. Scheme showing a GlpT protein opened toward bacteria periplasm space (Co: outward facing) allowing Pi (green filled circle) to reach a central pore when the GlpT execute change in conformation (Ci: inward facing) and molecule moves to the inside of cytoplast. Likewise, the conformation changing from Ci to Co transports the molecule from cytoplasm to periplasm spaces.

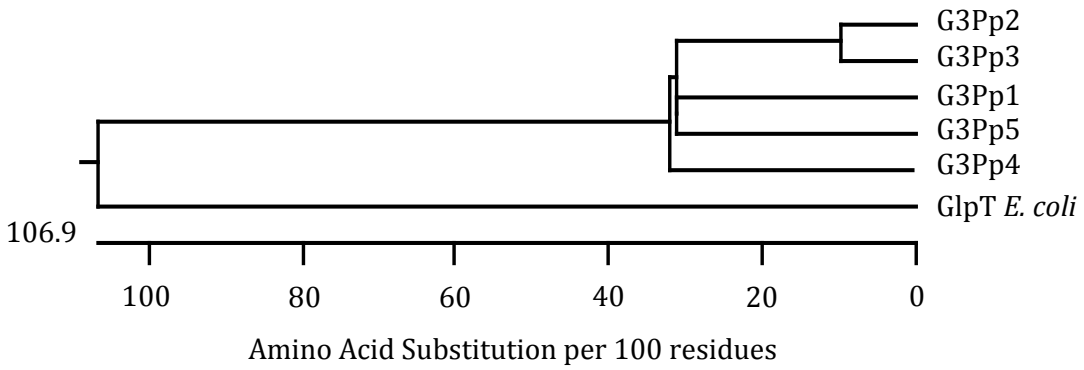

Figure 3.2. Inferred phylogenetic relationship of G3Pp isoforms.

Phylogenetic tree derived from ClustalW alignment of G3Pp Arabidopsis isoforms and GlpT from *E. coli*. The distance between sequence pairs and the number of substitutions events are indicated in the tree. To calculate distance values, the Kimura distance formula was used and the phylogenetic tree scale uses these values multiplied by 100 (https://www.dnastar.com).

Table 3.1. G3Pp protein isoforms and mutant alleles.

(A) Arabidopsis annotated information of the five isoforms of G3Pp from database TAIR (https://www.arabidopsis.org). **(B)** Arabidopsis microarray data from expression browser (http://www.expressionbrowser.com).

A

	AGI Locus Identifier	Mutant Allele Characterized	Protein length (aa)	Molecular weight (Da)	Splice variants
G3Pp1	AT3G47420	none	523	56309	2
G3Pp2	AT4G25220	*g3pp2* (GABI_742G10)	504	54376	0
G3Pp3	AT1G30560	*g3pp3* (SAIL452B07)	510	55088	0
G3Pp4	AT4G17550	*g3pp4-1* (SALK071338)	544	59075	0
		g3pp4-2 (GK-230D07)			
G3Pp5	AT2G13100	none	493	53056	3

B

***G3Pp1* At3G47420**	***G3Pp2* At4G25220**	***G3Pp3* At1G30560**	***G3Pp4* At4G17550**	***G3Pp5* At2G13100**
Psm *Pst* (avrRpm1) *Pst* (avrB) *Pst* (DC3000) Xanthomonas Phytophtora *Botrytis cinerea* *Blumeria graminis* f.sp. *hordei* Nutrient Starvation Dark Cold Drought	Not pathogen Nutrient Starvation	Not pathogen Nutrient Starvation	Cold Heat ABA Drought Osmotic *Pst* (DC3000) *Botrytis cinerea*	Osmotic Cold *Pst*(DC3000)

Table 3.2. Isoforms predicted subcellular localization.

Putative localization of G3Pp isoforms inferred by ChloroP, MitoProll, TargetP and SignalP protein sub-localization prediction programs.

	G3Pp1	G3Pp2	G3Pp3	G3Pp4	G3Pp5
ChloroP	Plasma mb	Plasma mb	Plasma mb	Chloroplast	Chloroplast
MitoProII	Plasma mb	Plasma mb	Plasma mb	Mitochondria	Plasma mb
TargetP	Plasma mb	Plasma mb	Plasma mb	Mitochondria	Plasma mb
SignalP	Plasma mb	Plasma mb	Plasma mb	Plasma mb	Plasma mb

Table 3.3. TDNA knockout lines isolated in this study.

Gene	Mutants identification number	Site of insertion	Knockout
G3Pp1	SAIL-261-A08	Promoter	No
	GK-696B08-024559	5'UTR	No
G3Pp2	GK-179F04-013562	3'UTR	No
	GK-742G10-023520	Exon	Yes
G3Pp3	SALK-028571	Promoter	No
	SAIL-452-B07	Exon	Yes
G3Pp4	SALK-028113	Promoter	No
	SALK-071338	Exon	Yes
	GK-230D07-014316	Exon	Yes
G3Pp5	SALK-097946	Promoter	No
	SALK-035552	Promoter	No

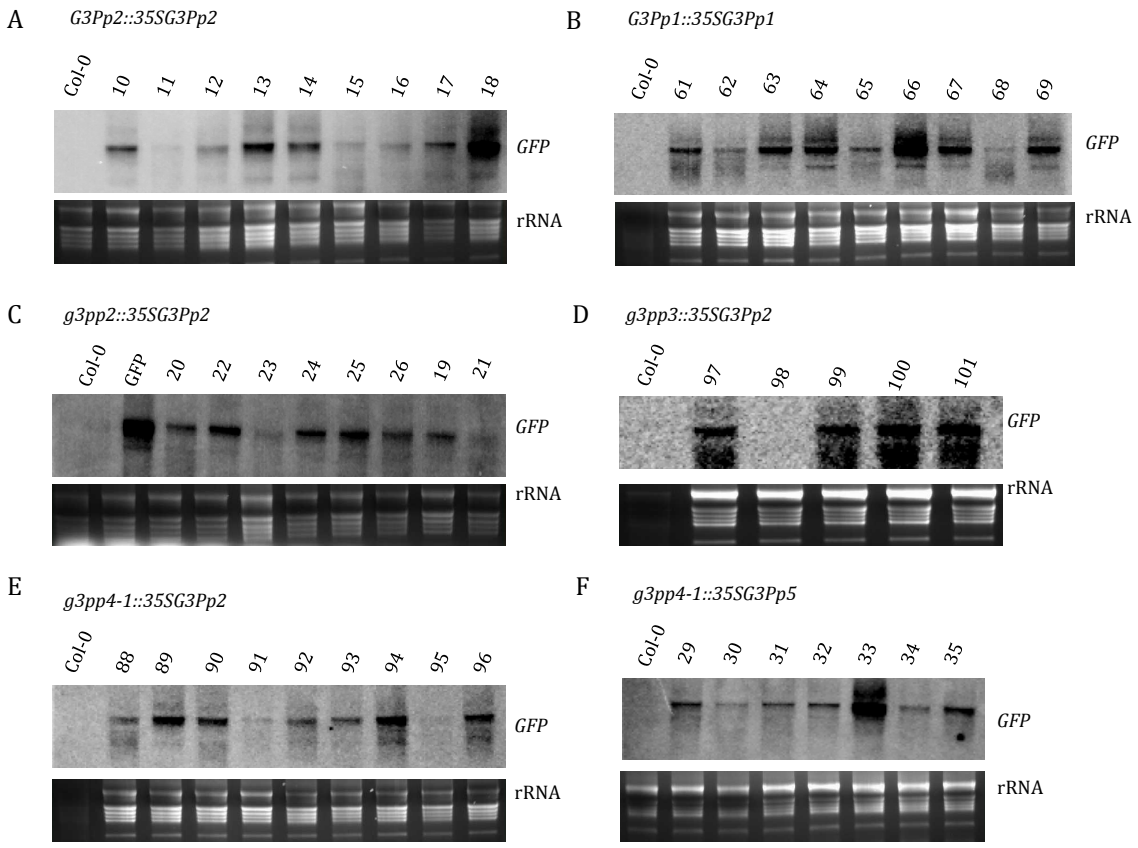

Figure 3.3. Transcript levels in the *35S-G3Pp-GFP* transgenic lines.

The membranes were probed with *GFP*. The transcript levels being showed are from the lines **(A)** *35SG3Pp1-GFP* and **(B)** *35SG3Pp2-GFP* are in wild type (WT) background. **(C-E)** Blots are showing *G3Pp-GFP* transcripts of *G3Pp2-GFP* in mutant backgrounds: **(C)** *g3pp2* **(D)** *g3pp3* and **(E)** *g3pp4-1* and **(F)** G3Pp5-GFP lines are in *g3pp4-1* background. RNA gel-blot analysis was performed on 7 µg of total RNA. Ethidium bromide staining of rRNA was used as a loading control. The predicted transcript size of the full-length transcript for the permease plus the *GFP* marker generated *in planta* from the transgenes are: *G3Pp1-GFP*: 2.8 Kb; *G2Pp2-GFP*: 2.7 Kb; *G3Pp3-GFP*: 2.5 Kb; *G3Pp5-GFP*: 3 Kb.

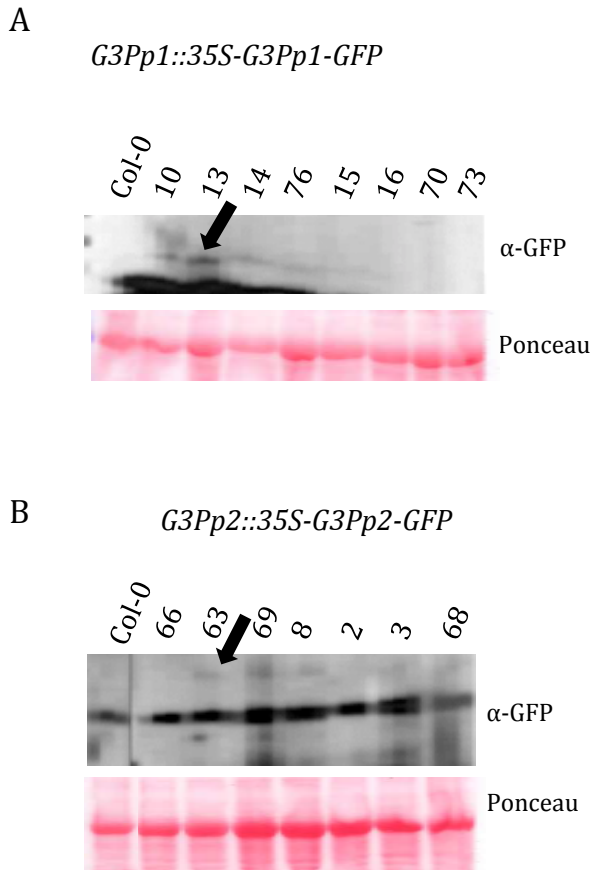

Figure 3.4. Protein levels in the *35S-G3Pp-GFP* transgenic lines.

Immunoblot showing relative levels of *35S-G3Pp-GFP* transgenic lines T1 generation of plants in WT background **(A)** *35S-G3Pp1* and **(B)** *35S-G3Pp2-GFP*. Ponceau-S staining of the immunoblot was used as the loading control. The protein molecular weight marker, included in each blot, clearly shows the predicted, translationally fused permease-marker protein size in all instances.

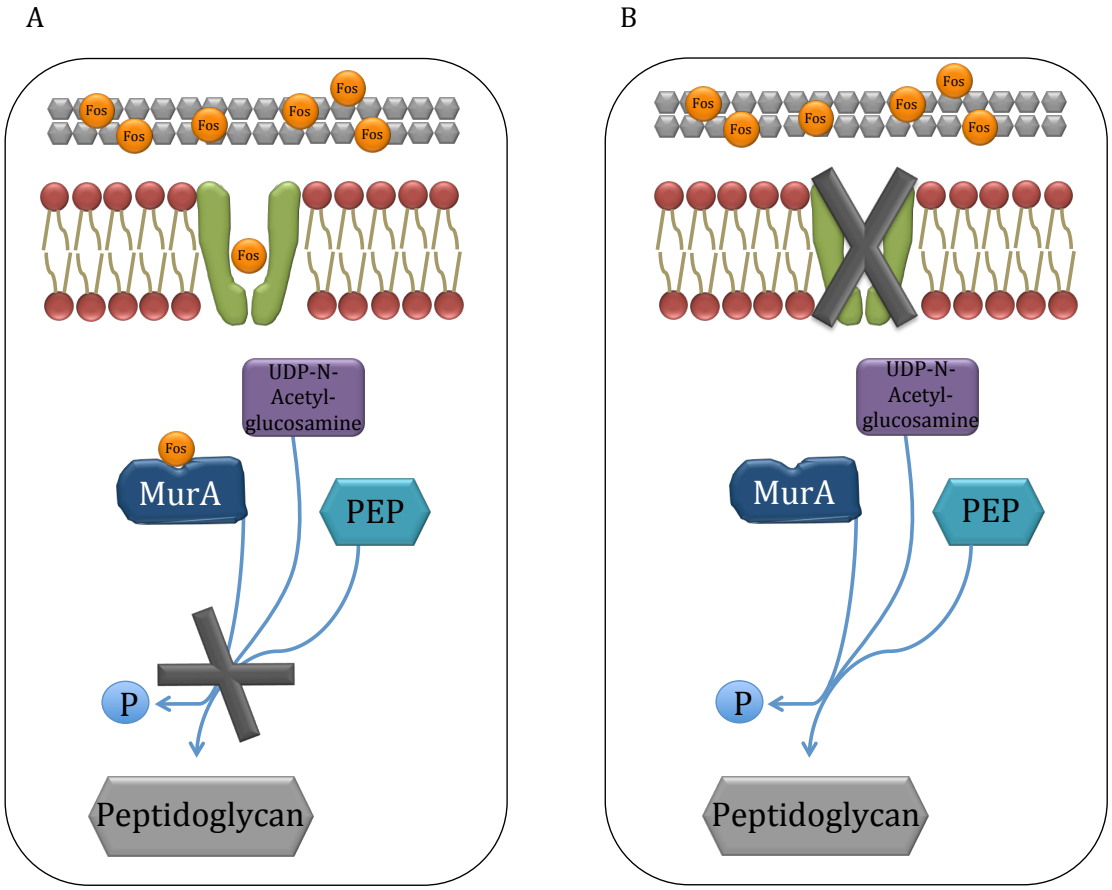

Figure 3.5. Fosfomycin mode of action adapted from (Blazquez & Alexandro, 2013).

(A) Fosfomycin using GlpT transporter to enter into the bacterial cell resulting in blockage of the peptidoglycan pathway. **(B)** GlpT transporter knockout preventing fosfomycin to get access to the bacterial cell and the bacterial cell wall is normally biosynthesized.

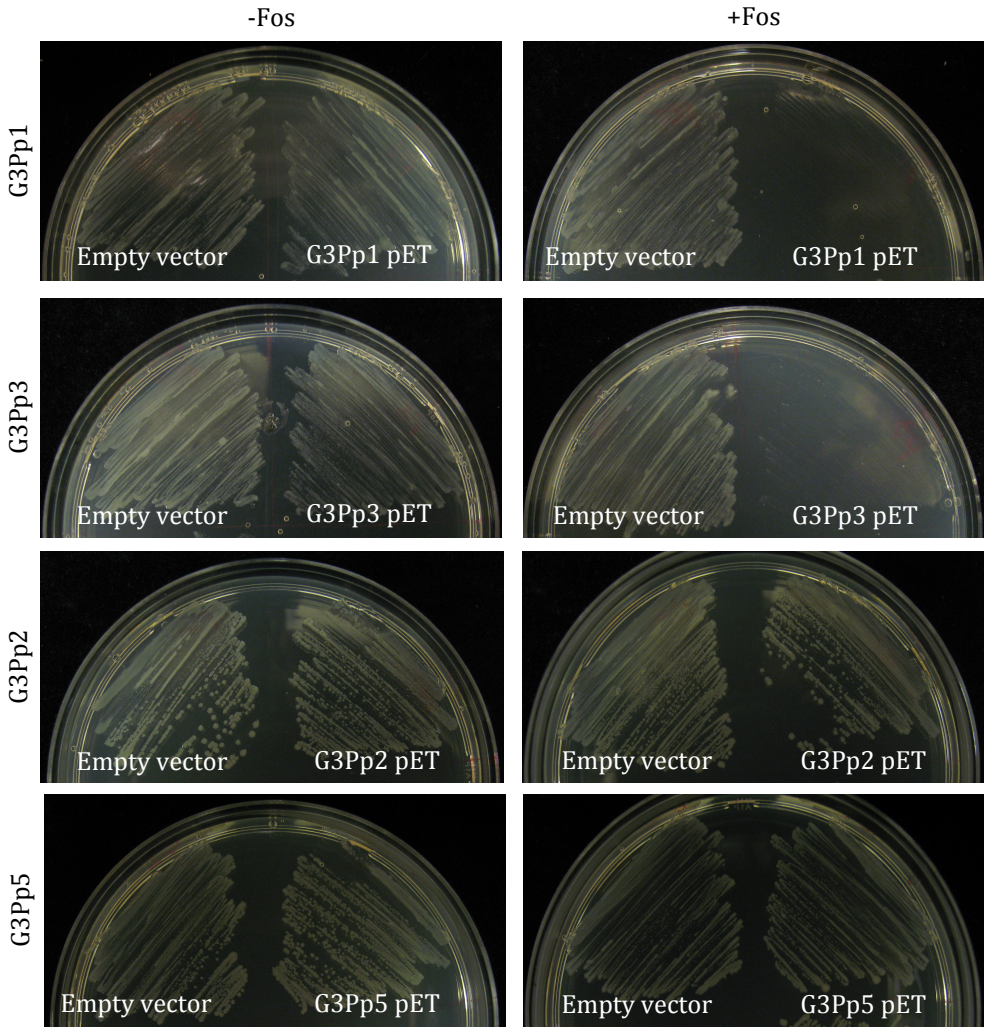

Figure 3.6. G3Pp complementation assay in ΔG3Pp *E. coli* strain.

Empty vectors and G3Pp-pET21 constructs transformed into ΔG3Pp *E. coli* strain and streaked in media with and without Fosfomycin. SOC plates were supplemented with 1 mM Arabinose and 1 mM IPTG. The left sets of pictures are showing the G3Pp constructs as well pET21 empty vector streaked in SOC media containing kanamycin (Kan: 50 μg/mL) and ampicillin (Amp: 100 μg/mL) antibiotics. The right sets of pictures are showing the bacteria cells streaked in SOC media with kananamycin, ampicillin and fosfomycin (128 μg/mL).

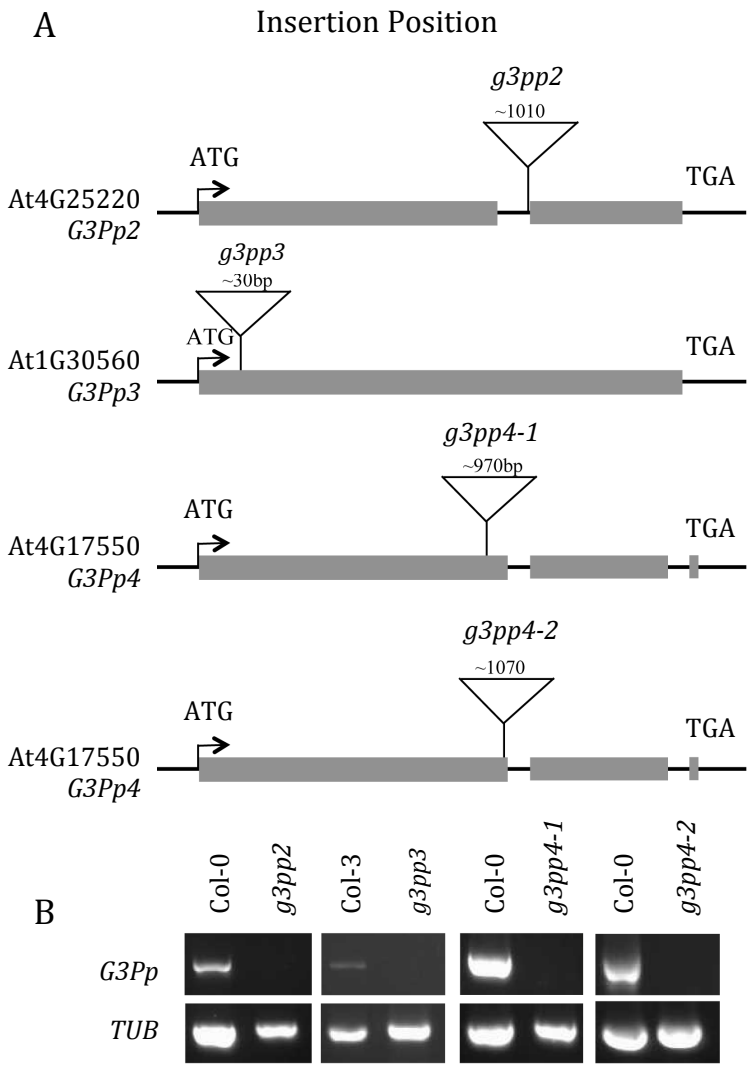

Figure 3.7. Insertion position and semi-quantitative RT-PCR of *g3pp* knockouts.

(A) Insertion position in the gene At4G25220 (*G3Pp2*) for the line GK742: 1010 bp downstream start codon; At1G30360 (*G3Pp3*) for the line SAIL452: 30 bp downstream ATG; At4G17550 (*G3Pp4*) for the lines SALK071338: 970 bp and GK230: 1070 bp downstream start codon. **(B)** Semi quantitative RT-PCR analysis of RNA extracted from Col-0 and *g3pp* using gene-specific primers for *G3Pp*. The level of β-tubulin was used as an internal control to normalize the amount of cDNA template.

A

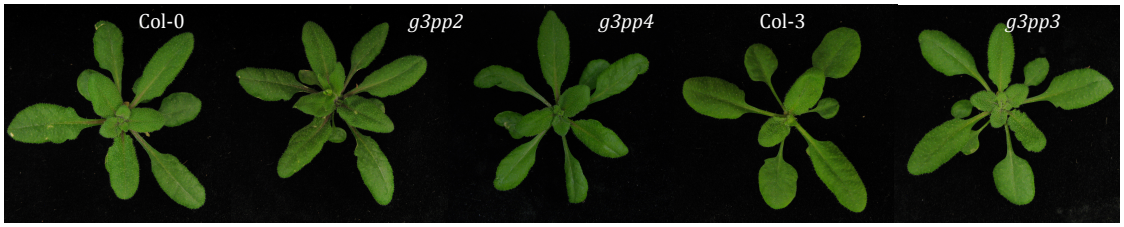

B

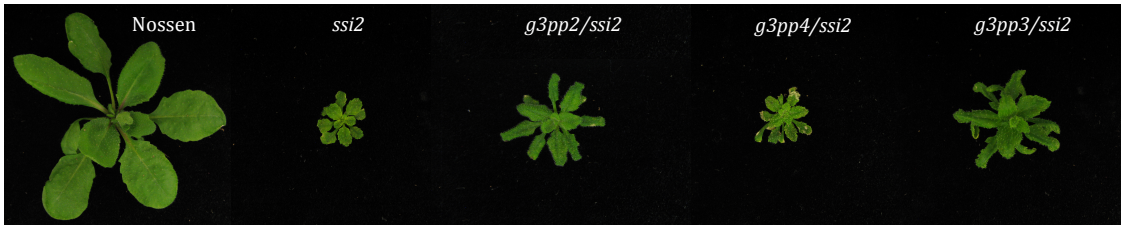

Figure 3.8. *g3pp3 ssi2* double and single mutant morphological phenotypes. **(A)** WT and *g3pp* single mutants morphological phenotypes: Col-0, *g3pp2* (GK742) and *g3pp4-1* (S071338) as well as Col-3 and *g3pp3* (SAIL452). **(B)** Morphology of *SSI2* and *ssi2* compared to double mutants *ssi2 g3pp*.

A

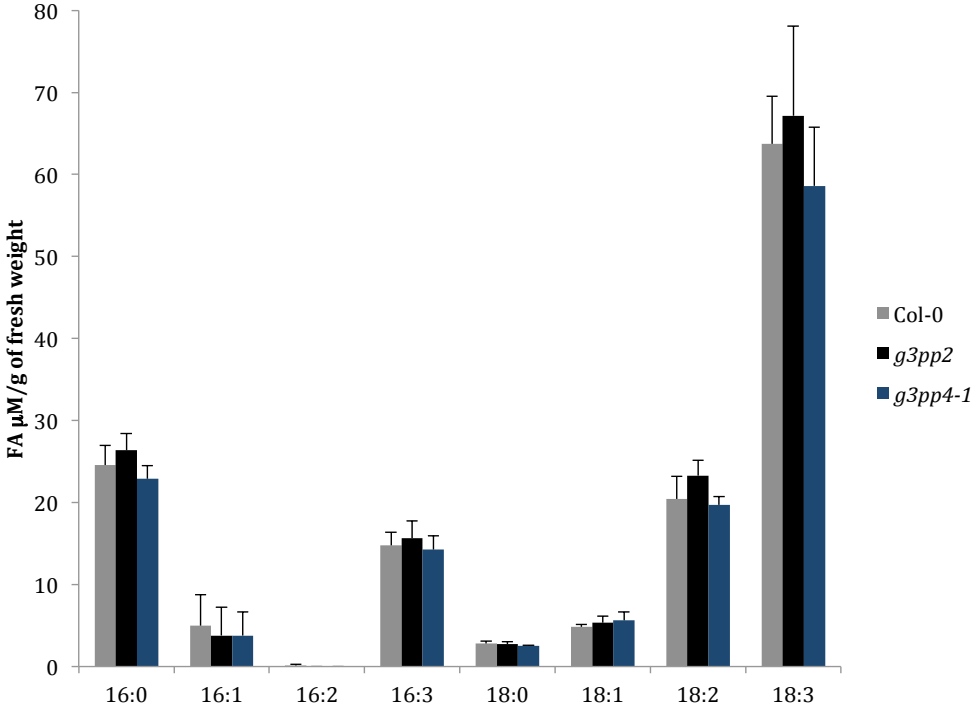

B

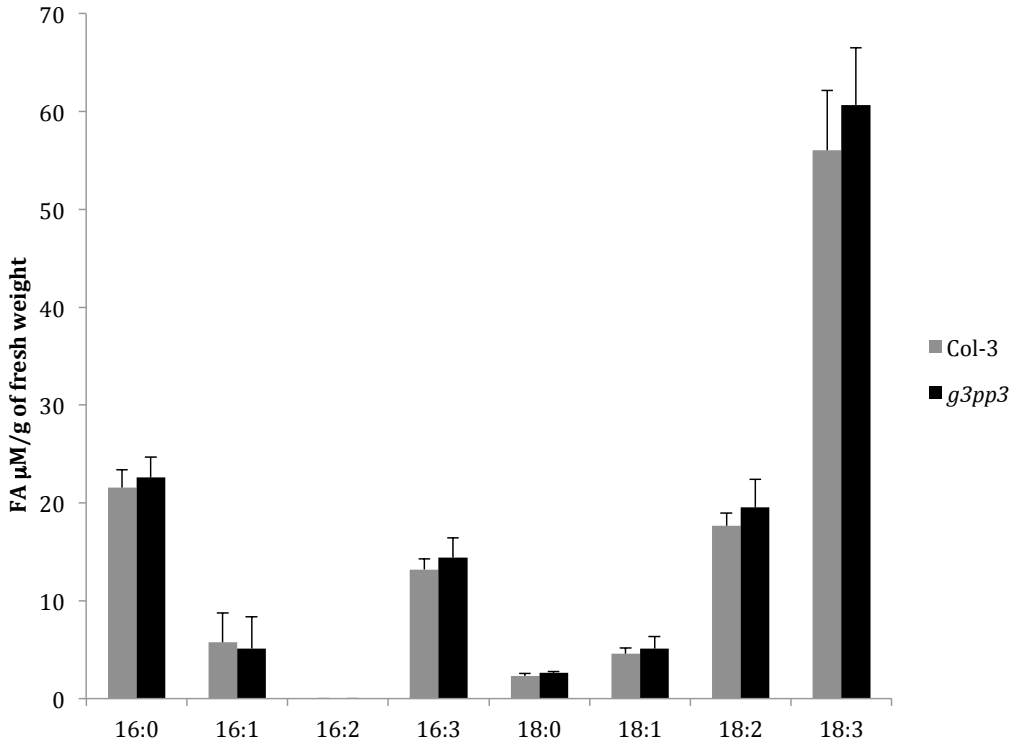

Figure 3.9. Fatty acid (FA) profile in *g3pp*.

(A-B) Relative levels of FA in leaves of 4-week-old Col-0, *g3pp2*, *g3pp4-1*, Col-3 and *g3pp3*. The values are presented as means of five replicates. Asterisks denote a significant difference with WT (t-test, $P < 0.05$). FW indicates fresh weight. Error bars represent standard deviation (SD) (n=4). Asterisks denote a significant difference with WT (t test, $P<0.05$).

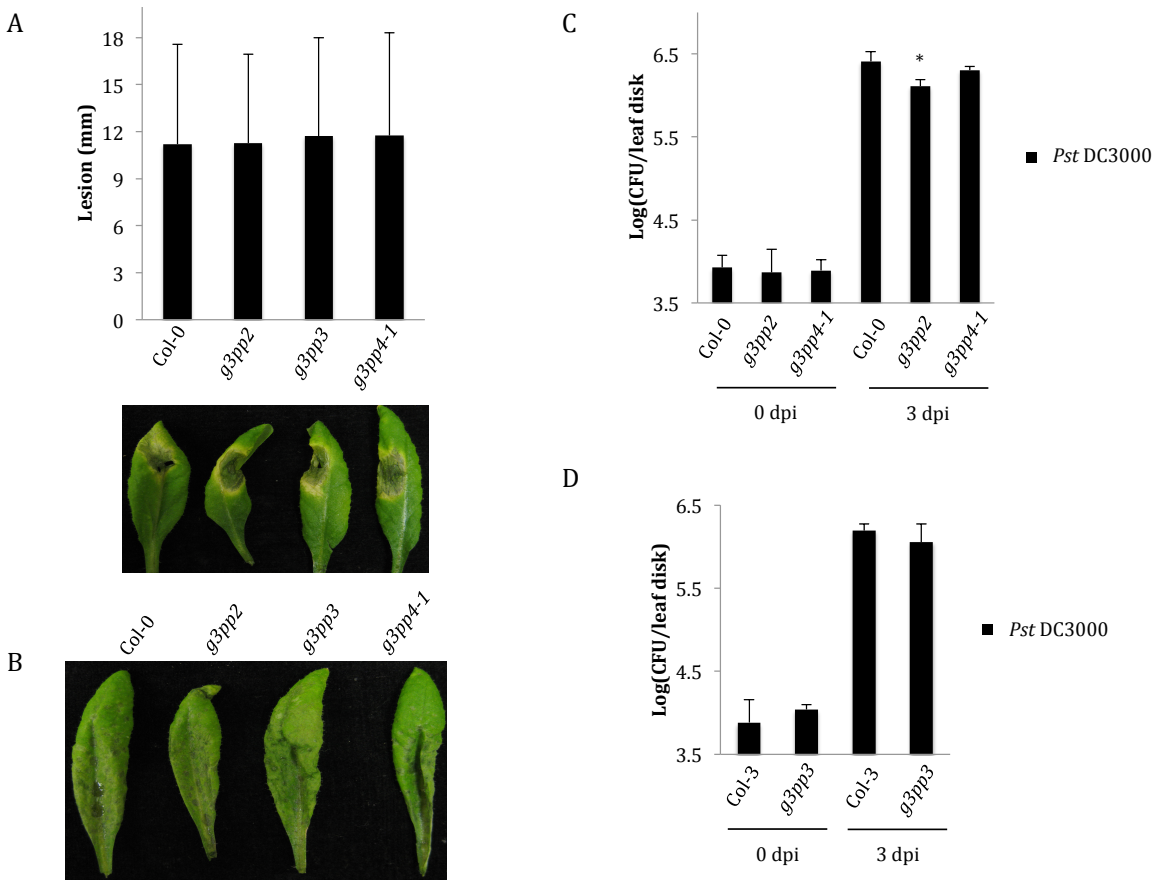

Figure 3.10. Basal defense in *g3pp* knockouts.

Disease symptoms in WT plants or *g3pp* inoculated with *C. higginsianum*. **(A)** Plants spot inoculated with $2x10^6$ spores/mL and lesion size measurements taken from 30 to 50 independent leaves at 5 dpi. Statistical significance was determined using Student's t test. Asterisks indicate statistical difference from mutant and WT. Error bars indicate SD. **(B)** Plants spray inoculated with $2x10^6$ spores/mL and the leaves photographed at 3 dpi. **(C-D)** Basal disease resistance inferred by bacterial colony counts of plants inoculated with *Pst* DC3000

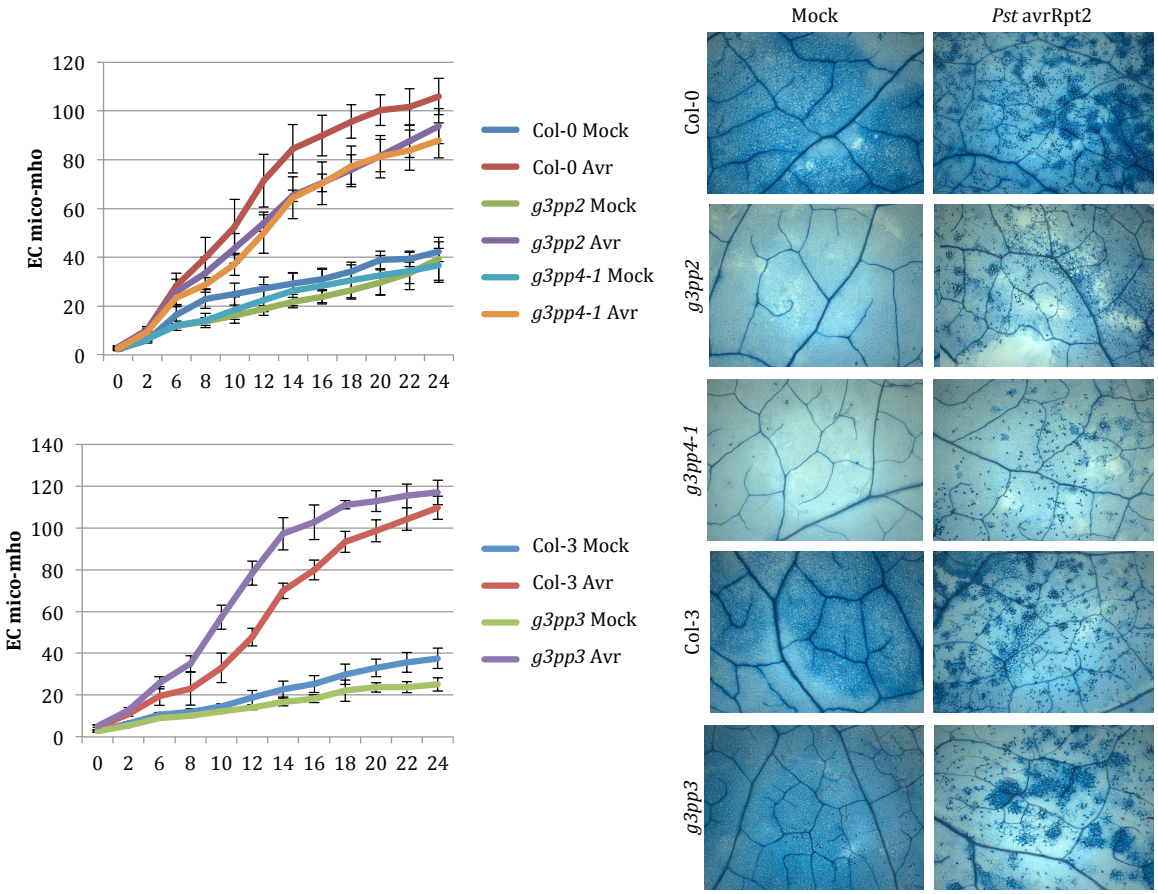

Figure 3.11. Cell death phenotype in *g3pp* mutants.

(A) Electrolyte leakage in Arabidopsis leaves inoculated with *Pst* avrRpt2 (10^7 CFU/ml). Ion leakage was measured on leaves sampled from 0, 2, 6, 8, 10, 12, 14, 16, 18, 20, 22, 24 h post treatments. Control plants were treated with 10 mM $MgCl_2$. Error bars represents SD. **(B)** Microscopy of trypan blue-stained leaves inoculated with *Pst* avrRpt2 (10^6 CFU/ml) and mock treatment as control (10 mM $MgCl_2$). Leaves were sampled 24 h after inoculation.

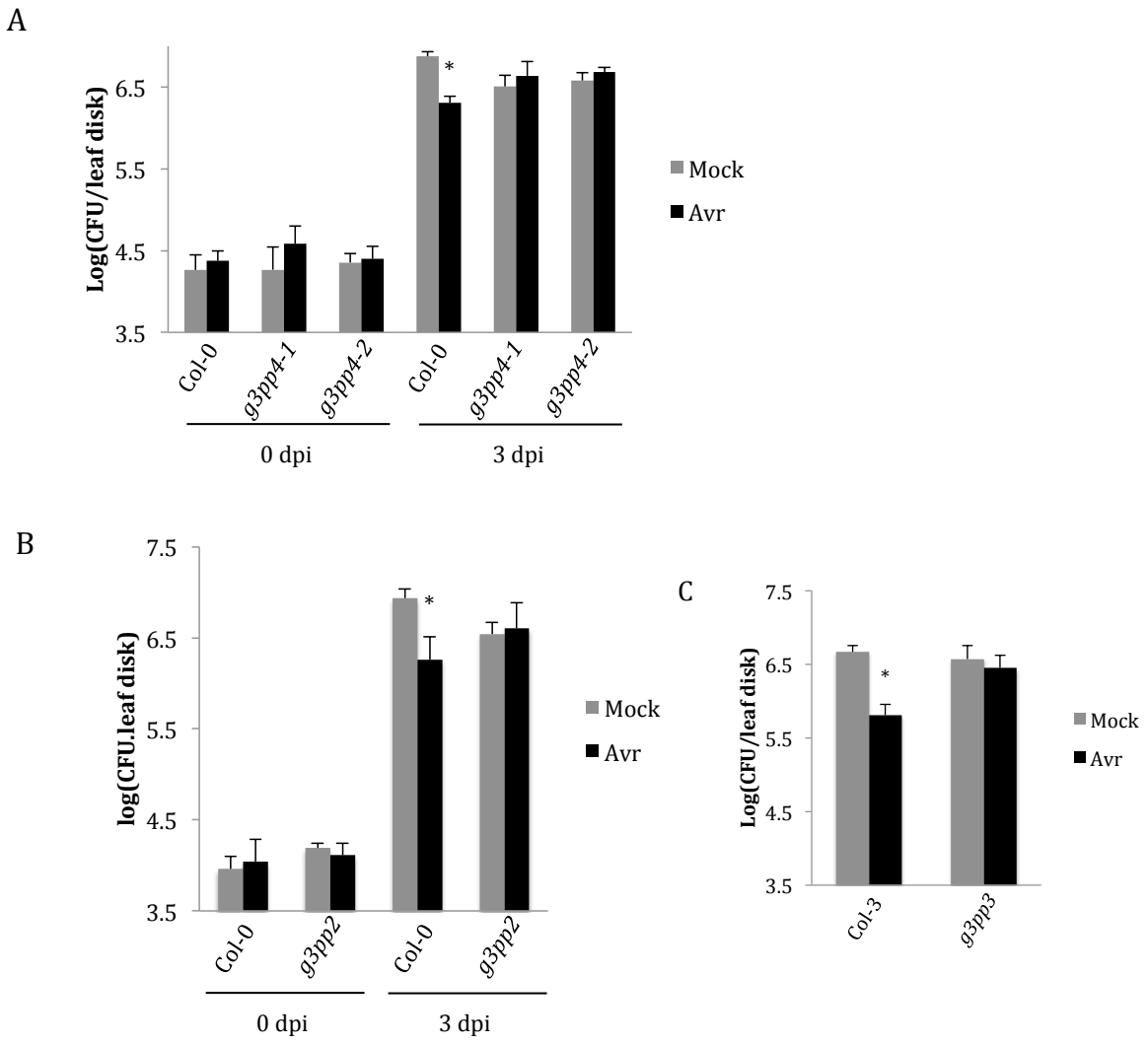

Figure 3.12. SAR phenotype in *g3pp* KOs.

SAR response in WT (Col-0 and Col-3) and *g3pp*. **(A-C)** Primary leaves inoculated with *Pst* avrRpt2 or 10 mM $MgCl_2$ (mock) and the distal leaves 48 h later infected with the virulent strain of *Pst* DC3000. Asterisks denote a significant difference between mock and treatment (t-test, $P < 0.05$). The error bars represent SD.

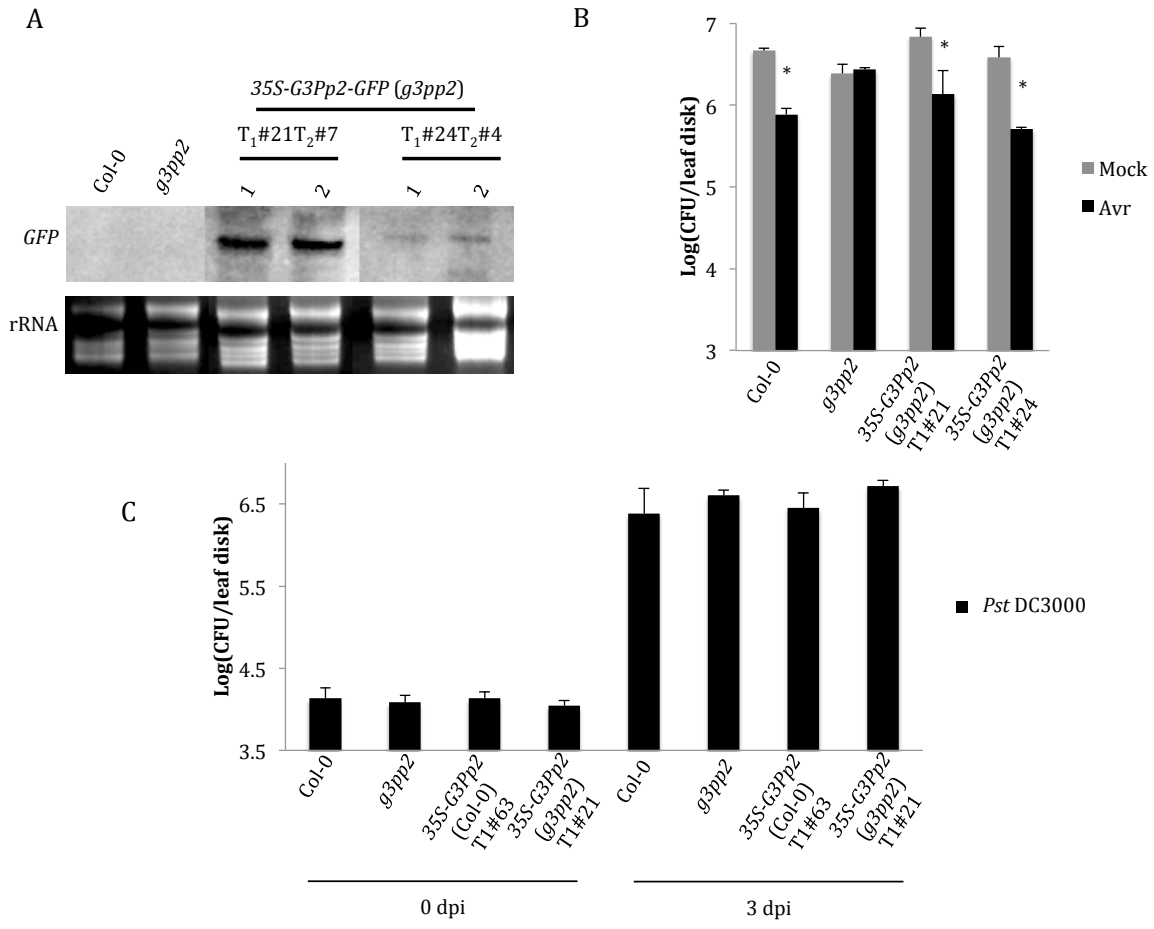

Figure 3.13. Analysis of transgenic lines overexpressing *35S-G3Pp2-GFP* in *g3pp2* mutant background.

(A) Northern blot analysis showing *35S-G3Pp2-GFP* transcripts in mutant background. RNA gel-blot analysis was performed on 7 µg of total RNA. Ethidium bromide staining of rRNA was used as a loading control. **(B)** SAR response in WT, mutants and transgenic lines infiltrated with 10 mM $MgCl_2$ or inoculated with *Pst* avrRpt2. The distal tissues, 48h after primary leaf treatment, were inoculated with a virulent strain of *P. syringae* (*Pst* DC3000). Asterisks denote a significant difference between mock and pathogen induction treatments. **(C)** Basal mediated responses to *Pst* DC3000. Plant inoculated leaves from Col-0, *g3pp2* and transgenic lines were sampled three days after inoculation. Error bars indicate SD (n=4).

A

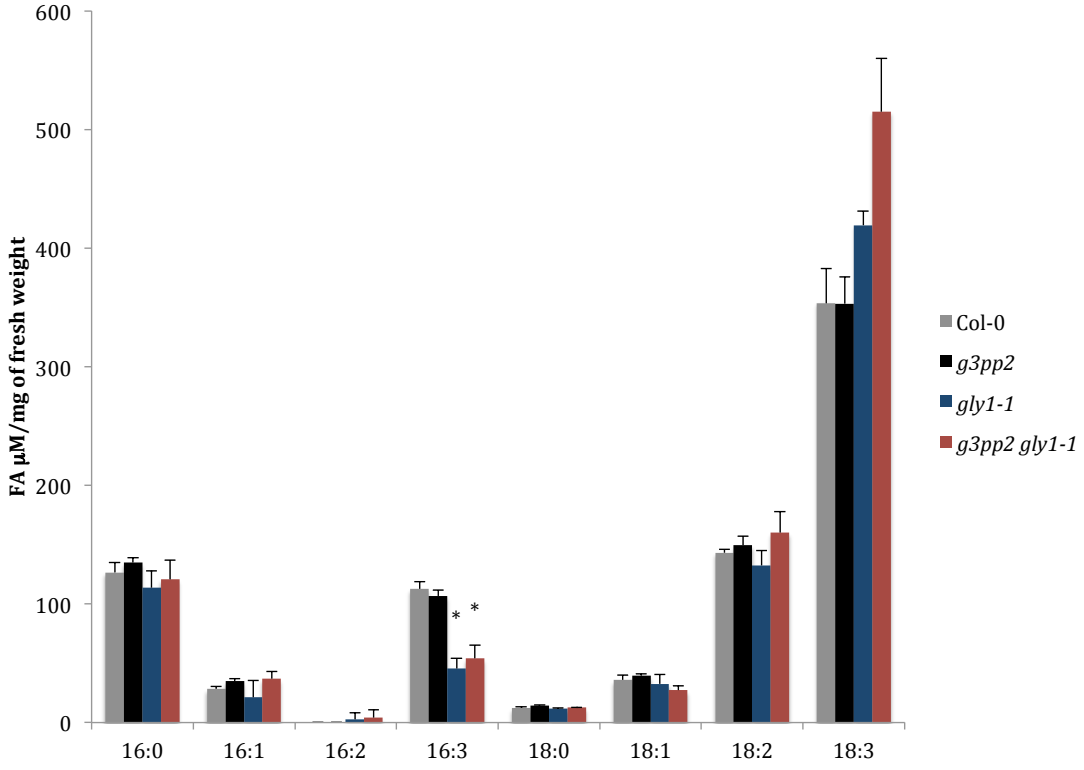
600
500
400
300
200
100
0
FA µM/mg of fresh weight
16:0
16:1
16:2
16:3
18:0
18:1
18:2
18:3
*
*
Col-0
g3pp2
gly1-1
g3pp2 gly1-1

B

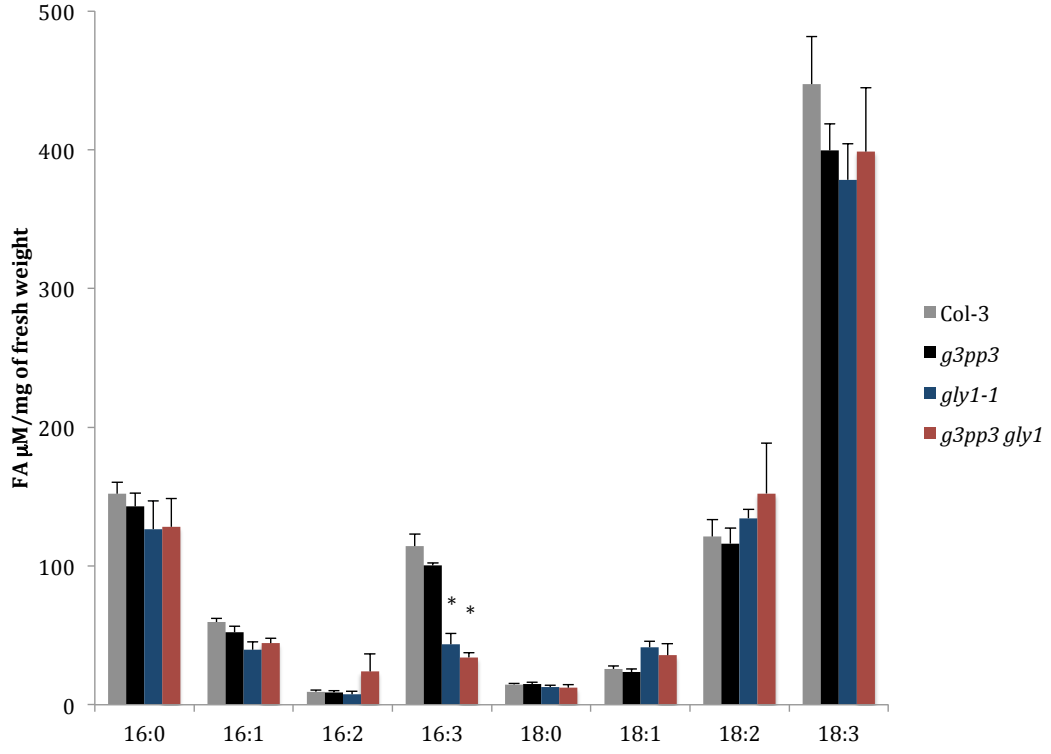
500
400
300
200
100
0
FA µM/mg of fresh weight
16:0
16:1
16:2
16:3
18:0
18:1
18:2
18:3
*
*
Col-3
g3pp3
gly1-1
g3pp3 gly1

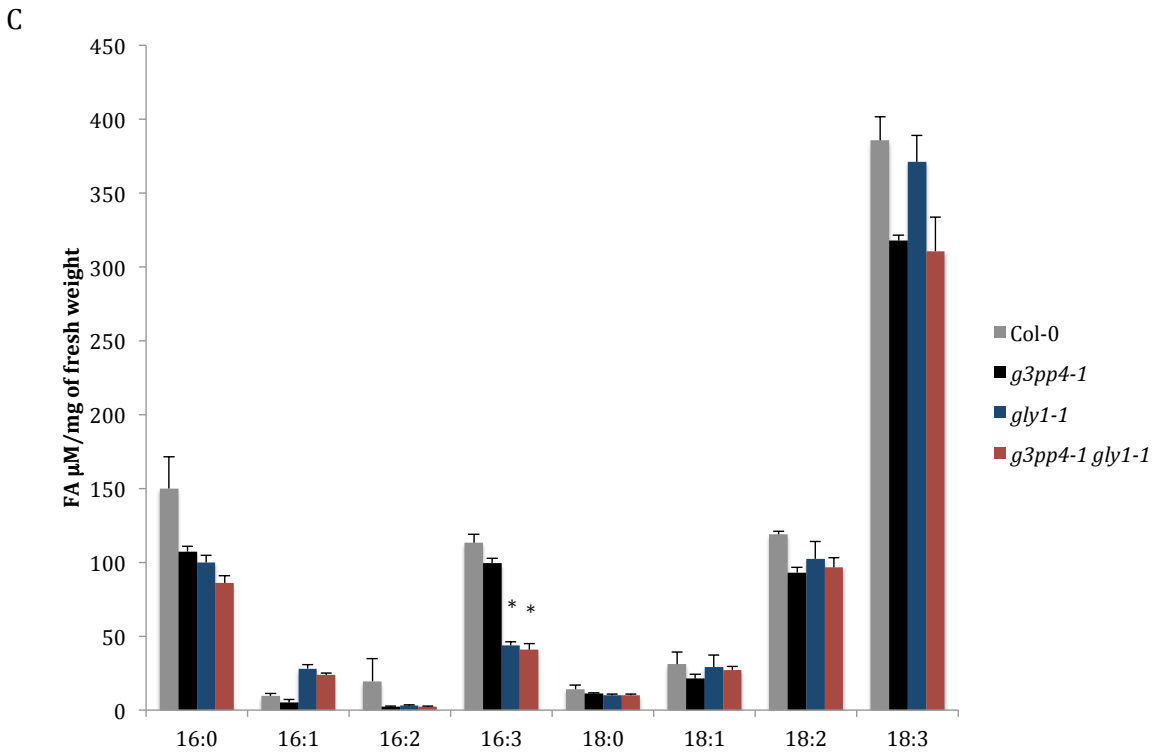

Figure 3.14. FA profile in *g3pp gly1-1* double and single mutants.

Leaf FA profile in double and single mutant analyzed along with their WT **(A)** *g3pp2 gly1-1* **(B)** *g3pp3 gly1-1* **(C)** *g3pp4-1 gly1-1*. The values are presented as a mean of five replicates. The error bars represent SD.

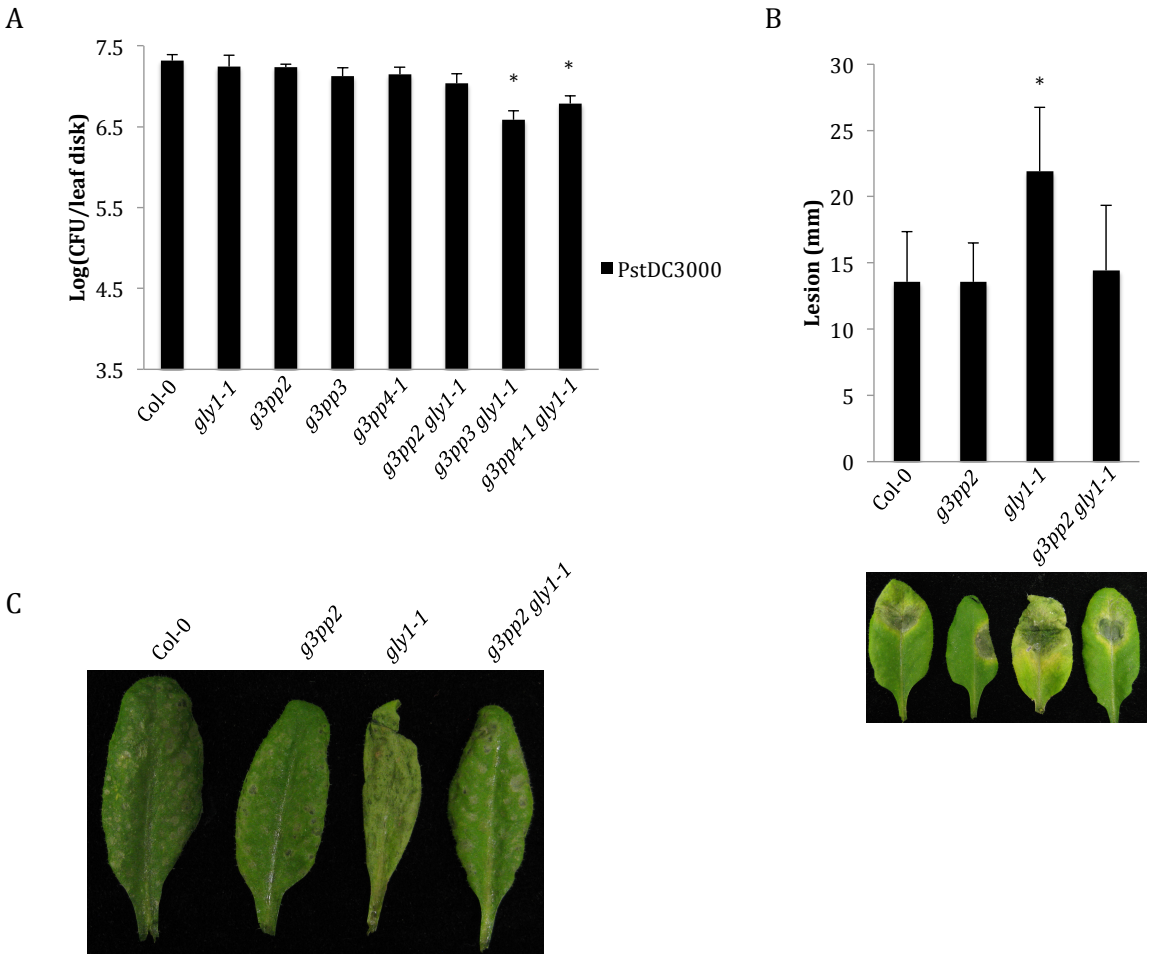

Figure 3.15. Basal defense phenotype in the double mutants *g3pp gly1-1*.

(A) Basal disease resistance against *Pst* DC3000 in WT, *g3pp* and *g3pp gly1-1* mutants. Plants were sampled three days after infection and disease amount was inferred by bacterial colony counting. **(B-C)** Disease symptoms in WT, *g3pp* and *g3pp2 gly1-1* plants inoculated with *C. higginsianum*. **(B)** Plants spot inoculated with $2x10^6$ spores/mL and lesion size measurements taken from 30 to 50 independent leaves at 5 dpi. Statistical significance was determined using Student's t test. Asterisks indicate data that are statistically significant from that of control. Error bars indicate SD. **(C)** Plants spray inoculated with $2x10^6$ spores/mL and the leaves photographed at 3 dpi.

A

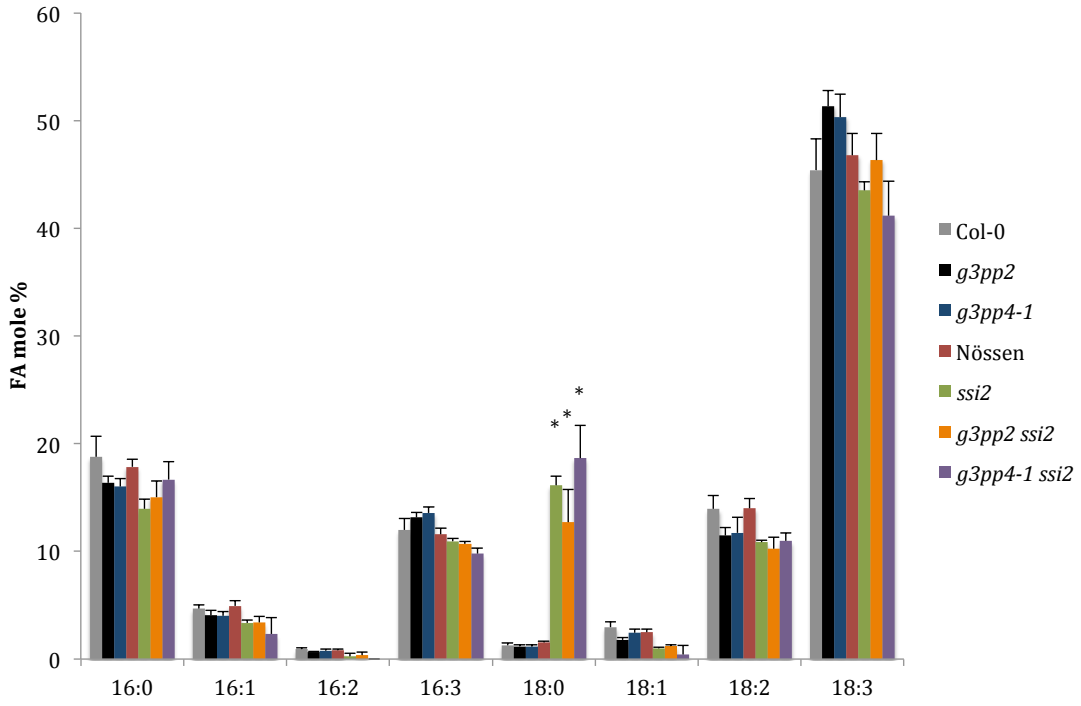
60
50
40
30
20
10
0
FA mole %
16:0
16:1
16:2
16:3
18:0
18:1
18:2
18:3
Col-0
g3pp2
g3pp4-1
Nössen
ssi2
g3pp2 ssi2
g3pp4-1 ssi2

B

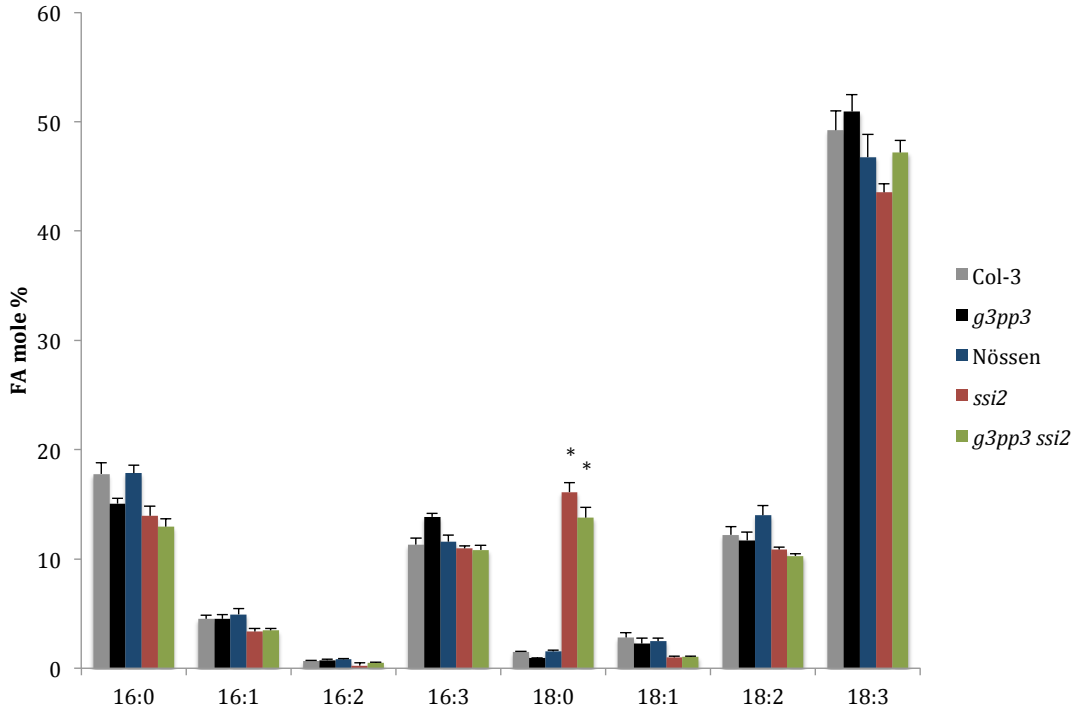
60
50
40
30
20
10
0
FA mole %
16:0
16:1
16:2
16:3
18:0
18:1
18:2
18:3
Col-3
g3pp3
Nössen
ssi2
g3pp3 ssi2

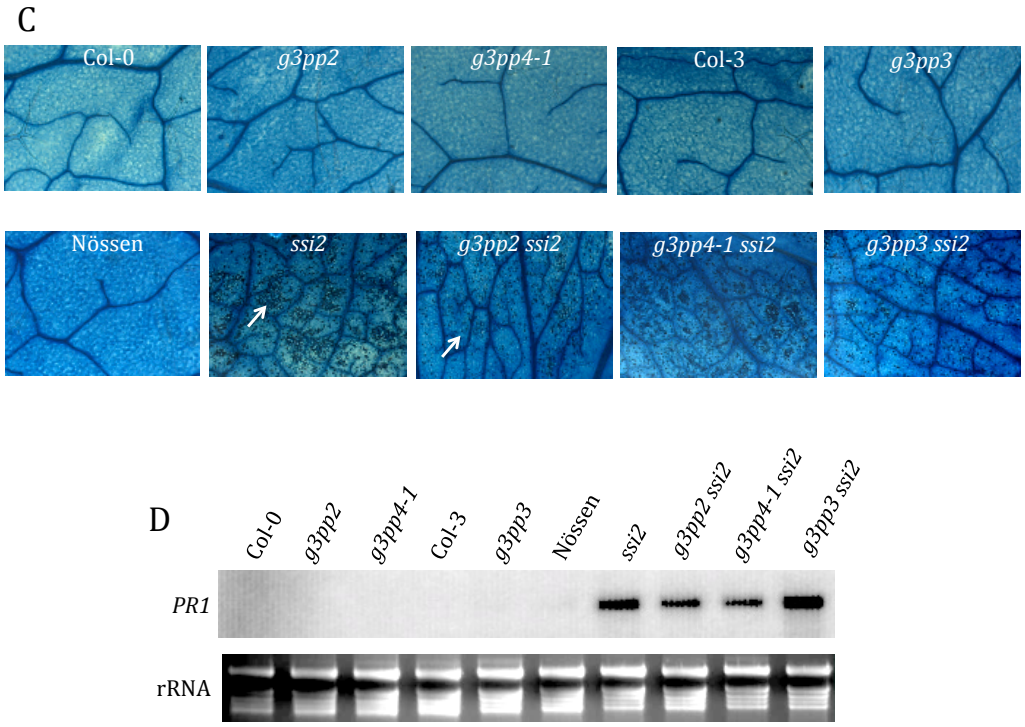

Figure 3.16. *g3pp ssi2* double mutant phenotypes.

(A-B) Profile of fatty acid in the double mutant *g3pp ssi2* analyzed along with WT and the respective single mutants **(A)** *g3pp2 ssi2* and *g3pp4-1 ssi2* **(B)** *g3pp3 ssi2*. The values are presented as a mean of four replicates. The error bars represent SD. **(C)** Microscopy of trypan blue-stained leaves showing cell death phenotypes of *ssi2* single and crossed with *g3pp* as well as their WTs (Col-0, Col-3 and Nössen). Three leaves of each genotype were stained and visualized using microscope. White arrows indicate dead cells. **(D)** Northern blot analysis of *PR-1* gene constitutive expression in single and double mutants along with WTs Col-0, Col-3 and Nössen. RNA gel-blot analysis was performed on 7 µg of total RNA. Ethidium bromide staining of rRNA was used as a loading control.

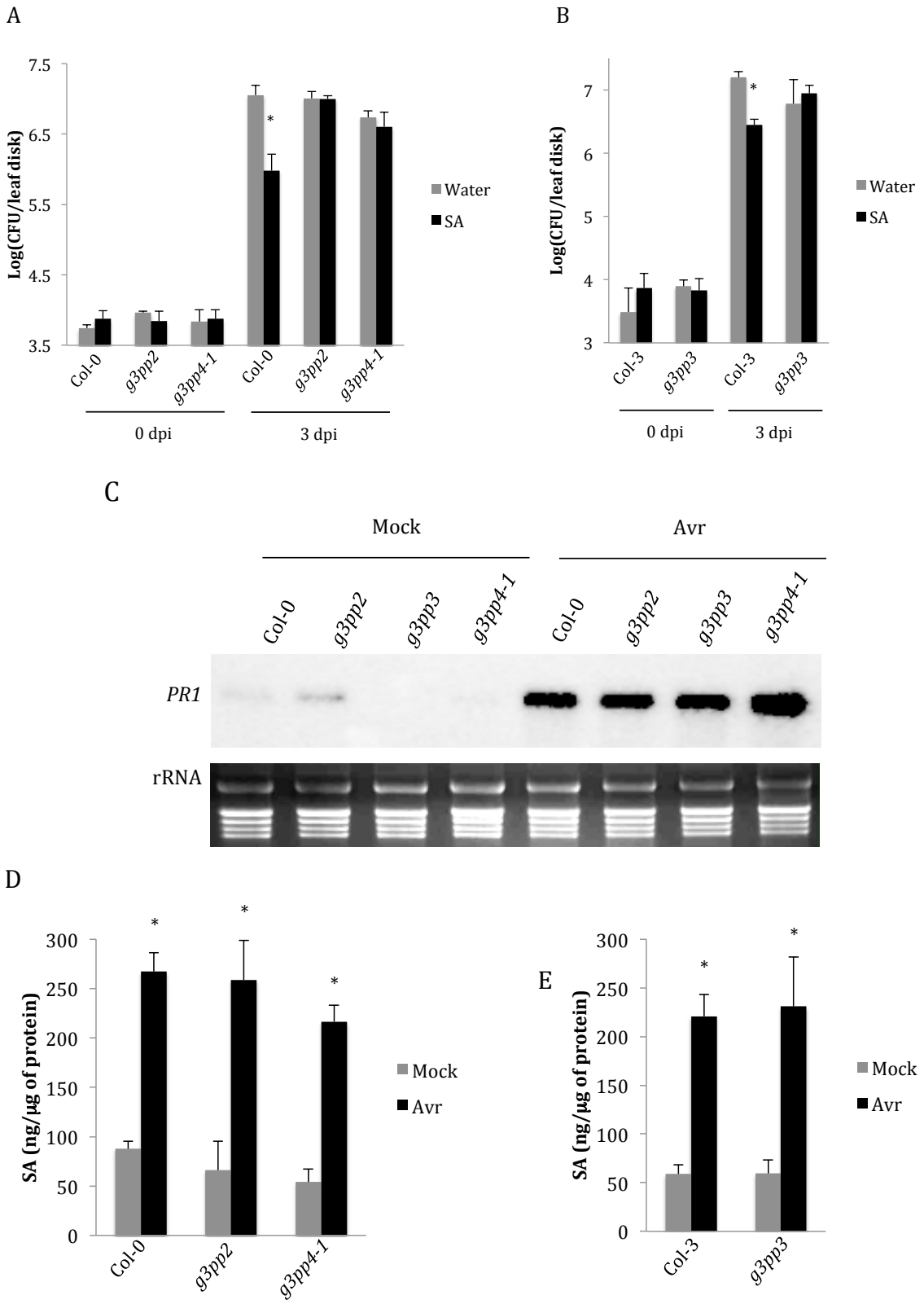

Figure 3.17. Effect of G3Pp mutation on the SA pathway.

Figure 3.17. Effect of G3Pp mutation on the SA pathway.

(A-B) SAR response in distal leaves of WT Col-0 plants treated locally with water or salicylic acid (SA-500μM). The virulent pathogen *Pst* DC3000 was inoculated 24 h after local treatments. Error bars indicate SD (n = 4). **(C)** Northern blot analysis of *PR-1* gene expression 24 after avirulent pathogen inoculation (*Pst* avrRpt2) in *g3pp* knockouts along with the WTs Col-0 and Col-3. RNA gel-blot analysis was performed on 7 μg of total RNA. Ethidium bromide staining of rRNA was used as a loading control. **(D-E)** SA levels in petiole exudates (PEX) collected from mock-infiltrated and *Pst* avrRpt2-inoculated plants. Error bars indicate SD (n = 4).

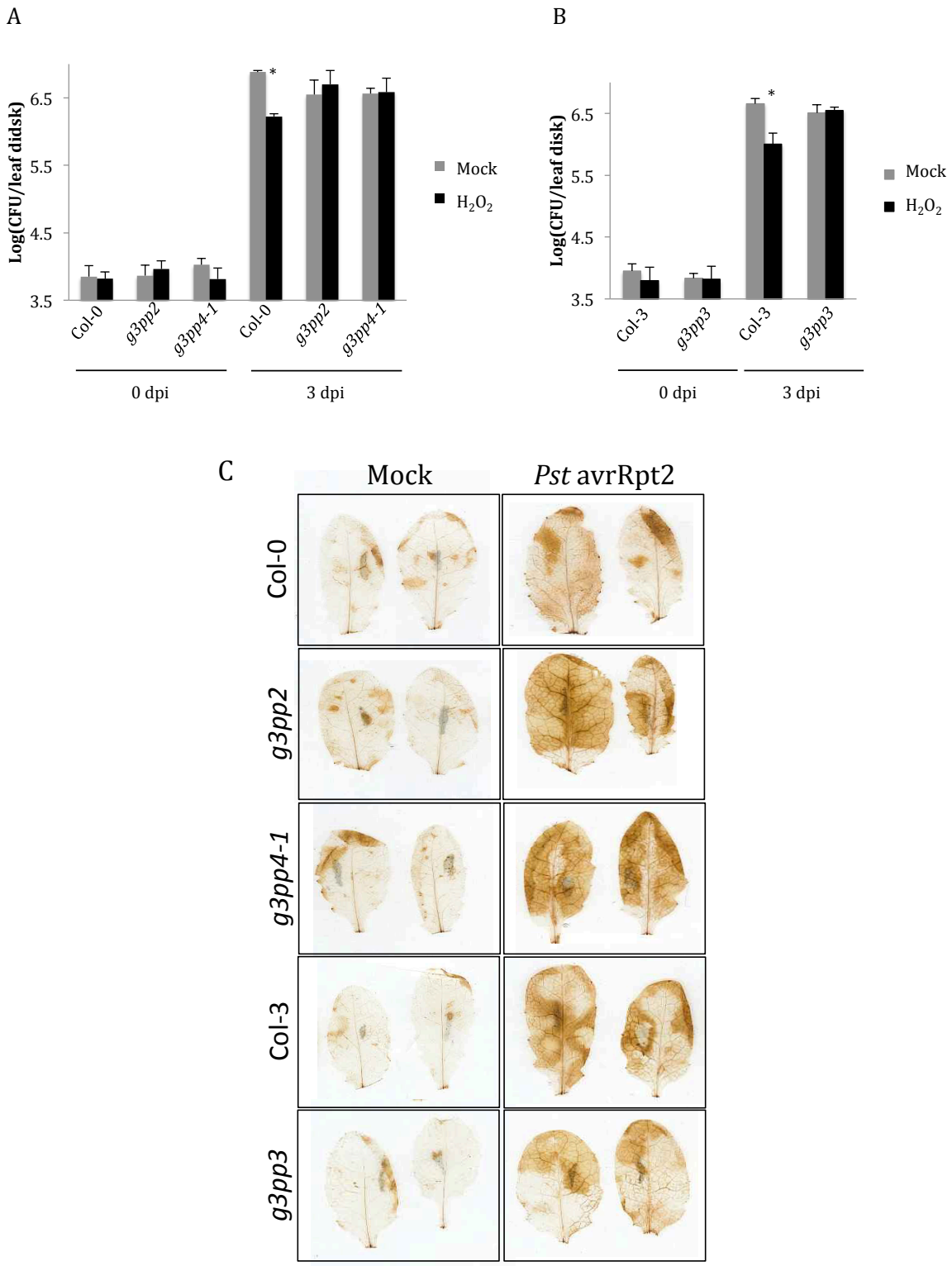

Figure 3.18. Effect of G3Pp mutation on H_2O_2 levels.

Figure 3.18. Effect of G3Pp mutation on H_2O_2 levels.

(A-B) SAR response in Col-0 and *g3pp* plants treated locally with water or hydrogen peroxide (H_2O_2-500μM) 24 h prior to inoculation of distal leaves with a virulent strain *(Pst* DC3000). Asterisks denote significant differences (t test, $p < 0.05$), and the error bars represent SD (n = 4). **(C)** Detection of H_2O_2 pathogen induced levels by DAB-mediated tissue staining. The right sets of pictures were mock treated leaves and the left panels were *Pst* avrRpt2 induced samples.

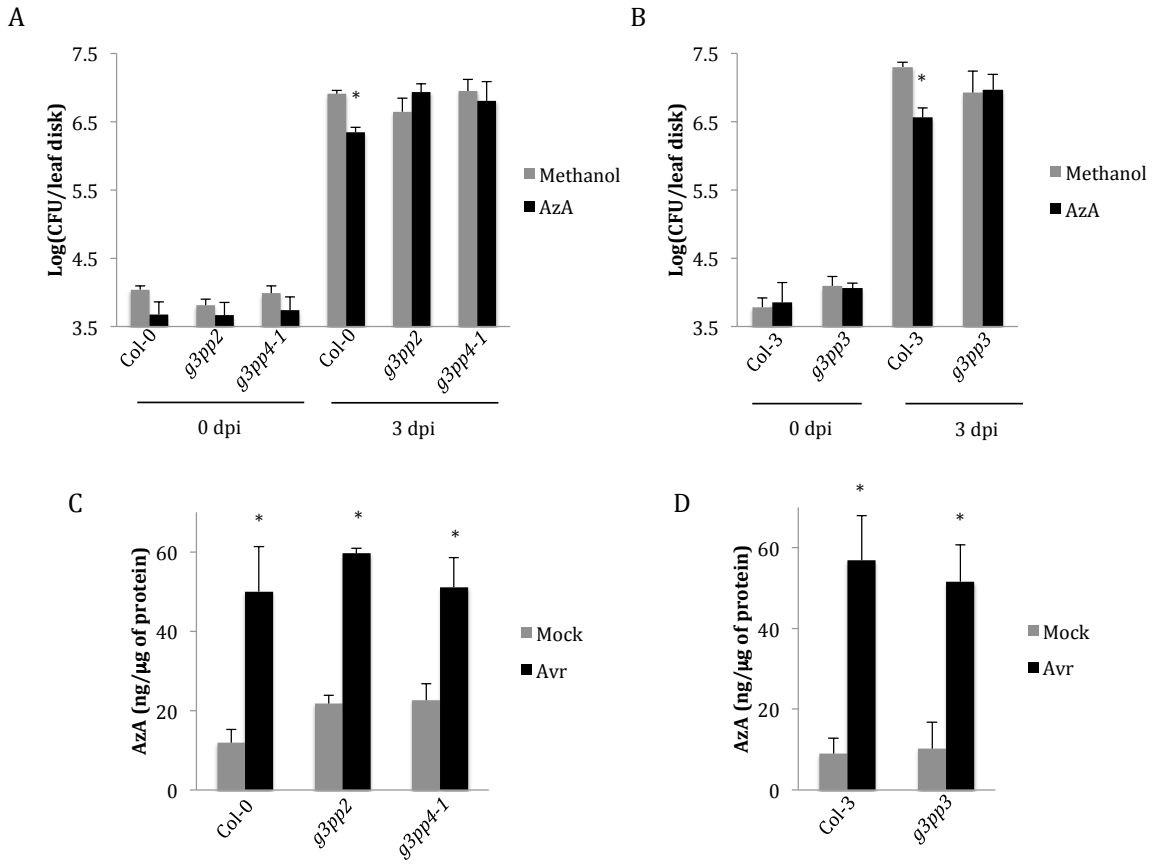

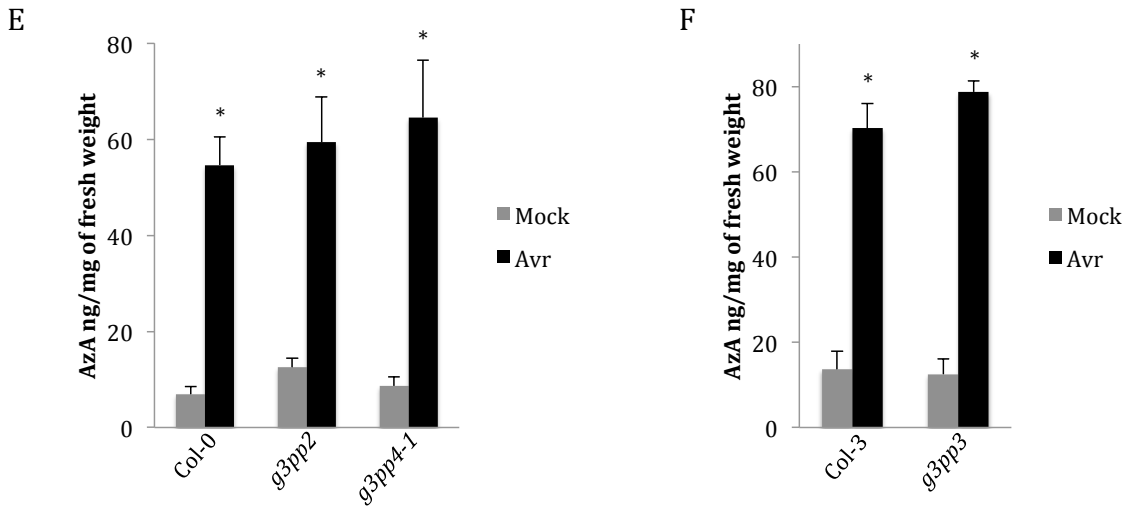

Figure 3.19. Effect of G3Pp mutation on AzA levels.

(A-B) SAR response to primary leaf treatment with methanol or 1 mM AzA in Col-0 and *g3pp*. At 24h post infiltration distal tissues were infected with *Pst* DC3000. Asterisks denote significant differences (t test, $p < 0.05$), and the error bars represent SD (n = 4). **(C-F)** AzA quantification in plant leaf tissues **(C-D)** and **(E-F)** petiole exudates of plants inoculated with *Pst* avrRpt2 in comparison to mock-treatment. Asterisks denote significant differences (t test, $p < 0.05$), and the error bars represent SD (n = 4).

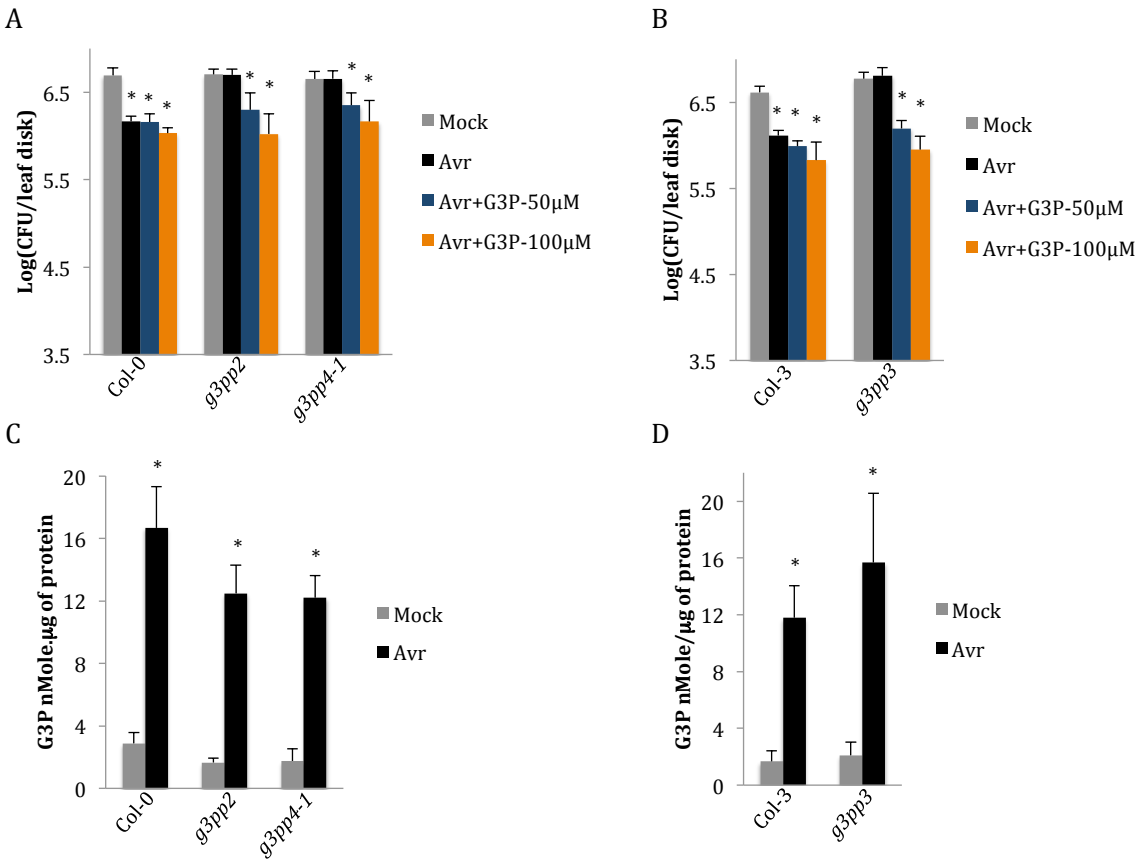

Figure 3.20. Effect of G3Pp mutation on G3P-mediated SAR and G3P levels. **(A-B)** SAR response in Col-0 and *g3pp* plants previously treated with 10 mM $MgCl_2$ or inoculated with *Pst* avrRpt2 supplied or not with 100 or 50 μM G3P. At 24h post infiltration distal tissues were infected with *Pst* DC3000. Asterisks denote significant differences (t test, $p < 0.05$), and the error bars represent SD (n = 4). **(C-D)** G3P levels PEX of plants inoculated with *Pst* avrRpt2 in comparison to mock-treatment. Asterisks denote significant differences (t test, $p < 0.05$), and the error bars represent SD (n = 4).

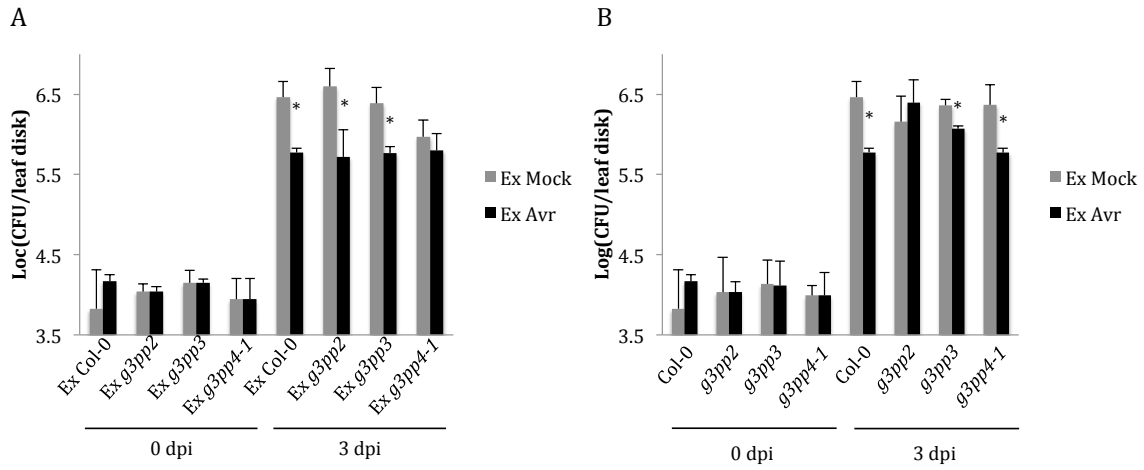

Figure 3.21. SAR signaling generation and perception in *g3pp* mutants.

(A) SAR response in Col-0 plants infiltrated with PEX from Col-0, *g3pp2*, *g3pp3* and *g3pp4-1* knockouts. **(B)** WT and mutant plants infiltrated with Col-0 PEX, 24h later, inoculated with *Pst* virulent strain and resistance quantified after 3 days. The error bars indicate SD (n = 4). Asterisks denote significant difference between treatments and mock infiltrated plants (t test, $p < 0.05$). Results are representative of one experiment.

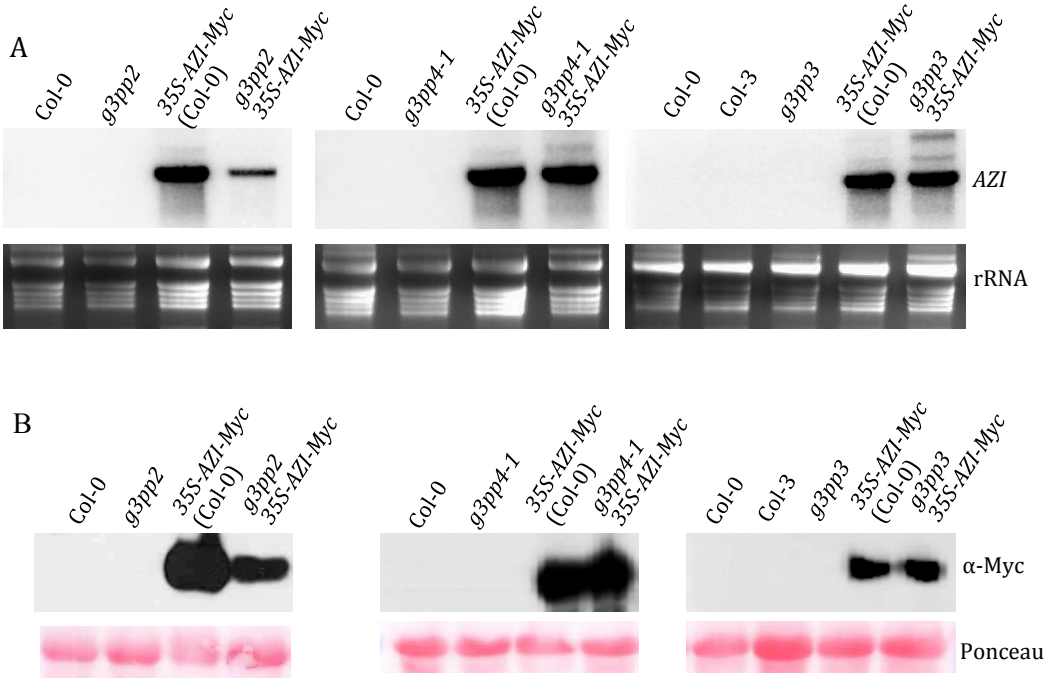

Figure 3.22. AZI stability in *g3pp* mutant backgrounds.

Figure 3.22. AZI stability in *g3pp* mutant backgrounds.

(A) Northern blot analysis of *AZI-Myc* gene expression in transgenic lines overexpressing *35S-AZI1-Myc* in WT and *g3pp* mutant backgrounds. RNA gel-blot analysis was performed on 7 µg of total RNA and *AZI1* probe was used. Ethidium bromide staining of rRNA was used as a loading control. **(B)** Immunoblot showing relative levels of AZI1-Myc protein in WT and *g3pp* mutant backgrounds. Membranes were probed with α-Myc antibody and Ponceau-S staining of the immunoblot was used as the loading control.

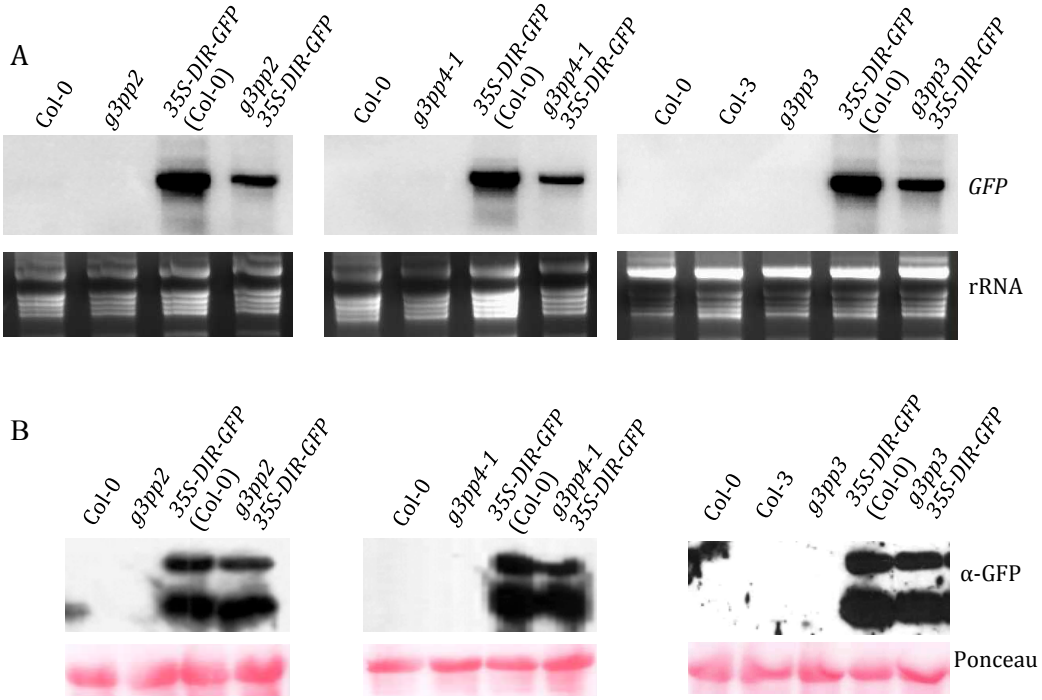

Figure 3.23. DIR stability in *g3pp* mutant backgrounds.

(A) Northern blot analysis of *DIR-GFP* gene expression in transgenic lines overexpressing *35S-DIR-GFP* in WT and *g3pp* mutant backgrounds. RNA gel-blot analysis was performed on 7 µg of total RNA and *GFP* probe was used. Ethidium bromide staining of rRNA was used as a loading control. **(B)** Immunoblot showing

relative levels of DIR-GFP protein in WT and *g3pp* mutant backgrounds. Membranes were probed with α-GFP antibody and Ponceau-S staining of the immunoblot was used as the loading control.

CHAPTER 4

Characterization of *gly1* suppressors

Introduction

Glycerol-3-phosphate (G3P) biosynthesis is catalyzed via Glycerol Kinase (GK) mediated phosphorylation of glycerol or G3P Dehydrogenase (G3Pdh)–mediated reduction of dihydroxy- acetone phosphate (DHAP) (Chanda et al, 2011; Lu et al, 2001; Nandi et al, 2004). The Arabidopsis genome contains five isoforms of G3Pdh that localize to the cytosol (designated as CYT1-At2G41540 and CYT2-At3G07690), chloroplast (designated as GLY1-At2g40690 and CHL-At5G40610) or mitochondria (SDP6-At3g10370) (Chanda et al, 2011; Quettier et al, 2008). A loss-of-function mutation in *CYT2*, *GLY1*, and *CHL* isoforms was shown to compromise systemic acquired resistance (SAR) as well as basal defense against necrotrophic pathogens (Chanda et al, 2008; Chanda et al, 2011). However, among G3Pdh isoforms only GLY1 was required for lipid biosynthesis and a mutation in *GLY1* results in reduced carbon flux through the prokaryotic pathway of lipid biosynthesis (Miquel & Cassagne, 1998). In contrast to *gly1*, a mutation in G3P Acyltransferase (designated as *ACT1*) or Fatty acid Desaturases (designated as *FAD*), also impaired prokaryotic pathway of lipid biosynthesis but did not alter SAR or local defense response (Chanda et al, 2011; Xia et al, 2010). This suggests that the altered carbon flux via the prokaryotic pathway might not contribute to compromise SAR phenotype of *gly1* plants. To identify factors that contributes to altered defense in *gly1*, a suppressor screen was initiated that led to isolation of three putative suppressors. These suppressors showed partial or complete restoration of SAR. This chapter describes characterization of *gly1* suppressors.

Results and discussion

Defense phenotypes are restored in the suppressor of *gly1-1*

An ethyl methanesulfonate (EMS) suppressor screen based on enhanced resistance of *gly1* to *Colletotrichum higginsianum* was carried out by the host laboratory and led to isolation of three putative suppressors. These were designated as *gly1-1 Sup1-Sup3*, and as expected the mutants showed *gly1* specific genotypes **(Figure 4.1A)**. Consistent with their genotype, all the suppressors show reduced levels of 16:3 fatty acids **(Figure 4.1B)**, suggesting that the suppressor mutation did not restore the altered prokaryotic pathway. Unlike the fatty acid phenotype, *gly1 Sup1* but not *gly1 Sup2* and *gly1-1 Sup3,* showed wild-type-like resistance to *C. higginsianum* **(Figure 4.2A-B)**. For SAR analysis, the wild type, *gly1* and suppressors were inoculated with *Pst* avrRpt2 and followed by inoculation with virulent *Pst* DC3000 two days post avirulent inoculation. As shown earlier (Chanda et al, 2011), the *gly1* plants showed compromised SAR **(Figure 4.3A)**. Unlike their response to *C. higginsianum*, the *gly1 Sup1* showed nominal or no SAR while *gly1 Sup2* and *gly1 Sup3* showed wild-type-like SAR **(Figure 4.3A)**. All three *gly1 Sup* mutants showed *gly1-1*-like basal resistance **(Figure 4.2C).** To determine the genetic basis of the suppressor mutation, I backcrossed *gly1 Sup3* plants with the *gly1* parent and analyzed the SAR phenotype in the individual F1 progeny. All the F1 plants showed compromised SAR **(Figure 4.3B)**, suggesting that the suppressor mutation was recessive in nature. To confirm this result I assayed SAR in F3 pools prepared from 16 *gly1* homozygous F2 plants derived from *gly1* x *gly1 Sup3* crosses. Two of 8 F3 plants showed normal SAR **(Figure 4.4C-D)**, which is consistent with monogenic recessive inheritance. This was further confirmed by analyzing *gly1* homozygous F3 pools derived from the Col-0 x *gly1 Sup3* cross; two of eight F3 pools showed normal SAR **(Figure 4.5A)**. One of these F3 pools showing normal SAR was used for a second backcross (BC) with Col-0 and the resulting BC2 F2 population was genotyped for the *gly1* locus and the *gly1* homozygous plants were assayed for SAR. The *gly1* homozygous plants from the second backcross also segregated for SAR in a monogenic recessive manner **(Figure**

4.5B-C). Together, these results suggested that *gly1-1 Sup3* was a recessive mutation that normalized the compromised SAR phenotype of the *gly1* plants.

AzA and SA confer SAR on *gly1 Sup3*

The induction of SAR is dependent on SA and AzA and as described above these chemical signals operate in parallel (Gao et al, 2014b; Wang et al, 2014). Furthermore, AzA acts upstream of G3P and consequently AzA is unable to confer SAR on mutants that are defective in G3P biosynthesis (like *gly1*). Consistent with previous results (Chanda et al, 2011), the *gly1* plants showed normal induction of the *PR-1* gene in response to *Pst* avrRpt2 **(Figure 4.6A)**, suggesting that these plants accumulate normal levels of SA. Likewise, *gly1 Sup3* also induced normal expression of *PR-1* in response to avirulent inoculation. However, unlike wild-type plants, exogenous SA was unable to confer SAR on *gly1* plants **(Figure 4.6B)**. This result was consistent with the fact that *gly1* plants do not accumulate G3P and therefore are unable to activate the AzA-G3P branch of the SAR pathway. However, SA treatment was able to confer SAR on *gly1 Sup3* plants **(Figure 4.6B)**. Next, AzA-mediated SAR was assayed on *gly1 Sup3* plants. Since AzA acts upstream of *GLY1*, exogenous AzA was unable to confer SAR on *gly1* plants. Interestingly, AzA treatment conferred normal SAR on *gly1 Sup3* plants **(Figure 4.6C)**. Together, these results suggested that the suppressor mutation was able to restore wild-type-like SAR signaling in the *gly1* background. It is possible that the *gly1-1 Sup3* mutation restored SAR by normalizing G3P levels or signaling downstream of G3P. Further characterization of *SUP3* should yield novel insights into factors modulating G3P-mediated signaling in plants.

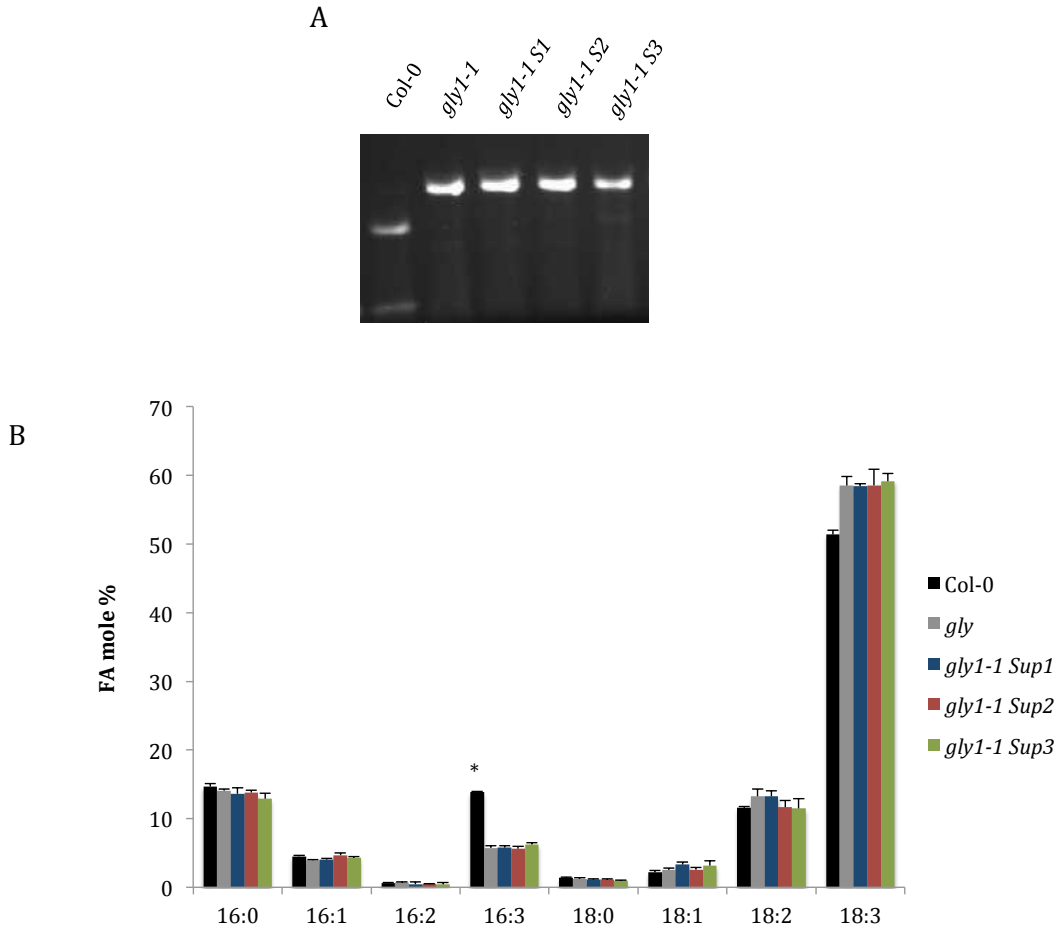

Figure 4.1. *gly1-1 Sup* genotyping and FA profile.

(A) PCR-amplified products from Col-0, *gly1-1*, *gly1-1 Sup1*, *gly1-1 Sup2*, *gly1-1 Sup3* digested with BstNI and resolved on a 3.5% w/v agarose gel. **(B)** Moles percentage of leaf FA levels in 4-week-old Col-0, *gly1-1*, *gly1-1 Sup1*, *gly1-1 Sup2*, *gly1-1 Sup3*. The values are presented as means of four replicates. Asterisks denote a significant difference with wild type (t-test, $P < 0.05$). FW indicates fresh weight. Error bars represent SD (n=4). Asterisks denote a significant difference with wild type (t test, $P<0.05$).

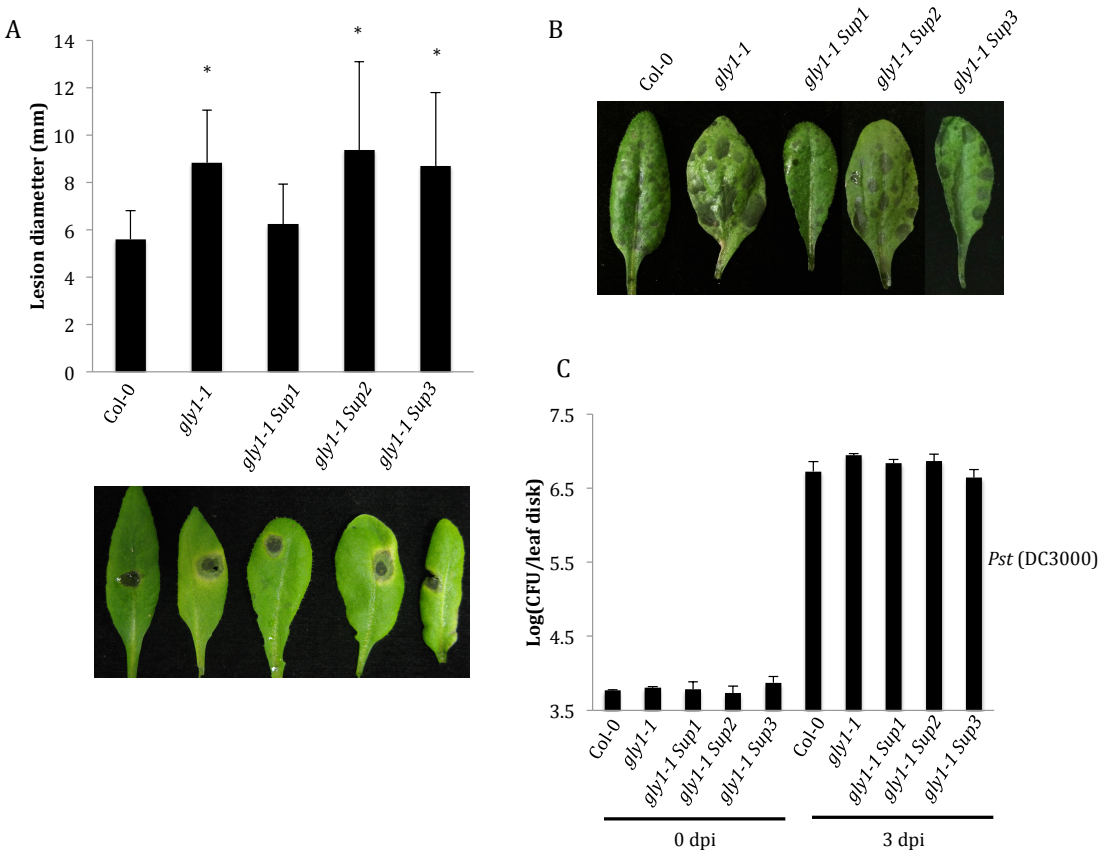

Figure 4.2. Basal defense responses in the *Sup* plants.

Disease symptoms on Col-0, *gly1-1*, *gly1-1 Sup1*, *gly1-1 Sup2*, *gly1-1 Sup3* inoculated with *C. higginsianum*. **(A)** The plants were spot inoculated with $2x10^6$ spores/mL of *C. higginsianum* and the lesion size was measured from 30 to 50 independent leaves at 5 dpi. Statistical significance was determined using Student's t test. Asterisks indicate data that are statistically significant from that of control. Error bars indicate standard deviation. **(B)** Plants were spray inoculated with $2x10^6$ spores/mL and the leaves were photographed at 3 dpi. **(C)** Basal disease resistance inferred by bacterial colony counts of plants inoculated with *Pst* DC3000

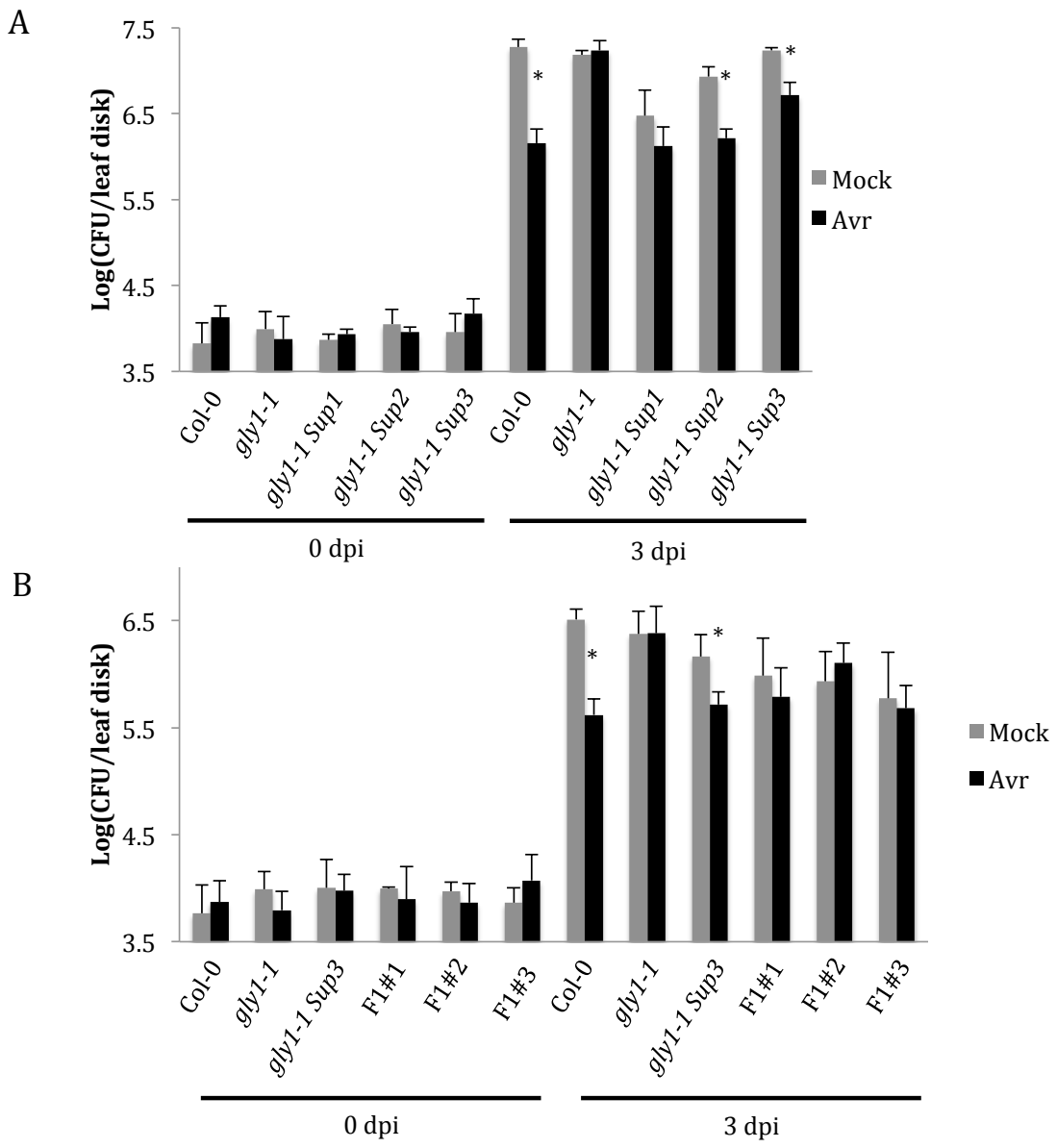

Figure 4.3. SAR phenotype in *gly1-1 Sup* plants.

(A) SAR response in distal leaves of WT, *gly1-1* mutant plants and *gly1-1 Sup*. **(B)** SAR phenotype of F1 population of *gly1-1 Sup3* backcrossed to *gly1-1*. The plants were treated locally with $MgCl_2$ or inoculated with *Pst* avrRpt2. The virulent pathogen *Pst* DC3000 was inoculated in distal leaves 48 h after local treatments. Error bars indicate SD (n = 4).

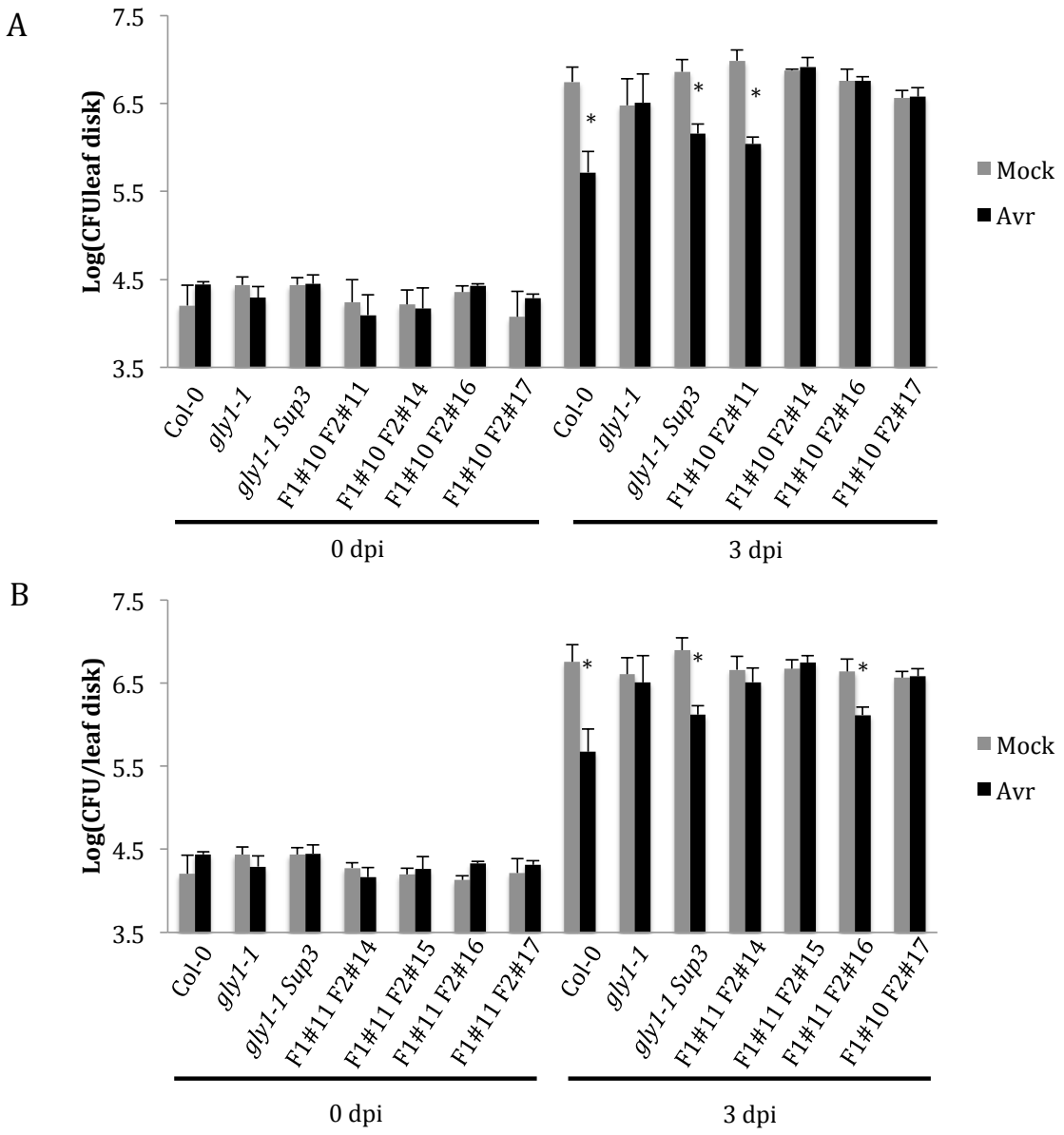

Figure 4.4. SAR response in F3 population derived from *gly1-1 Sup3* x *gly1-1* backcross.

SAR phenotype of wild type, *gly1-1* and backcrosses between *gly1-1 Sup3* and *gly1-1* **(A)** F1#10 and **(B)** F1#11. Plants were treated locally with $MgCl_2$ or inoculated with pathogen. The virulent pathogen *Pst* DC3000 was inoculated 48 h after local treatments. Error bars indicate SD (n = 4).

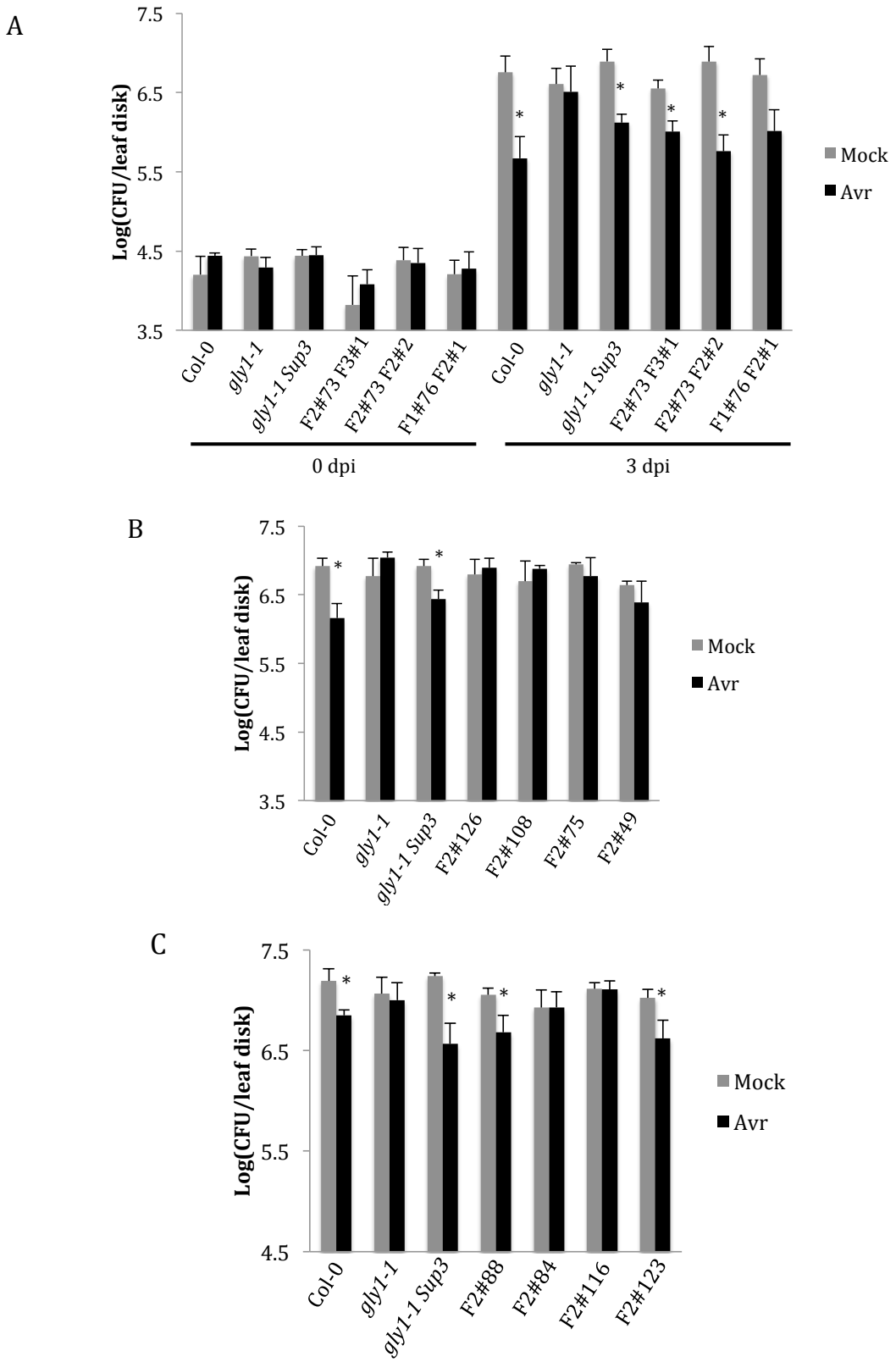

Figure 4.5. SAR response in F3 plants derived from the *gly1-1 S3* x Col-0 cross.

Figure 4.5. SAR response in F3 plants derived from the *gly1-1 S3* x Col-0 cross. **(A-C)** SAR response in distal leaves of wild type and mutants treated locally with $MgCl_2$ or inoculated with pathogen. The virulent pathogen *Pst* DC3000 was inoculated 48 h after local treatments. Error bars indicate SD (n = 4). **(A)** SAR phenotype in Col-0, gly1-1 and F3 plants of *gly1-1 Sup3* backcrossed to Col-0 F1#4 F2#73 and F1#4 F2#76. **(B-C)** SAR induction in F3 plants of a second backcross between Col-0 and *gly1-1 Sup3* x Col-0 F1#4 F2#73

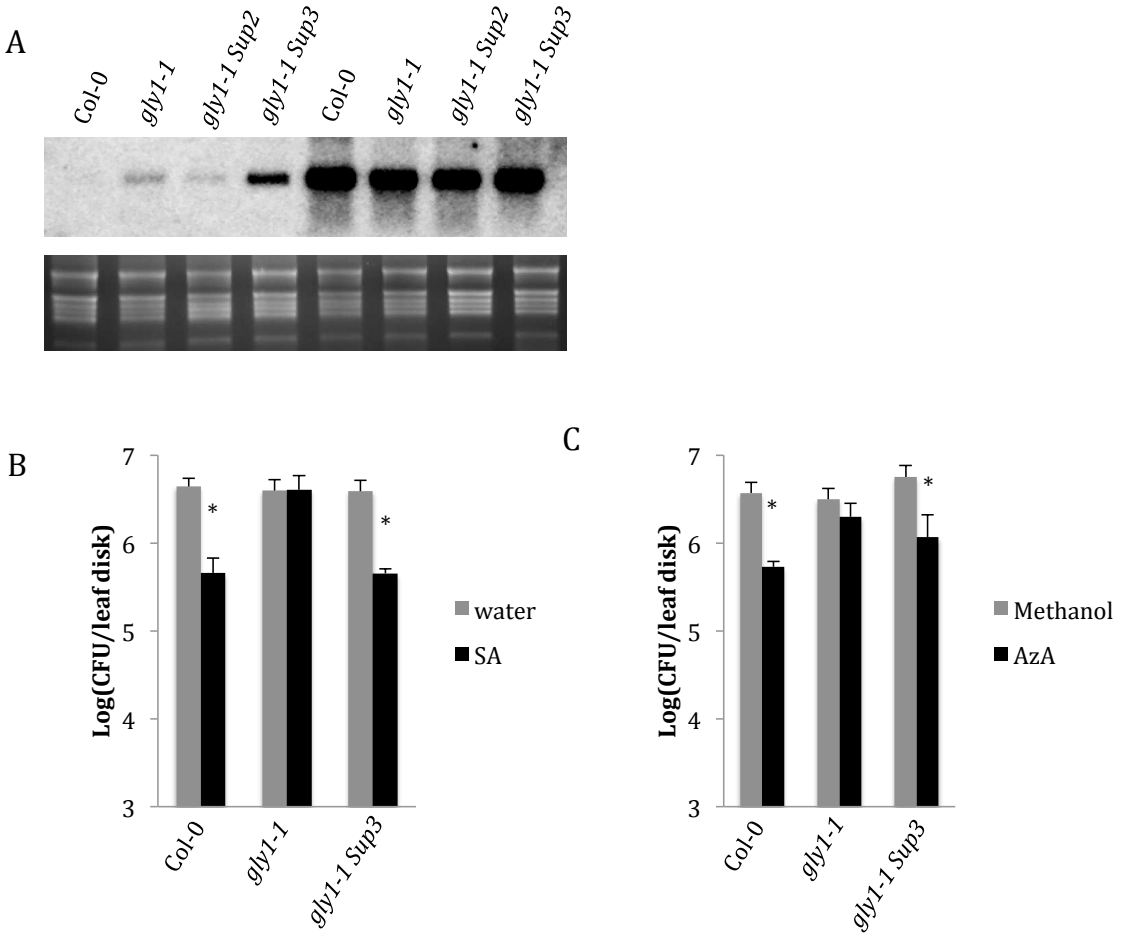

Figure 4.6. AzA and SA chemically induced SAR on *gly1 Sup3*.

Figure 4.6. AzA and SA chemically induced SAR on *gly1 Sup3*.

(A) Northern blot analysis of *PR-1* gene expression after avr pathogen infection (*Pst* avrRpt2) in Col-0, *gly1-1*, *gly1-1 Sup1*, *gly1-1 Sup2*, *gly1-1 Sup3*. RNA gel-blot analysis was performed on 7 µg of total RNA. Ethidium bromide staining of rRNA was used as a loading control. **(B-C)** SAR response in distal leaves of WT and mutant plants treated locally with **(B)** water or SA and **(C)** 0.01% v/v methanol or AzA. The virulent pathogen *Pst* DC3000 was inoculated 48 h after local treatments. Error bars indicate SD (n = 4).

CHAPTER 5

Conclusion and future prospects

The data presented in this study suggests that G3Pp2, G3Pp3 and G3Pp4 play an important role in SAR, possibly via regulating G3P levels. This is based on the results that exogenous G3P was able to restore normal SAR in *g3pp* mutants and *G3Pp1* and *G3Pp3* complemented *E. coli GlpT* mutation. Since G3Pp isoforms are predicted to localize in chloroplast, mitochondria or plasma membrane, a non-redundant requirement for three G3Pp proteins in SAR suggests that G3P partitioning might play an important role. It is possible that infiltration of G3P allows diffusion across various sub-cellular compartments, thereby restoring SAR. More is required to establish a role of G3Pp proteins in sub-cellular transport of G3P. Likewise, the *gly1* suppressor mutation might also regulate cellular pool of G3P or a factor that operates downstream of G3P. Further characterization of *gly1 Sup3* plants and cloning of *SUP3* should yield exciting insights into G3P-mediated signaling in plants.

APPENDIX

LIST OF ABREVIATION

Acronym/ abbreviation	Expansion
aa	Amino acid
A_{260}	Absorbance measured at a wavelength of 260 nm
A_{600}	Absorbance measured at a wavelength of 600 nm
ACT1	G3P Acyltransferase
AGTC	Advanced Genetic Technologies Center
AGI	Arabidopsis Genome Initiative
ALD1	AGD2-like Defense Response Protein1
Avr	Avirulence
AzA	Azelaic Acid
AZI1	AzA Insensitive
BC	Backcross
BHT	Butylated Hydroxytoluene
BSA	Bovine serum albumin
C18	Fatty acid of 18 carbon
$CaCl_2$	Calcium chloride
CAPS	Cleaved Amplified Polymorphic Sequence
CC	Coiled-coil
cDNA	Complementary DNA
CERK1	Chitin Elicitor Receptor Kinase 1
CFU	Colony-forming unit
CH_3CO_2K	Potassium Acetate
CNL	CC-Nucleotide Binding Site-Leucine Rich Repeat
CUL3	Cullin Homolog 3
DA	Dehydroabietinal
DAB	3,3'-diaminobenzidine
dATP	Deoxyadenosine triphosphate
dCAPS	Derived Cleaved Amplified Polymorphic Sequence
dCTP	Deoxycytidine triphosphate
DGDG	Digalactosyldiacylglycerol
dGTP	Deoxyguanosine triphosphate
DNA	Deoxyribonucleic Acid
dpi	Days Post Inoculation
DTT	Dithiothreitol
dTTP	Thymidine triphosphate
EDTA	Ethylenediaminetetraacetic acid
EMS	Ethyl methanesulfonate
ETI	Effector-triggered immunity
FA	Fatty Acid

Acronym/ abbreviation	Expansion
FAD	Fatty Acid Desaturases
fl22	Flagellin
FLS2	Flagellin Sensing 2
FW	Fresh weight
GFP	Green Fluorescent Protein
G3P	Glycerol-3-phosphate
G3Pdh	G3P Dehydrogenase
G3Pp	G3P Permeases
GK	Glycerol Kinase
g	Gram
GC	Gas Chromatography
GC-MS	GC–mass spectrometry
h	Hours
H_2O_2	Hydrogen Peroxide
H_2SO_4	Sulfuric acid
HPLC	High-performance liquid chromatography
HR	Hypersensitive Response
ISR	Induced Systemic Resistance
Ci	Inward Facing
Co	Outward Facing
JW22-34	*E. coli* knockout strain (ΔG3Pp)
K_2HPO_4	Potassium phosphate dibasic
KCl	Potassium Chloride
kDA	kilodalton
KO	knock-out
KOH	Potassium Hydroxide
Kb	Kilobase
L	Liter
LB	Luria-Bertani medium
LRR	Leucine Rich Repeat
LTP	Lipid Transfer Proteins
M	Mol
mb	Membrane
MeSA	Methylatyl Salicylate
mg	miligram
$MgCl_2$	Magnesium chloride
MGDG	Monogalactosyldiacylglycerol
min	Minutes
mL	Milliliter
mM	Millimolar
MOPS	3-morpholinopropane-1-sulfonic acid
MS	Murashige and Skoog

Acronym/ abbreviation	Expansion
$MgSO_4$ $7H_20$	Magnesium Sulfate Heptahydrate
MSTFA	N-Methyl-N-(trimethylsilyl)trifluoroacetamide
MTBSTFA	N-tert-Butyldimethylsilyl-N-methyltrifluoroacetamide
N-terminus	Amino-terminus, NH2-terminus
NaCl	Sodium Chloride
NaOAc	Sodium acetate
NaOH	Sodium Hydroxide
NBS	Nucleotide Binding Site
ng	nanogram
NHR	Non-host resistance
NO	Nitric Oxide
NPR1	Non-Expressor of Pathogenesis-Related Protein 1
o/n	Overnight
OD	Optical Density
PAMP	Pathogen Associated Molecular Pattern
PCR	Polymerase Chain Reaction
PD	Plasmodesmata
PDLP	Plasmodesmata Localizing Protein
PFD	Photon Flux Density
pH	Potential of Hydrogen
Pi	Inorganic Phosphate
Pip	Pipecolic Acid
PR-1	Pathogenesis-Related Protein 1
PRR	PATTERN RECOGNITION RECEPTORS
Pst avrRpt2	*Pseudomonas syringae* pv *tomato* (avrRpt2)
Pst DC3000	*Pseudomonas syringae* pv *tomato* (DC3000)
PTI	Pathogen Associated Molecular Pattern-triggered immunity
PVDF	Polyvinylidene difluoride
R	Resistance protein
$RbCl_2$	Rubidium chloride
RIN4	RPM1-INTERACTING PROTEIN 4
RNA	Ribonucleic Acid
RNase	Ribonuclease
ROS	Reactive Oxygen Species
RPM	Rotations in one minute
RPM1	Resistance to *Pseudomonas syringae* pv. *maculicola* 1
RPS2	Resistant to *Pseudomonas syringae* 2
RT-PCR	Reverse Transcription Polymerase Chain Reaction
SD	Standard deviation
SDS	Sodium dodecyl sulfate
SSC	3 M NaCl and 0.3 M Na citrate
SA	Salicylic Acid

Acronym/ abbreviation	Expansion
SAR	Systemic acquired resistance
tDNA	Transfer DNA
TIR1	Toll Interleukin-1
TMDs	Transmembrane Domains
TNL	TIR1-Nucleotide Binding Site-Leucine Rich Repeat
Tris-HCl	Tris(hydroxymethyl)aminomethane hydrochloride
TUB	Tubulin
UV	Ultraviolet
v/v	volume/volume
w/v	Weight/volume
w/w	Weight/weight
WT	Wild type
x g	Times gravity
µF	Microfarad
µg	Microgram
µL	Microliter
µmole	Micromole
µCi	Microcurie
µM	micromolar
%	Percentage
~	Approximately
Ω	Omega
^{o}C	Degrees Celsius
17:0	Heptadecanoic Acid
Δ	Delta: meaning deletion

REFERENCES

Agrios GN (2005) Plant Pathology. 5th eds. *Elsevier Academic Press USA* **8:** 1-40

Baba T, Ara T, Hasegawa M, Takai Y, Okumura Y, Baba M, Datsenko KA, Tomita M, Wanner BL, Mori H (2006) Construction of Escherichia coli K‐12 in‐frame, single‐gene knockout mutants: the Keio collection. *Molecular systems biology* **2**

Bartoloni L, Wattenhofer M, Kudoh J, Berry A, Shibuya K, Kawasaki K, Wang J, Asakawa S, Talior I, Bonne-Tamir B (2000) Cloning and characterization of a putative human glycerol 3-phosphate permease gene (SLC37A1 or G3PP) on 21q22. 3: mutation analysis in two candidate phenotypes, DFNB10 and a glycerol kinase deficiency. *Genomics* **70:** 190-200

Blazquez J, Alexandro R-R. (2013) Molecular Mechanisms and Clinical Impact of Acquired and Intrinsic Fosfomycin Resistance. Antibiotics, Vol. 2, pp. 217-236.

Boller T, Felix G (2009) A renaissance of elicitors: perception of microbe-associated molecular patterns and danger signals by pattern-recognition receptors. *Annual review of plant biology* **60:** 379-406

Bradford MM (1976) A rapid and sensitive method for the quantitation of microgram quantities of protein utilizing the principle of protein-dye binding. *Analytical biochemistry* **72:** 248-254

Cao H, Bowling SA, Gordon AS, Dong X (1994) Characterization of an Arabidopsis mutant that is nonresponsive to inducers of systemic acquired resistance. *The Plant Cell* **6:** 1583-1592

Castaneda-García A, Rodríguez-Rojas A, Guelfo JR, Blazquez J. (2009) Glycerol-3-Phosphate Permease GlpT Is the Only Fosfomycin Transporter in Pseudomonas aeruginosa. JOURNAL OF BACTERIOLOGY, pp. 6968–6974.

Chanda B, Venugopal SC, Kulshrestha S, Navarre DA, Downie B, Vaillancourt L, Kachroo A, Kachroo P (2008) Glycerol-3-phosphate levels are associated with basal resistance to the hemibiotrophic fungus Colletotrichum higginsianum in Arabidopsis. *Plant physiology* **147:** 2017-2029

Chanda B, Xia Y, Mandal MK, Yu K, Sekine KT, Gao Q-m, Selote D, Hu Y, Stromberg A, Navarre D (2011) Glycerol-3-phosphate is a critical mobile inducer of systemic immunity in plants. *Nature genetics* **43:** 421-427

Chaturvedi R, Venables B, Petros RA, Nalam V, Li M, Wang X, Takemoto LJ, Shah J (2012) An abietane diterpenoid is a potent activator of systemic acquired resistance. *The Plant Journal* **71:** 161-172

Chinchilla D, Bauer Z, Regenass M, Boller T, Felix G (2006) The Arabidopsis receptor kinase FLS2 binds flg22 and determines the specificity of flagellin perception. *The Plant Cell* **18:** 465-476

Choudhary DK, Prakash A, Johri BN (2007) Induced systemic resistance (ISR) in plants: mechanism of action. *Indian Journal of Microbiology* **47:** 289-297

Delledonne M, Zeier J, Marocco A, Lamb C (2001) Signal interactions between nitric oxide and reactive oxygen intermediates in the plant hypersensitive disease resistance response. *Proceedings of the National Academy of Sciences* **98:** 13454-13459

Downie BA (1994) Sugar content and endo-beta-mannanase activity in white spruce (Picea glauca (Moench.), Voss.) seeds during germination.

Eiglmeier K, Boos W, Cole ST (1987) Nucleotide sequence and transcriptional startpoint of the glpT gene of Escherichia coli: extensive sequence homology of the glycerol‐3‐phosphate transport protein with components of the hexose‐6‐phosphate transport system. *Molecular microbiology* **1:** 251-258

Elashvili I, DeFrank JJ, Culotta VC (1998) phnE and glpT Genes Enhance Utilization of Organophosphates in Escherichia coliK-12. *Applied and environmental microbiology* **64:** 2601-2608

Elvin CM, Hardy CM, Rosenberg H (1985) Pi exchange mediated by the GlpT-dependent sn-glycerol-3-phosphate transport system in Escherichia coli. *Journal of bacteriology* **161:** 1054-1058

Freialdenhoven A, Peterhansel C, Kurth J, Kreuzaler F, Schulze-Lefert P (1996) Identification of genes required for the function of non-race-specific mlo resistance to powdery mildew in barley. *The Plant Cell* **8:** 5-14

Frohlich KM, Roberts RAW, Housley NA, Audia JP (2010) Rickettsia prowazekii uses an sn-glycerol-3-phosphate dehydrogenase and a novel dihydroxyacetone phosphate transport system to supply triose phosphate for phospholipid biosynthesis. *Journal of bacteriology* **192:** 4281-4288

Gaffney T, Friedrich L, Vernooij B, Negrotto D, Nye G, Uknes S, Ward E, Kessmann H, Ryals J (1993) Requirement of salicylic acid for the induction of systemic acquired resistance. *SCIENCE-NEW YORK THEN WASHINGTON-* **261:** 754-754

Gao Q-m, Kachroo A, Kachroo P (2014a) Chemical inducers of systemic immunity in plants. *Journal of experimental botany* **65:** 1849-1855

Gao Q-m, Yu K, Xia Y, Shine MB, Wang C, Navarre D, Kachroo A, Kachroo P (2014b) Mono-and digalactosyldiacylglycerol lipids function nonredundantly to regulate systemic acquired resistance in plants. *Cell reports* **9:** 1681-1691

Gill US, Lee S, Mysore KS (2015) Host versus nonhost resistance: distinct wars with similar arsenals. *Phytopathology* **105:** 580-587

Glazebrook J, Zook M, Mert F, Kagan I, Rogers EE, Crute IR, Holub EB, Hammerschmidt R, Ausubel FM (1997) Phytoalexin-deficient mutants of Arabidopsis reveal that PAD4 encodes a regulatory factor and that four PAD genes contribute to downy mildew resistance. *Genetics* **146:** 381-392

Gómez-Gómez L, Boller T (2000) FLS2: An LRR receptor–like kinase involved in the perception of the bacterial elicitor flagellin in Arabidopsis. *Molecular cell* **5:** 1003-1011

Gubellini F, Verdon G, Karpowich NK, Luff JD, Boël G, Gauthier N, Handelman SK, Ades SE, Hunt JF (2011) Physiological response to membrane protein overexpression in E. coli. *Molecular & Cellular Proteomics* **10:** M111. 007930

Hirai T, Heymann JAW, Maloney PC, Subramaniam S (2003) Structural model for 12-helix transporters belonging to the major facilitator superfamily. *Journal of bacteriology* **185:** 1712-1718

Hirai T, Heymann JAW, Shi D, Sarker R, Maloney PC, Subramaniam S (2002) Three-dimensional structure of a bacterial oxalate transporter. *Nature Structural & Molecular Biology* **9:** 597-600

Huang Y, Lemieux MJ, Song J, Auer M, Wang D-N (2003) Structure and mechanism of the glycerol-3-phosphate transporter from Escherichia coli. *Science* **301:** 616-620

Jenns AE, Kuc J (1979) Graft transmission of systemic resistance of cucumber to anthracnose induced by Colletotrichum lagenarium and tobacco necrosis virus. *Phytopathology*

Jomaa H, Wiesner J, Sanderbrand S, Altincicek B, Weidemeyer C, Hintz M, Türbachova I, Eberl M, Zeidler J, Lichtenthaler HK (1999) Inhibitors of the nonmevalonate pathway of isoprenoid biosynthesis as antimalarial drugs. *Science* **285:** 1573-1576

Jones JD, Dangl JL (2006) The plant immune system. *Nature* **444:** 323-329

Jung HW, Tschaplinski TJ, Wang L, Glazebrook J, Greenberg JT (2009) Priming in systemic plant immunity. *Science* **324:** 89-91

Kaback HR, Wu J (1997) From membrane to molecule to the third amino acid from the left with a membrane transport protein. *Quarterly reviews of biophysics* **30:** 333-364

Kachroo A, Lapchyk L, Fukushige H, Hildebrand D, Klessig D, Kachroo P (2003) Plastidial fatty acid signaling modulates salicylic acid–and jasmonic acid–mediated defense pathways in the Arabidopsis ssi2 mutant. *The Plant Cell* **15:** 2952-2965

Kachroo A, Robin GP (2013) Systemic signaling during plant defense. *Current opinion in plant biology* **16:** 527-533

Kachroo A, Venugopal SC, Lapchyk L, Falcone D, Hildebrand D, Kachroo P (2004) Oleic acid levels regulated by glycerolipid metabolism modulate defense gene expression in Arabidopsis. *Proceedings of the National Academy of Sciences of the United States of America* **101:** 5152-5157

Kachroo P, Kachroo A (2018) Plants pack a quiver full of arrows. *Cell Host & Microbe*

Kachroo P, Shanklin J, Shah J, Whittle EJ, Klessig DF (2001) A fatty acid desaturase modulates the activation of defense signaling pathways in plants. *Proceedings of the National Academy of Sciences* **98:** 9448-9453

Kawai H, Ishikawa T, Mitsui T, Kore-eda S, Yamada-Kawai M, Ohnishi J-i (2014) Arabidopsis glycerol-3-phosphate permease 4 is localized in the plastids and involved in the accumulation of seed oil. *Plant Biotechnology* **31:** 159-165

Khandjian EW (1986) UV crosslinking of RNA to nylon membrane enhances hybridization signals. *Molecular biology reports* **11:** 107-115

King EO, Ward MK, Raney DE (1954) Two simple media for the demonstration of pyocyanin and fluorescin. *Translational Research* **44:** 301-307

Konieczny A, Ausubel FM (1993) A procedure for mapping Arabidopsis mutations using co‐dominant ecotype‐specific PCR‐based markers. *The Plant Journal* **4:** 403-410

Kulik A, Noirot E, Grandperret V, Bourque S, Fromentin J, Salloignon P, Truntzer C, Dobrowolska G, Simon‐Plas F, Wendehenne D (2015) Interplays between nitric oxide and reactive oxygen species in cryptogein signalling. *Plant, cell & environment* **38:** 331-348

Lee J-Y (2015) Plasmodesmata: a signaling hub at the cellular boundary. *Current opinion in plant biology* **27:** 133-140

Lim G-H, Shine MB, de Lorenzo L, Yu K, Cui W, Navarre D, Hunt AG, Lee J-Y, Kachroo A, Kachroo P (2016) Plasmodesmata localizing proteins regulate transport and signaling during systemic acquired immunity in plants. *Cell host & microbe* **19:** 541-549

Lindermayr C, Sell S, Müller B, Leister D, Durner J (2010) Redox regulation of the NPR1-TGA1 system of Arabidopsis thaliana by nitric oxide. *The Plant Cell* **22:** 2894-2907

Liu T, Liu Z, Song C, Hu Y, Han Z, She J, Fan F, Wang J, Jin C, Chang J (2012) Chitin-induced dimerization activates a plant immune receptor. *Science* **336:** 1160-1164

Lu M, Tang X, Zhou J-M (2001) Arabidopsis NHO1 is required for general resistance against Pseudomonas bacteria. *The Plant Cell* **13:** 437-447

Luna E, Bruce TJ, Roberts MR, Flors V, Ton J (2012) Next-generation systemic acquired resistance. *Plant physiology* **158:** 844-853

Mackey D, Belkhadir Y, Alonso JM, Ecker JR, Dangl JL (2003) Arabidopsis RIN4 is a target of the type III virulence effector AvrRpt2 and modulates RPS2-mediated resistance. *Cell* **112:** 379-389

Mackey D, Holt BF, Wiig A, Dangl JL (2002) RIN4 interacts with Pseudomonas syringae type III effector molecules and is required for RPM1-mediated resistance in Arabidopsis. *Cell* **108:** 743-754

Maiden MCJ, Davis EO, Baldwin SA, Moore DCM, Henderson PJF (1987) Mammalian and bacterial sugar transport proteins are homologous. *Nature* **325:** 641-643

Maldonado AM, Doerner P, Dixon RA, Lamb CJ, Cameron RK (2002) A putative lipid transfer protein involved in systemic resistance signalling in Arabidopsis. *Nature* **419:** 399-403

McHale L, Tan X, Koehl P, Michelmore RW (2006) Plant NBS-LRR proteins: adaptable guards. *Genome biology* **7:** 212

Meinken J, Min J (2012) Computational prediction of protein subcellular locations in eukaryotes: an experience report. *Computational Molecular Biology* **2**

Miquel M, Cassagne C (1998) A new class of Arabidopsis mutants with reduced hexadecatrienoic acid fatty acid levels. *Plant physiology* **117:** 923-930

Miya A, Albert P, Shinya T, Desaki Y, Ichimura K, Shirasu K, Narusaka Y, Kawakami N, Kaku H, Shibuya N (2007) CERK1, a LysM receptor kinase, is essential for chitin elicitor signaling in Arabidopsis. *Proceedings of the National Academy of Sciences* **104:** 19613-19618

Moradi M, Enkavi G, Tajkhorshid E (2015) Atomic-level characterization of transport cycle thermodynamics in the glycerol-3-phosphate: phosphate antiporter. *Nature communications* **6:** 8393

Mou Z, Fan W, Dong X (2003) Inducers of plant systemic acquired resistance regulate NPR1 function through redox changes. *Cell* **113:** 935-944

Mysore KS, Ryu C-M (2004) Nonhost resistance: how much do we know? *Trends in plant science* **9:** 97-104

Nakagawa T, Kurose T, Hino T, Tanaka K, Kawamukai M, Niwa Y, Toyooka K, Matsuoka K, Jinbo T, Kimura T (2007) Development of series of gateway binary vectors, pGWBs, for realizing efficient construction of fusion genes for plant transformation. *Journal of bioscience and bioengineering* **104:** 34-41

Nandi A, Welti R, Shah J (2004) The Arabidopsis thaliana dihydroxyacetone phosphate reductase gene SUPPRESSOR OF FATTY ACID DESATURASE DEFICIENCY1 is required for glycerolipid metabolism and for the activation of systemic acquired resistance. *The Plant Cell* **16:** 465-477

Návarová H, Bernsdorff F, Döring A-C, Zeier J (2012) Pipecolic acid, an endogenous mediator of defense amplification and priming, is a critical regulator of inducible plant immunity. *The Plant Cell* **24:** 5123-5141

Neff MM, Neff JD, Chory J, Pepper AE (1998) dCAPS, a simple technique for the genetic analysis of single nucleotide polymorphisms: experimental applications in Arabidopsis thaliana genetics. *The Plant Journal* **14:** 387-392

Oparka KJ (1993) Signalling via plasmodesmata—the neglected pathway, Vol. 4, pp 131-138

Pao SS, Paulsen IT, Saier MH (1998) Major facilitator superfamily. *Microbiology and molecular biology reviews* **62:** 1-34

Park S-W, Kaimoyo E, Kumar D, Mosher S, Klessig DF (2007) Methyl salicylate is a critical mobile signal for plant systemic acquired resistance. *Science* **318:** 113-116

Peart JR, Lu R, Sadanandom A, Malcuit I, Moffett P, Brice DC, Schauser L, Jaggard DAW, Xiao S, Coleman MJ (2002) Ubiquitin ligase-associated protein SGT1 is required for host and nonhost disease resistance in plants. *Proceedings of the National Academy of Sciences* **99:** 10865-10869

Pieterse CMJ, Leon-Reyes A, Van der Ent S, Van Wees SCM (2009) Networking by small-molecule hormones in plant immunity. *Nature chemical biology* **5:** 308-316

Pitzschke A, Datta S, Persak H (2014) Salt stress in Arabidopsis: lipid transfer protein AZI1 and its control by mitogen-activated protein kinase MPK3. *Molecular plant* **7:** 722-738

Quettier A-L, Shaw E, Eastmond P (2008) SUGAR-DEPENDENT6 encodes a mitochondrial FAD-dependent glycerol-3-phosphate dehydrogenase, which is required for glycerol catabolism and post-germinative seedling growth in Arabidopsis. *Plant Physiology*

Ramaiah M, Jain A, Baldwin JC, Karthikeyan AS, Raghothama KG (2011) Characterization of the phosphate starvation-induced glycerol-3-phosphate permease gene family in Arabidopsis. *Plant physiology* **157:** 279-291

Robatzek S, Bittel P, Chinchilla D, Köchner P, Felix G, Shiu S-H, Boller T (2007) Molecular identification and characterization of the tomato flagellin receptor LeFLS2, an orthologue of Arabidopsis FLS2 exhibiting characteristically different perception specificities. *Plant molecular biology* **64:** 539-547

Robert HS, Friml J (2009) Auxin and other signals on the move in plants. *Nature chemical biology* **5:** 325-332

Shah J, Kachroo P, Nandi A, Klessig DF (2001) A recessive mutation in the Arabidopsis SSI2 gene confers SA‐and NPR1‐independent expression of PR genes and resistance against bacterial and oomycete pathogens. *The Plant Journal* **25:** 563-574

Shah J, Tsui F, Klessig DF (1997) Characterization of a s alicylic a cid-i nsensitive mutant (sai1) of Arabidopsis thaliana, identified in a selective screen utilizing the SA-inducible expression of the tms2 gene. *Molecular Plant-Microbe Interactions* **10:** 69-78

Shen W, Li JQ, Dauk M, Huang Y, Periappuram C, Wei Y, Zou J (2010) Metabolic and transcriptional responses of glycerolipid pathways to a perturbation of glycerol 3-phosphate metabolism in Arabidopsis. *Journal of Biological Chemistry* **285:** 22957-22965

Shine MB, Yang JW, El‐Habbak M, Nagyabhyru P, Fu DQ, Navarre D, Ghabrial S, Kachroo P, Kachroo A (2016) Cooperative functioning between phenylalanine ammonia lyase and isochorismate synthase activities contributes to salicylic acid biosynthesis in soybean. *New Phytologist* **212:** 627-636

Singh A, Lim GH, Kachroo P (2017) Transport of chemical signals in systemic acquired resistance. *Journal of Integrative Plant Biology* **59:** 336-344

Slaughter A, Daniel X, Flors V, Luna E, Hohn B, Mauch-Mani B (2012) Descendants of primed Arabidopsis plants exhibit resistance to biotic stress. *Plant physiology* **158:** 835-843

Spoel SH, Dong X (2012) How do plants achieve immunity? Defence without specialized immune cells. *Nature Reviews Immunology* **12:** 89-100

Spoel SH, Mou Z, Tada Y, Spivey NW, Genschik P, Dong X (2009) Proteasome-mediated turnover of the transcription coactivator NPR1 plays dual roles in regulating plant immunity. *Cell* **137:** 860-872

Stahl Y, Faulkner C (2016) Receptor complex mediated regulation of symplastic traffic. *Trends in plant science* **21:** 450-459

Tada Y, Spoel SH, Pajerowska-Mukhtar K, Mou Z, Song J, Wang C, Zuo J, Dong X (2008) Plant immunity requires conformational charges of NPR1 via S-nitrosylation and thioredoxins. *Science* **321:** 952-956

Takahashi Y, Miyata M, Zheng P, Imazato T, Horwitz A, Smith JD (2000) Identification of cAMP analogue inducible genes in RAW264 macrophages. *Biochimica et Biophysica Acta (BBA)-Gene Structure and Expression* **1492:** 385-394

Toyooka K, Matsuoka K (2009) Exo-and endocytotic trafficking of SCAMP2. *Plant signaling & behavior* **4:** 1196-1198

Truman WM, Bennett MH, Turnbull CG, Grant MR (2010) Arabidopsis auxin mutants are compromised in systemic acquired resistance and exhibit aberrant accumulation of various indolic compounds. *Plant physiology* **152:** 1562-1573

Tuzun S, Kuć J (1985) Movement of a factor in tobacco infected with Peronospora tabacina Adam which systemically protects against blue mold. *Physiological Plant Pathology* **26:** 321-330

van der Hoorn RAL, Kamoun S (2008) From guard to decoy: a new model for perception of plant pathogen effectors. *The Plant Cell* **20:** 2009-2017

Venkateswaran PS, Wu HC (1972) Isolation and characterization of a phosphonomycin-resistant mutant of Escherichia coli K-12. *Journal of bacteriology* **110:** 935-944

Wang C, El-Shetehy M, Shine MB, Yu K, Navarre D, Wendehenne D, Kachroo A, Kachroo P (2014) Free radicals mediate systemic acquired resistance. *Cell Reports* **7:** 348-355

Wang C, Liu R, Lim G-H, De Lorenzo L, Yu K, Zhang K, Hunt AG, Kachroo A, Kachroo P (2018) Pipecolic acid confers systemic immunity by regulating free radicals. *Science Advances*

Wendehenne D, Gao Q-m, Kachroo A, Kachroo P (2014) Free radical-mediated systemic immunity in plants. *Current opinion in plant biology* **20:** 127-134

West IC (1997) Ligand conduction and the gated-pore mechanism of transmembrane transport. *Biochimica et Biophysica Acta (BBA)-Reviews on Biomembranes* **1331:** 213-234

Wildermuth MC, Dewdney J, Wu G, Ausubel FM (2001) Isochorismate synthase is required to synthesize salicylic acid for plant defence. *Nature* **414:** 562-565

Williams TA (2014) Evolution: rooting the eukaryotic tree of life. *Current Biology* **24:** R151-R152

Xia Y, Gao Q-M, Yu K, Lapchyk L, Navarre D, Hildebrand D, Kachroo A, Kachroo P (2009) An intact cuticle in distal tissues is essential for the induction of systemic acquired resistance in plants. *Cell Host & Microbe* **5:** 151-165

Xia Y, Yu K, Gao Q-m, Wilson E, Navarre D, Kachroo P, Kachroo A (2012) Acyl CoA binding proteins are required for cuticle formation and plant responses to microbes. *Frontiers in plant science* **3:** 224

Xia Y, Yu K, Navarre D, Seebold K, Kachroo A, Kachroo P (2010) The glabra1 mutation affects cuticle formation and plant responses to microbes. *Plant physiology* **154:** 833-846

Yang H-C, Fu H-L, Lin Y-F, Rosen BP (2012) Pathways of arsenic uptake and efflux. In *Current topics in membranes* Vol. 69, pp 325-358. Elsevier

Yu K, Soares JM, Mandal MK, Wang C, Chanda B, Gifford AN, Fowler JS, Navarre D, Kachroo A, Kachroo P. (2013) A FeedbackRegulatory Loop betweenG3P and Lipid Transfer Proteins DIR1 and AZI1 Mediates Azelaic-Acid-Induced Systemic Immunity.

Zhang M, Zhang Y, Liu L, Yu L, Tsang S, Tan J, Yao W, Kang MS, An Y, Fan X (2010) Gene Expression Browser: large-scale and cross-experiment microarray data integration, management, search & visualization. *BMC bioinformatics* **11:** 433

Zipfel C, Robatzek S, Navarro L, Oakeley EJ, Jones JD, Felix G, Boller T (2004) Bacterial disease resistance in Arabidopsis through flagellin perception. *Nature* **428:** 764-767

VITA

JULIANA MOREIRA SOARES

EDUCATION

M. Sc. in Plant Pathology, Universidade Federal de Lavras (Brazil)……..2009-2011
Thesis title: Morphological, molecular and pathogenic characterization of pineapple fusariosis in Brazil.

B. Sc. in Agronomy Engineer, Universidade Federal de Viçosa (Brazil)…….2003-2009
Project title: Silicon in the management of sorghum anthracnose: resistance components and biochemical defense responses.

PROFESSIONAL EXPERIENCE

Volunteer trainee, Plant Disease Diagnostic, Universidade Federal de Viçosa, Brazil……..……..……2008-2009

Trainee in Agriculture by Communicating for Agricultural Exchange Program, Methuen-MA, Mattituck-NY, Rockledge-FL, Saint Paul-MN, USA……..…..2007-2008

Undergraduate Research Assistant, Pathogen/Host Interaction, Universidade Federal de Viçosa, Brazil ……..……..2006-2007

Volunteer trainee, Pathogen/Host Interaction, Universidade Federal de Viçosa, Brazil……..……..2004-2006

HONORS AND AWARDS

Graduate student travel award from University of Kentucky for Annual meeting of the American Phytopathological Society, Minneapolis, MN……..……..2014

Graduate student travel award from APS Foundation Student Travel Awards, travel award for APS National Meeting, Minneapolis, MN…….…… 2014

Fellowship CAPES, recipient as graduate research assistant, Plant Pathology department at laboratory of Ecology and Systematics of Fungi, Universidade Federal de Lavras……2009-2011

Fellowship CNPq, recipient as undergraduate research assistant, Plant Pathology department at laboratory of pathogen/host interaction, Universidade Federal de Viçosa……..…2006-2007

PUBLICATIONS

1. Araujo, L., **Soares, J. M.**, De Filippi, M. C. C., Rodrigues, F. A. Cytological aspects of incompatible and compatible interactions between rice, wheat and the blast pathogen *Pyricularia oryzae*. Scientia Agricola (2016).

2. *Yu, K., ***Soares, J. M.**, Mandal, M. K., Wang, C., Chanda, B., Gifford, A. N., Fowler, J. S., Navarre, D., Kachroo, A., Kachroo, P. A Feedback Regulatory Loop between G3P and Lipid Transfer Proteins DIR1 and AZI1 Mediates Azelaic Acid-Induced Systemic Immunity, Cell Reports (2013). * These authors contributed equally to this work.

3. **Soares, J. M.**, Crado, F., Mesquita, D. M., Barreto, R. W. *Sclerotium rolfsii* causing stem-rot of *Impatiens walleriana* in Brazil. Plant Disease (2009).

4. Resende, R. S., Rodrigues, F. A., **Soares, J. M.**, Casela, C. R. Influence of silicon on some components of resistance to anthracnose in susceptible and resistant sorghum lines. European Journal of Plant Pathology (2009).

OTHER PUBLICATIONS

1. **Soares, J. M.**, Yu, K., Mandal, M., Wang, C., Kachroo A., Kachroo, P. A feedback regulatory loop between G3P, DIR1 and AZI1 mediates azelaic acid-induced systemic immunity (2014). Poster (presenter).

2. **Soares, J. M.**, Abreu, L. M., Pinto, P. P., Ventura, J. A., Pfenning, L. H. Phylogenetic analysis in a population of Fusarium pathogenic to pineapple in Brazil (2011). Poster (presenter).

3. Castro, A. R., **Soares, J. M.**, Pfenning, L. H. Pathogeniciy test in *Ananas* spp. with isolates of *Fusarium guttiforme* e *Fusarium subglutinans* associated to wild and cultivated pinapple (2010). Poster (contributor).

4. **Soares, J. M**., Resende, R. S., Rodrigues, F. A. Silicon in control of sorghum anthracnose: evaluation of resistance components (2007). Poster (contributor).

EXTRACURRICULAR ACTIVITIES

Administrative Coordinator of a student association in Plant Pathology, Lavras, Brazil

Juliana Moreira Soares